Seismic Isolation and Protection Systems

SEISMIC ISOLATION AND PROTECTIVE SYSTEMS

http://pjm.math.berkeley.edu/siaps/

LETTER FROM THE PRESIDENT

Dear Readers,

It gives me great pleasure to introduce you to the first issue of Seismic Isolation and Protection Systems, the journal of ASSISi. The Society has felt for some time that these technologies have lacked the focussed forum that their own specialist journal could provide. The aim is to complement the biennial ASSISi Conference, and bring together refereed articles covering research, development and implementation from academia, research institutes, consultancies, device suppliers and the construction industry. We hope that those in any of these sectors will find the journal an essential aid to keeping abreast of the latest advances, and that they will regard it as the obvious choice for publication of their own work.

Initially, the journal will be published three times a year, in electronic format only. Members of ASSISi will have free access to the journal, thus ensuring a strong readership base from the outset.

This first issue covers a range of topics, including device performance, industrial and civil applications, state of the art, design criteria and health monitoring. We expect to maintain the same, high standard of articles in future.

Earthquakes continue to cause material devastation and human suffering, the recent events in China, Haiti, Italy, Chile and New Zealand being the most recent examples. Given the potential of seismic isolation and energy dissipation systems to minimize the seismic risk to structures, it is the hope and wish of ASSISi that this new journal, by improving the dissemination of ideas, will facilitate the work of the earthquake engineering community towards its goal of reducing the casualties and financial losses associated with structural damage and collapse.

KEITH FULLER: keithngfuller@aol.com
President, Anti-Seismic Systems International Society (ASSISi)

ASSESSMENT OF PERFORMANCE DEGRADATION IN ENERGY DISSIPATORS INSTALLED ON BRIDGE STRUCTURES

GIANMARIO BENZONI AND CARMEN AMADDEO

A health monitoring technique for estimating the performance degradation of antiseismic devices is presented. The approach was validated through data obtained from a 3D finite element model of a bridge structure as well as through records obtained from a real bridge equipped with viscous dampers. The records from the real structure were collected during ambient vibrations as well as a seismic event. The procedure appears capable of detecting early stages of performance variation in the devices, both in terms of location and severity level. It also requires a rather limited number of sensors, typical of a basic monitoring installation. The procedure appears feasible for application to many devices commonly installed in bridges.

1. Introduction

An effective health monitoring approach for the assessment of changes in the performance of energy dissipators in service is defined. The devices specifically considered in this study are viscous dampers (energy dissipators), but the proposed algorithm, and particularly the general procedure, can be adapted to structures equipped with other antiseismic devices. Variations in the performance characteristics of these protection systems have proved difficult to detect by traditional approaches that belong to the broad category of global (macro) methods. These approaches use measurements from a dispersed set of sensors to obtain global information about the condition of the entire structure [Housner et al. 1997]. The scope of monitoring the performance of bridges with seismic response modification devices (SRMDs), due to the concentration of nonlinear, large deformation behavior into one group of elements, pertains instead naturally to the category of local (micro) methods, which are designed to monitor specific components of the overall structural system. The ideal approach should provide a level of integration between global and local performance in order to allow for the assessment of the impact on the overall bridge response of the performance degradation detected at the local level. The proposed algorithm follows this approach by providing an assessment of the performance degradation of local components obtained from changes in modal characteristics of the overall structure.

The main case study in this research is the Vincent Thomas Bridge, a cable-suspension structure retrofitted in different stages, and lately equipped with 48 viscous dampers. The study was conducted by means of nonlinear time-history analyses of a detailed three-dimensional FE model of the bridge, provided by the California Department of Transportation (Caltrans), used in the validation phase of the procedure. Real acceleration records, obtained from the bridge under ambient vibrations and a seismic event, were used, in a second phase of development, to demonstrate the validity and accuracy of the procedure.

2. Definition of the damage detection algorithm

The core of the proposed algorithm consists of an existing damage detection algorithm modified and extended to the specific case of a bridge structure equipped with energy dissipators. The method can identify whether damage has occurred and can determine the location and severity of the damage. The sequence of procedural steps is summarized hereafter and is shown schematically in Figure 1.

Step 1. Two sources of records of the structural response were used. A three-dimensional finite element model of the Vincent Thomas Bridge provided acceleration records under white noise excitations. Records from ambient vibrations and a recent seismic event, obtained with the existing sensor network of the same bridge, were also analyzed. A model of a simplified frame, with applied viscous dampers, was used, in the early development phase, in order to validate the approach. The results of this initial phase are not reported here, but details can be found in [Benzoni et al. 2007]. Through the finite element model, the bridge structure was initially analyzed in an undamaged configuration and subsequently modified to artificially create localized degradation conditions in the viscous dampers, at different levels of severity. The simulated damages were introduced as a reduction of both stiffness and viscous dissipative properties of the energy dissipators. The data obtained from the sensor network available on the real bridge structure were also used and indicated, through the proposed procedure, that the viscous devices were at different
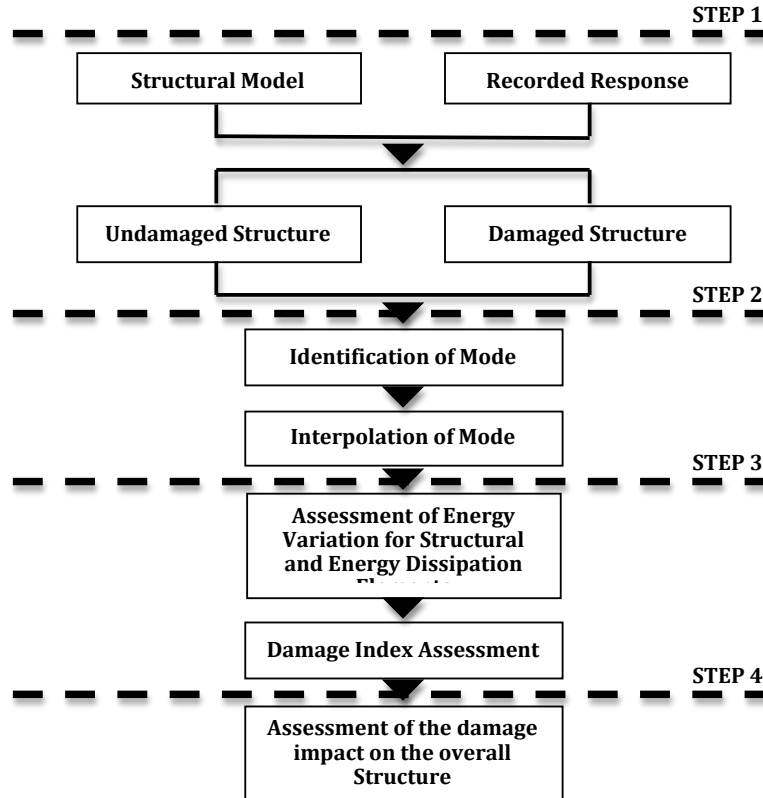

Figure 1. Layout of analytical approach.

levels of functionality. Four dampers on the bridge, in fact, suffered different degrees of damage and had to be replaced with new, identical devices. Data were recorded from the bridge with dampers in new as well as degraded conditions.

Step 2. For both the bridge model and the real structure, the natural frequencies and mode shapes of the first three significant modes were extracted. The procedure can be extended to a larger number of modes, but for the purposes of this investigation the first three modes appeared to provide sufficient information for the damage identification process. The covariance-driven stochastic subspace identification method (SSI-Cov) [Peeters 2000] was used for the assessment of the modal characteristics.

Step 3. The nondestructive damage evaluation method was applied by comparing pre-damage and post-damage configurations of the structure in terms of energy content, obtained from flexural and axial deformations. Deformations were calculated from the previously assessed mode shapes through interpolating polynomial functions. A damage index, associated with arbitrary structural elements as well as with the damping devices, was calculated.

Step 4. The structural degradation thus detected was then assigned a damage severity level.

2.1. *Implementation of the original procedure.* The original procedure was introduced in [Stubbs et al. 1992]. If a linear elastic beam is considered, the i-th modal stiffness is obtained as

$$K_i = \int_0^L EI(x)[\psi_i''(x)]^2 dx,$$

where L is the total length of the beam, ψ_i is the i-th mode shape and $EI(x)$ is the beam bending stiffness. Assuming the beam discretized into a number of elements and nodes, the contribution to the i-th modal stiffness of the j-th element can be expressed as

$$K_{ij} = EI_j \int_a^b [\psi_i''(x)]^2 dx,$$

where EI_j is the stiffness of the j-th element integrated along the length of the single element. The limits a and b generically indicate the boundary of the element length. For simplicity, EI_j is considered here as constant along the element.

The term F_{ij} represents the fraction of modal energy for the i-th mode that is concentrated in the j-th element. and is given by

$$F_{ij} = \frac{K_{ij}}{K_i}.$$

The same quantities for the damaged structure are indicated by asterisks:

$$F_{ij}^* = \frac{K_{ij}^*}{K_i^*}.$$

The ratio between the modal energy in the damaged and undamaged states can be expressed as

$$\frac{F_{ij}^*}{F_{ij}} = \frac{K_{ij}^*/K_i^*}{K_{ij}/K_i} = \frac{EI_j^* \int_a^b [\psi_i^{*\prime\prime}(x)]^2 dx \big/ \int_0^L EI^*(x)[\psi_i^{*\prime\prime}(x)]^2 dx}{EI_j \int_a^b [\psi_i''(x)]^2 dx \big/ \int_0^L EI(x)[\psi_i''(x)]^2 dx}. \tag{2-1}$$

The assumption that $EI(x)$ is constant over the length of the beam, for both the undamaged and damaged structure, allows us to reorganize (2-1) and define the damage localization index (DI_{ij}) for the j-th element and the i-th mode as

$$DI_j = \frac{F_{ij}^*}{F_{ij}} = \frac{\int_a^b [\psi_i^{*\prime\prime}(x)]^2 dx \big/ \int_0^L [\psi_i^{*\prime\prime}(x)]^2 dx}{\int_a^b [\psi_i^{\prime\prime}(x)]^2 dx \big/ \int_0^L [\psi_i^{\prime\prime}(x)]^2 dx}. \tag{2-2}$$

In general terms, the existence of damage is indicated, for the j-th element, by $DI_{ij} > 1$. It must be noted that the possibility of very small numbers for the denominator of (2-2), for instance obtained when the j-th member is at or near a node of the i-th mode, can result in a false prediction of damage. For this reason, in some cases, a value of unity is added to the fractions of modal energy to avoid division by zero, resulting in the following equation for the damage index:

$$DI_j = \frac{F_{ij}^* + 1}{F_{ij} + 1} = \frac{\left(\int_a^b [\psi_i^{*\prime\prime}(x)]^2 dx + \int_0^L [\psi_i^{*\prime\prime}(x)]^2 dx \right) \int_0^L [\psi_i^{\prime\prime}(x)]^2 dx}{\left(\int_a^b [\psi_i^{\prime\prime}(x)]^2 dx + \int_0^L [\psi_i^{\prime\prime}(x)]^2 dx \right) \int_0^L [\psi_i^{*\prime\prime}(x)]^2 dx}.$$

In the original approach, the contribution of N_{mod} different modes was taken into account as a simple sum in the definition of the damage index for the j-th element:

$$DI_j = \frac{\sum_{i=1}^{N_{\mathrm{mod}}} \left(\int_a^b [\psi_i^{*\prime\prime}(x)]^2 dx + \int_0^L [\psi_i^{*\prime\prime}(x)]^2 dx \right) \int_0^L [\psi_i^{\prime\prime}(x)]^2 dx}{\sum_{i=1}^{N_{\mathrm{mod}}} \left(\int_a^b [\psi_i^{\prime\prime}(x)]^2 dx + \int_0^L [\psi_i^{\prime\prime}(x)]^2 dx \right) \int_0^L [\psi_i^{*\prime\prime}(x)]^2 dx}. \tag{2-3}$$

From the damage index DI_{ij} it is possible to obtain the normalized index for the j-th element and the i-th mode as

$$z_{ij} = \frac{DI_{ij} - \mu_{DI_{ij}}^i}{\sigma_{DI_{ij}}^i},$$

where $\mu_{DI_{ij}}^i$ and $\sigma_{DI_{ij}}^i$ represent the mean and standard deviation of the damage index of all the elements for the i-th mode. As indicated above, the normalized index z_j for the j-th element, taking into account the relevant number of mode shapes, is obtained as

$$z_j = \frac{DI_j - \mu_{DI}}{\sigma_{DI}},$$

where μ_{DI} and σ_{DI} represent the mean and standard deviation of the damage index of all the elements for all the considered modes. At a 98% significance level the procedure indicates the existence of damage in the j-th element if $z_j \geq 2$. The severity of damage at a given location is obtained as

$$\alpha_j = \frac{K_j^* - K_j}{K_j} = \frac{1}{DI_j - 1}, \tag{2-4}$$

where K_j and K_j^* are the stiffness terms of the elements in the undamaged and damaged configuration, respectively. The existence of damage is indicated by $\alpha_j \leq 0$.

2.2. *Modified approach: structure with energy dissipators.* The procedure required initially a new formulation in order to take into account the existence of the energy dissipators. The energy contribution provided by the dampers is expressed as function of the equivalent stiffness of the damper (k_{eq}):

$$E_{\text{damp}} = k_{\text{eq}} s^2,$$

where s is the length variation of the damper in relation to the modal displacements. The equivalent stiffness is obtained as

$$k_{\text{eq}} = \frac{F_{\max}}{x_{F_{\max}}},$$

where $F_{\max}$ is the peak force and $x_{F_{\max}}$ is the damper stroke (relative displacement) corresponding to the peak force value. In the definition of the damage index the energy contributions for the structural elements and for the dampers need to be combined as homogeneous quantities. For this reason the stiffness associated to the dampers is normalized to the bending stiffness of the other structural elements:

$$k_m = \frac{k_{\text{eq}}}{EI},$$

where the index m is the number of the damper. However, this level of simplification can be removed by taking into account the energy variation of each element with its pertinent level of stiffness. From the numerical point of view, an additional requirement of normalization was needed in order to maintain a level of homogenous contribution to the total energy for both the structural elements and the energy dissipators. The amplitude of the energy dissipated by the dampers is, in fact, generally much larger than the contribution from the structural elements. Numerically, this effect tends to reduce the sensitivity of the approach to changes experienced in the structural elements when the dampers are mobilized with a significant level of stroke involved. For this reason, an additional coefficient t_{im} (for each mode i and damper m) was introduced to normalize the maximum contribution of energy in the structural elements to the maximum value of energy in the dampers:

$$t_{im} = \frac{\max_{j=1,\ldots,N_{\text{el}}}\left(\int_a^b [\psi_i''(x)]^2 dx\right)}{\max(k_m s_{im}^2)},$$

where the index i indicates the mode under consideration, the index m refers to the damper, k_m is the normalized damper stiffness, and s_{im} is the m-th damper length variation for the i-th mode. The numerator represents the maximum modal stiffness of each j-th element for the i-th mode shape. The denominator is the maximum modal stiffness for each m-th damper for the i-th mode shape. The index m is also needed to take into account configurations with dampers of different length, connecting nonsymmetric elements and/or having different performance characteristics.

For the damage index, the two components, for structural elements (DI_{ij}) and dampers (DI_{im}), can be obtained, respectively, as

$$DI_{ij} = \frac{\int_a^b [\psi_i^{*\prime\prime}(x)]^2 dx + \sum\limits_{n=1}^{N_{\text{el}}} \int_0^{L_n} [\psi_i^{*\prime\prime}(x)]^2 dx + \sum\limits_{m=1}^{N_{\text{damp}}} t_{im}(s_{im}^*)^2}{\int_a^b [\psi_i''(x)]^2 dx + \sum\limits_{n=1}^{N_{\text{el}}} \int_0^{L_n} [\psi_i''(x)]^2 dx + \sum\limits_{m=1}^{N_{\text{damp}}} t_{im}(s_{im})^2} \cdot \frac{\sum\limits_{n=1}^{N_{\text{el}}} \int_0^{L_n} [\psi_i''(x)]^2 dx + \sum\limits_{m=1}^{N_{\text{damp}}} t_{im}(s_{im})^2}{\sum\limits_{n=1}^{N_{\text{el}}} \int_0^{L_n} [\psi_i^{*\prime\prime}(x)]^2 dx + \sum\limits_{m=1}^{N_{\text{damp}}} t_{im}(s_{im}^*)^2},$$

$$(2\text{-}5)$$

$$DI_{im} = \frac{t_{im}(s_{im}^*)^2 + \sum_{n=1}^{N_{el}} \int_0^{L_n} [\psi_i^{*\prime\prime}(x)]^2 dx + \sum_{m=1}^{N_{damp}} t_{im}(s_{im}^*)^2}{t_{im}(s_{im})^2 + \sum_{n=1}^{N_{el}} \int_0^{L_n} [\psi_i^{\prime\prime}(x)]^2 dx + \sum_{m=1}^{N_{damp}} t_{im}(s_{im})^2} \cdot \frac{\sum_{n=1}^{N_{el}} \int_0^{L_n} [\psi_i^{\prime\prime}(x)]^2 dx + \sum_{m=1}^{N_{damp}} t_{im}(s_{im})^2}{\sum_{n=1}^{N_{el}} \int_0^{L_n} [\psi_i^{*\prime\prime}(x)]^2 dx + \sum_{m=1}^{N_{damp}} t_{im}(s_{im}^*)^2}, \quad (2\text{-}6)$$

where N_{el} is the number of subcomponents of the structure. Subcomponents are intended here as assemblies of single portions of the structure with physical significance: columns, beams, and so on. N_{damp} is the total number of dampers. The combination of the N_{mod} different modes results in a damage index for the j-th structural element, defined as

$$DI_j = \frac{\sum_{i=1}^{N_{mod}} \left(\int_a^b [\psi_i^{*\prime\prime}(x)]^2 dx \sum_{n=1}^{N_{el}} \int_0^{L_n} [\psi_i^{*\prime\prime}(x)]^2 dx + \sum_{m=1}^{N_{damp}} t_{im}(s_{im}^*)^2 \right)}{\sum_{i=1}^{N_{mod}} \left(\int_a^b [\psi_i^{\prime\prime}(x)]^2 dx + \sum_{n=1}^{N_{el}} \int_0^{L_n} [\psi_i^{\prime\prime}(x)]^2 dx + \sum_{m=1}^{N_{damp}} t_{im}(s_{im})^2 \right)}$$

$$\cdot \frac{\sum_{i=1}^{N_{mod}} \left(\sum_{n=1}^{N_{el}} \int_0^{L_n} [\psi_i^{\prime\prime}(x)]^2 dx + \sum_{m=1}^{N_{damp}} t_{im}(s_{im})^2 \right)}{\sum_{i=1}^{N_{mod}} \left(\sum_{n=1}^{N_{el}} \int_0^{L_n} [\psi_i^{*\prime\prime}(x)]^2 dx + \sum_{m=1}^{N_{damp}} t_{im}(s_{im}^*)^2 \right)}, \quad (2\text{-}7)$$

and in a damage index for the m-th damper, defined as

$$DI_m = \frac{\sum_{i=1}^{N_{mod}} \left(t_{im}(s_{im}^*)^2 + \sum_{n=1}^{N_{el}} \int_0^{L_n} [\psi_i^{*\prime\prime}(x)]^2 dx + \sum_{m=1}^{N_{damp}} t_{im}(s_{im}^*)^2 \right)}{\sum_{i=1}^{N_{mod}} \left(t_{im}(s_{im})^2 + \sum_{n=1}^{N_{el}} \int_0^{L_n} [\psi_i^{\prime\prime}(x)]^2 dx + \sum_{m=1}^{N_{damp}} t_{im}(s_{im})^2 \right)}$$

$$\cdot \frac{\sum_{i=1}^{N_{mod}} \left(\sum_{n=1}^{N_{el}} \int_0^{L_n} [\psi_i^{\prime\prime}(x)]^2 dx + \sum_{m=1}^{N_{damp}} t_{im}(s_{im})^2 \right)}{\sum_{i=1}^{N_{mod}} \left(\sum_{n=1}^{N_{el}} \int_0^{L_n} [\psi_i^{*\prime\prime}(x)]^2 dx + \sum_{m=1}^{N_{damp}} t_{im}(s_{im}^*)^2 \right)}. \quad (2\text{-}8)$$

As indicated in (2-3) and applied in (2-7) and (2-8), consistently with the original formulation, the contribution of the different modes is combined as a simple sum, for each structural element. However, in the original format, the combination of modal contributions introduced numerical irregularities, particularly when extended to modes beyond the second. It was also noted that, in the comparison between undamaged and damaged response signals, the variation of the natural frequencies of the significant modes seems to be a reliable indicator of the importance of the modal contribution. For this reason a modal coefficient was introduced in order to take into account the variation of the natural frequencies from undamaged to damaged configuration. This coefficient, c_i, is obtained as

$$c_i = \frac{\text{abs}(f_i^* - f_i)}{\max\left(\text{abs}(f_i^* - f_i)\right)}, \quad (2\text{-}9)$$

where f_i^* and f_i are the natural frequencies of the i-th mode for the damaged and undamaged case, respectively. The coefficient c_i is multiplied by the damage index (DI_{ij}) and allows the definition of the normalized damage index Z_{ij} and Z_j, as

$$Z_{ij} = \frac{c_i DI_{ij} - \mu(c_i DI_{ij})}{\sigma(c_i DI_{ij})}, \qquad Z_j = \frac{\sum_{i=1}^{N_{\text{mod}}} c_i DI_{ij} - \mu\left(\sum_{i=1}^{N_{\text{mod}}} c_i DI_{ij}\right)}{\sigma\left(\sum_{i=1}^{N_{\text{mod}}} c_i DI_{ij}\right)}. \qquad (2\text{-}10)$$

Here DI_{ij} stands for either DI_{ij} or DI_{im} when referring to structural elements or dampers, respectively. As in the original procedure, the existence of damage in the j-th element is indicated by $Z_j \geq 2$. The damage severity index α_j is obtained as in (2-4).

3. Validation of the procedure

The proposed procedure was initially applied to a simplified portal structure with applied viscous damper elements. It was tested with positive results under a large number of simulated cases of damage in both the structural elements as well as in the dampers. Unsymmetric configurations of damper locations and performance characteristics were simulated as well. Results of these preliminary analyses are not included here, but can be found in [Benzoni et al. 2007]. The validation of the approach by use of the response of a real bridge structure was initially obtained through a 3D finite element model of the Vincent Thomas Bridge (Figure 2). It must be noted that the numerical model is utilized here only to produce accelerometric response signals associated to different levels of degradation of some bridge components.
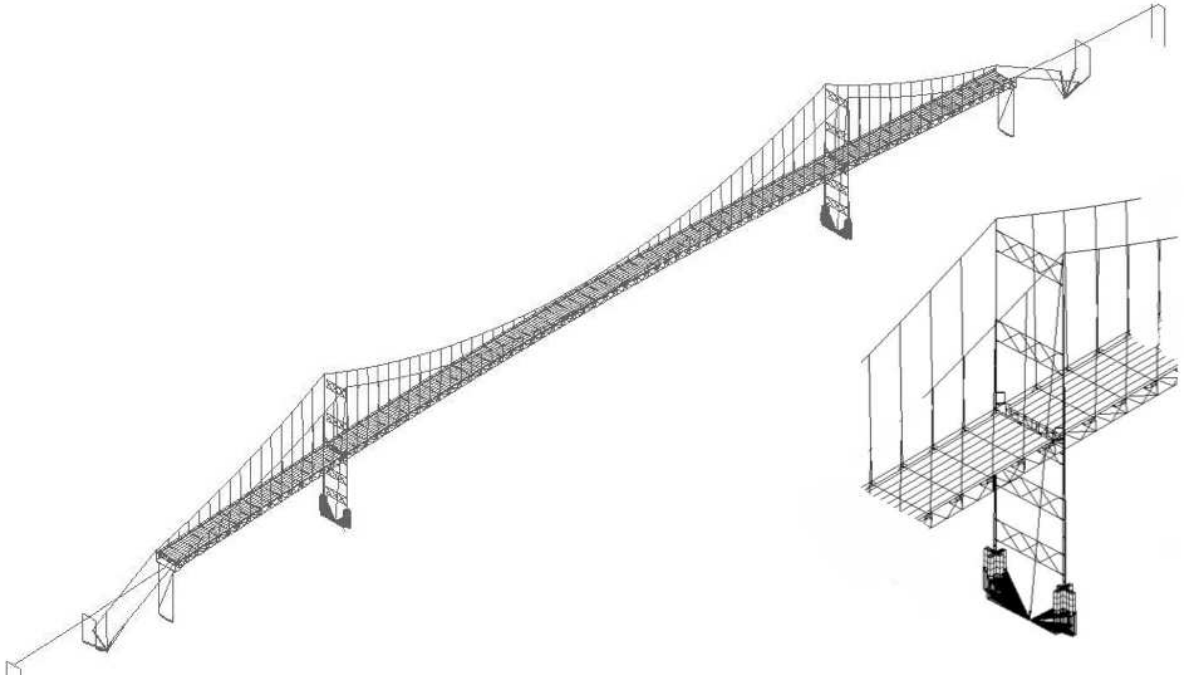

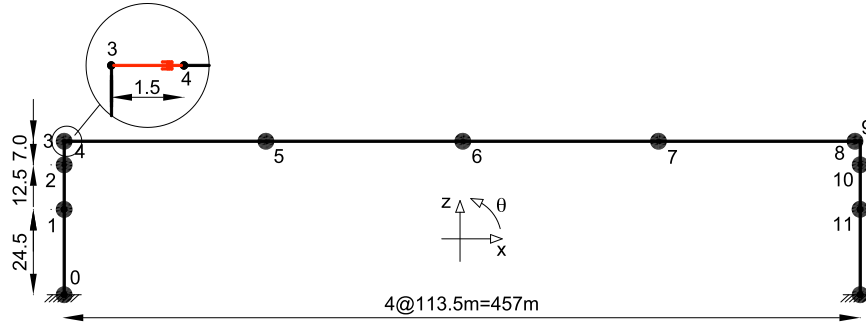**Figure 2.** Finite element model of the Vincent Thomas Bridge.

Figure 3. Bridge interpretative scheme with 12 elements (measurements in meters).

The application of the damage identification procedure does not require, in fact, the support of an FE model. The procedure requires, instead, a simplified interpretative scheme, as illustrated in the following subsection. The scheme is used for the discretization of the real structure in subcomponents (pylons, deck, and so on) and single elements, to allow the calculation of the normalized damage index for each element j, via (2-10)$_2$. The number and length of the elements that constitute the interpretative scheme is arbitrary. In addition, not every portion of the existing structure needs to be included in the interpretative scheme. In the following application, for instance, the main focus on damper performance verification justified the simplified interpretative scheme of Figure 3 to be limited to the bridge central span and the pylons. It must be noted that the interaction between all the structural components, and not only the ones represented in the simplified scheme, is accounted for in the response signals.

3.1. *Vincent Thomas Bridge application: numerical data.* The Vincent Thomas Bridge, located in the Los Angeles metropolitan area, is a cable-suspension bridge, 1849 m long, consisting of a main suspended span of approximately 457.5 m, two suspended side spans of 154 m each, ten spans in the San Pedro approach of approximately 560.6 m total length and ten spans in the Terminal Island approach of 522 m total length. The roadway width between curbs is typically 16 m and accommodates four lanes of traffic. The bridge construction was completed by the California Department of Transportation (Caltrans) in 1964. A substantial intervention of seismic upgrading was performed in 1980 and included, among others, the modification to the vertical cross frames, the lateral bracings near the bents, the cables restrainers, shear key abutment seats etc. In 1988 an additional seismic retrofit intervention included the stiffening of the bridge towers, the installation of structural fuses in the side spans and the installation of viscous dampers.

The dampers of interest for this research are located at the connection between pylons and deck, on both sides of the pylons (pylons to midspan and pylons to side-span). Other devices were not considered in this case study.

The finite element model of the bridge (Figure 2) consists of 3D elastic truss elements to represent the main suspension cables and suspender cables, 2D solid and shell elements to model the bridge deck, and beam elements to model the stiffening trusses and tower shafts. The viscous dampers are modeled by means of nonlinear spring elements with assigned stiffness and damping properties represented by a classic force-velocity relationship of the type $F = CV^a$. Here C and a represent the damping and velocity coefficients, respectively, while V is the velocity term.

Case	Frequency (Hz)			Coefficient c_i		
	Mode 1	Mode 2	Mode 3	Mode 1	Mode 2	Mode 3
D0	0.260	0.480	0.739	—	—	—
D30	0.274	0.477	0.746	1.000	0.116	0.176
D50	0.276	0.477	0.750	1.000	0.232	0.553

Table 1. Modal frequencies and coefficients of mode importance for bridge model.

Acceleration records were obtained from the numerical model of the bridge in three different configurations: bridge undamaged (case D0) and bridge with reduction of the performance characteristic of the dampers by 30% (case D30) and 50% (case D50). The degradation of the damper performance was simulated for the main span-tower dampers in terms of reduction of their damping coefficient with respect to the nominal values. The input excitation was provided through a white noise signal with frequencies between 0 and 60 Hz. The same signal was utilized for the bridge in undamaged and damaged condition.

Only the portion of the structure mostly affected by the dampers, specifically the pylons and the main span deck (see interpretative scheme of Figure 3), was considered in this phase. As indicated above, additional portions of the overall bridge can be added, like the complete height of the towers and the structure from the towers to the abutments, but the selected part of the bridge seemed appropriate for the goal of initial validation of the procedure. The dampers connecting the bridge towers and the main-span deck are also grouped, in the schematic of Figure 3, in two elements (element between node 3 and 4 and element between nodes 8 and 9). Each element represents a set of 4 dampers in the real structure. An higher level of analysis could represent each single damper by one specific element of the interpretative scheme.

The assessment of the mode shapes from the FE model response signals was obtained by use of the output-only response method proposed in [Peeters 2000], based on SSI-Cov. The output-only characteristic of the method is considered of paramount importance for the proposed application because the structure is treated as excited by unmeasurable input force and only output measurements (such as accelerations) are available. This condition closely represents the reality of a complex structure under a program of monitoring for structural health assessment purposes. For the SSI-Cov method the deterministic knowledge of the input is replaced by the assumption that the input is a realization of a stochastic process (white noise). An efficient construction of the stabilization diagram was achieved by computing the single value decomposition (SVD) of the covariance Toeplitz matrix only once. The natural frequencies for the first three modes and the coefficient c_i, as defined in (2-9), are reported in Table 1.

The normalized damage index Z_{ij}, for the 50% damage scenario, is reported in Figure 4 for the first three modes. For visualization purposes, the elements that represent the east pylon, the deck and the west pylon are projected on the same x axis. The damage indexes for the two energy dissipators, at the pylon to main-span location, are reported at the right end side of the diagram. In Figure 4, at the damper locations, the index Z_j exceeds the value of 2, indicating a degradation associated with these elements. Figure 5, left, shows the normalized damage index given in $(2\text{-}10)_2$ after the combination of the first
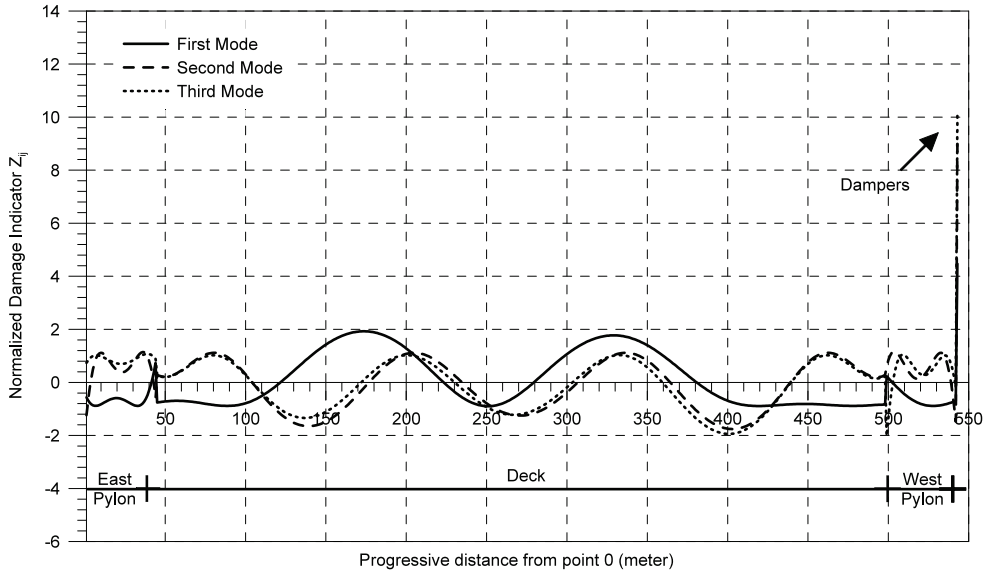
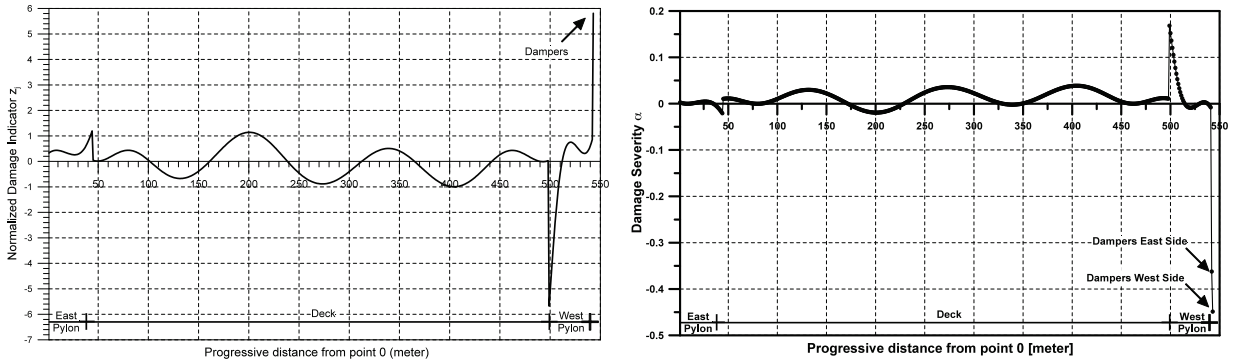**Figure 4.** Damage 50%: normalized damage index Z_{ij} of the first three modes.

Figure 5. Damage 50%: normalized damage index Z_j (left) and damage severity α_j (right).

three modes. The severity index α_j, plotted in Figure 5, right, indicates a degradation level of $\sim 37\%$ for the dampers on the East side of the main span and of $\sim 45\%$ for the dampers on the West side.

3.2. *Vincent Thomas Bridge application: experimental data.* Ambient vibration data were collected on the bridge by the sensor network indicated in Figure 6. Only the East side of the bridge is presently monitored by 26 accelerometers. Data were recorded on different events dated April 2003, June 2006 and December 2006. The data set represents a unique opportunity for validation of the proposed approach. In fact, April 2003 and June 2006 data sets correspond to a bridge configuration with degraded dampers, as observed by on site investigations and post-removal laboratory tests. By December 2006, four dampers were removed from the bridge and replaced with new identical units. For these reasons, reverting the time sequence of events, the December 2006 data were used as undamaged configuration and the April 2003 to June 2006 data were used to verify the damper conditions.

Los Angeles - Vincent Thomas Bridge
Caltrans Bridge No. 53-1471 (07-LA-47-0.86)
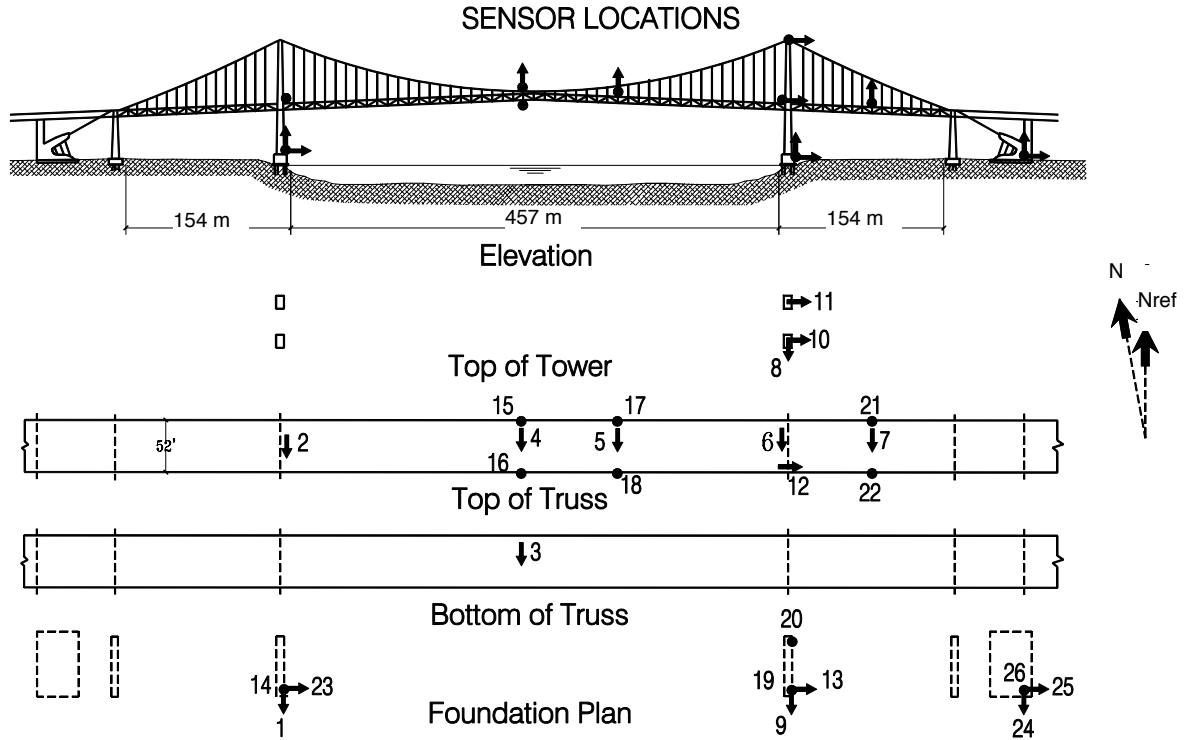CSMIP Station No. 14406

SENSOR LOCATIONS

Figure 6. Sensor locations, from [Smyth et al. 2003].

A set of records from the Chino Hills earthquake (July 2008) were finally compared with the records of December 2006 in order to verify the damper characteristics, with the expectation to obtain a nondamaged scenario due to the early replacement during year 2006. As outlined in the paragraphs above, the recorded data were initially used to estimate mode shapes for the first three significant modes of the deck and pylons. Three acceleration time histories (Channels 15, 17 and 21) were used for the deck's mode shapes and three sensor readouts (Channels 13, 12 and 10) were used for the pylon's mode shapes. The natural frequencies for the first three modes and the coefficients of mode importance — see (2-9) — are reported in Table 2.

The interpretative scheme of the bridge under consideration is shown in Figure 7. The node selection reflects both the availability of sensor readouts (numbers in parenthesis) as well as the need of providing points of connection between elements (nodes 3, 4, 8) and boundary locations (node 6). After the assessment of the mode shape functions, each segment of the structure between nodes was further subdivided in a larger number of elements, each 1 m long, used for the computation of the damage indices. The damage detection algorithm was applied here only to the deck portion of the bridge and to the viscous damper elements. Pylons were not analyzed, in terms of damage evaluation, due to the limited number of sensors installed on them. Pylon mode shapes, however, were obtained in order to estimate the relative
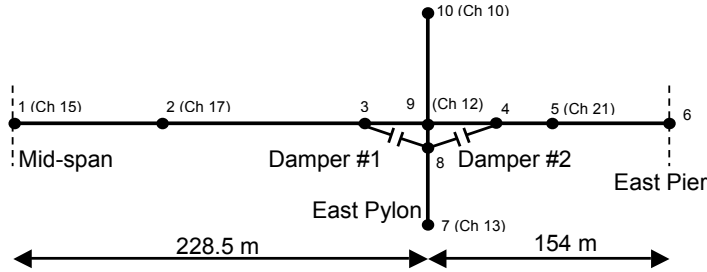
Figure 7. Interpretative scheme of the Vincent Thomas Bridge (measurements in meters).

displacements across the dampers. Figure 8 shows the damage index Z_j obtained as combination of the first three modal contributions. The estimate of the modes shapes was performed from acceleration data recorded on the bridge in December 2006 and April 2003 at the locations 1, 2, 9 and 5 corresponding to sensors in Channels 15, 17, 12 and 21, respectively (see Figure 7).

An interpolating function of the modes shapes was obtained in order to estimate the modal displacements at locations 3, 4 and 6 where sensors are not available. The mode shape of the pylon allowed the assessment of the relative modal displacement across the two sets of dampers (#1 and #2), located, for graphical representation, at the right side of Figure 8. The left part of the figure indicates damage in

	Frequency (Hz)			Coefficient c_i		
	Mode 1	Mode 2	Mode 3	Mode 1	Mode 2	Mode 3
Dec. 2006	0.25	0.39	0.46	—	—	—
Apr. 2003	0.22	0.37	0.46	1.0	0.40	0.30
June 2006	0.24	0.34	0.54	1.0	0.40	0.30
July 2008	0.32	0.43	0.62	1.0	0.30	0.70

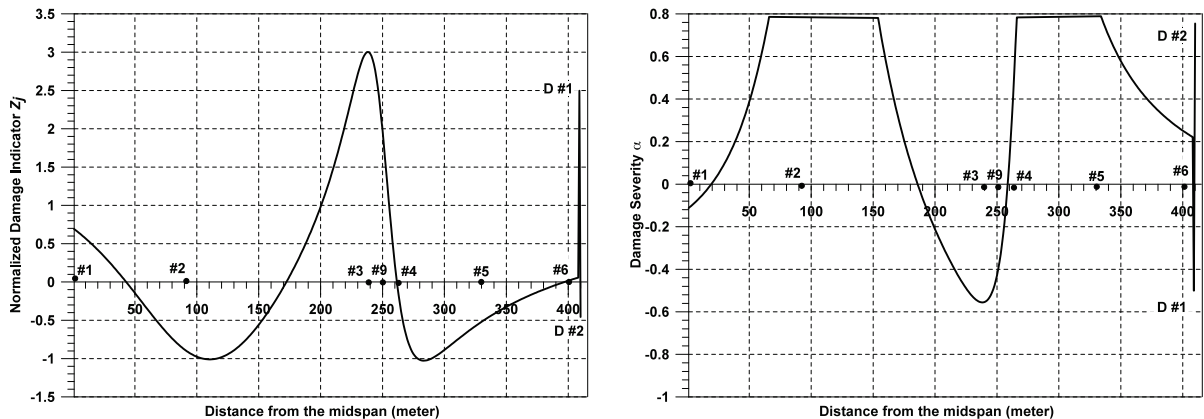**Table 2.** Modal frequencies and coefficients of mode importance for real structure.

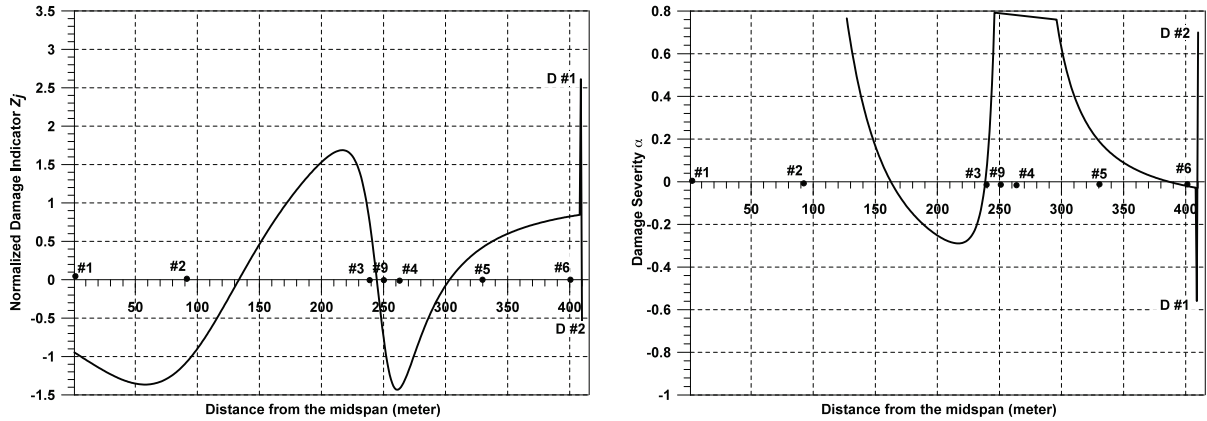**Figure 8.** Data from December 2006 and April 2003: normalized damage index Z_j (left) and damage severity α_j (right).

Figure 9. Data from December 2006 and June 2006: normalized damage index Z_j (left) and damage severity α_j (right).
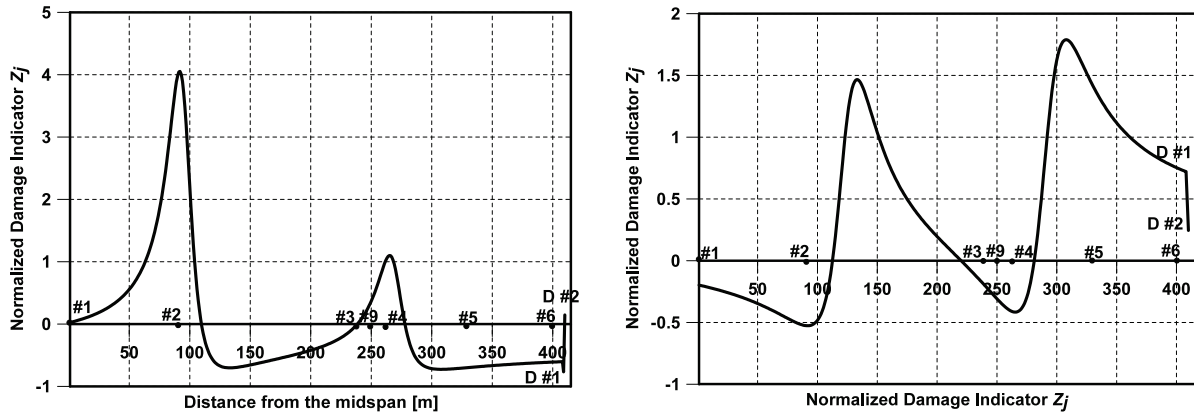

Figure 10. Data from December 2006 and July 2008: normalized damage index Z_j (left) and damage severity α_j (right).

the first damper set (#1) and for the deck elements between 220 to 250 m from the bridge midspan. For these elements the normalized damage index Z_j is, in fact, greater than 2. The severity of the damage, confirmed by the negative value of the coefficient α_j in Figure 8, right, is approximately 50% when compared with the undamaged configuration of the dampers. An additional analysis was performed using the data set obtained in June 2006 and using as reference configuration the December 2006 records. The results, presented in Figure 9, confirm the degradation of the damper performance for device #1 as well as the probable damage of deck elements in the region at 220–250 m from midspan. The last comparison, between bridge conditions in December 2006 and during the seismic event of July 2008 does not indicate any degradation of the dampers, as expected due to their replacement with new devices.

4. Conclusions

An existing structural health monitoring technique was adapted and improved in order to be used for bridge structures equipped with the use of viscous dampers. The procedure appears quite accurate for the detection of variations in the performance of the dissipation devices as well as in the remaining structural elements. One of the benefits of the procedure is the requirement of traditional sensors (accelerometers) not specifically installed in the proximity of the devices. The minimum number of installed sensors must however allow a reasonable assessment of the fundamental mode shapes of the bridge components (pylons, deck, and so on). The approach is presently under study for his potential application to bridges protected by common antiseismic devices such as elastomeric bearings and friction-based sliders.

Acknowledgements

References

[Benzoni et al. 2007] G. Benzoni, C. Amaddeo, A. D. Cesare, and P. Palermo, "A damage identification procedure for bridge structures with energy dissipation devices", technical report SRMD-2007/08, Department of Structural Engineering, University of California San Diego, La Jolla, CA, 2007.

[Housner et al. 1997] G. W. Housner, L. A. Bergman, T. K. Caughey, A. G. Chassiakos, R. O. Claus, S. F. Masri, R. E. Skelton, T. T. Soong, B. F. Spencer, and J. T. P. Yao, "J.T.P, "Structural control: past, present and future"", *J. Eng. Mech.* (*ASCE*) **123**:9 (1997), 897–971.

[Peeters 2000] B. Peeters, *System identification and damage detection in civil engineering*, Ph.D. thesis, Department of Civil Engineering, Katholieke Universiteit Leuven, Louvain, Belgium, 2000, available at www.kuleuven.be/bwm/papers/peet00a.pdf.

[Smyth et al. 2003] A. W. Smyth, J. S. Pei, and S. F. Masri, "System identification of the Vincent Thomas suspension bridge using earthquake records", *Earthquake Engin. Struct. Dyn.* **32** (2003), 339–367.

[Stubbs et al. 1992] N. Stubbs, J.-T. Kim, and K. Topole, "An efficient and robust algorithm for damage localization in offshore platforms", pp. 543–546 in *Proc. ASCE 10th Structures Congress* (San Antonio, TX), ASCE, New York, 1992.

GIANMARIO BENZONI: benzoni@ucsd.edu
University of California San Diego, Department of Structural Engineering, 9500 Gilman Drive, Mail Code 0085, La Jolla, CA 92093, United States

CARMEN AMADDEO: camaddeo@gmail.com
Università Mediterranea di Reggio Calabria, Loc. Feo di Vito, I-89100 Reggio Calabria, Italy

BASE ISOLATION: DESIGN AND OPTIMIZATION CRITERIA

PAOLO CLEMENTE AND GIACOMO BUFFARINI

Use of new antiseismic techniques is certainly suitable for buildings of strategic importance and, in general, in the case of very high risk. For ordinary buildings, instead, the cost of base isolation system should be balanced by an equivalent saving in the structure. In this paper the comparison criteria have been first defined, and then a large numerical investigation has been carried out to analyze the effectiveness and the economic suitability of seismic isolation, using elastomeric isolators and sliders, in reinforced concrete buildings.

1. Introduction

The number of seismic isolated buildings is increasing all over the world where the seismic hazard is particularly high. Besides, the very good performance of such buildings, even under very strong earthquakes, encouraged the use of seismic isolation, but a very spread diffusion of this technology has found an obstacle in its cost up to now. In fact, choose of new antiseismic technologies is quite obvious for strategic structures, which should be operational even during and just after a strong earthquake, and for buildings such as schools, banks and public offices in general, which can be very crowded. When the risk is very high or the safety requirements are very strong, such as in the cases mentioned, traditional technologies, based on an increase in structural resistance, cannot guarantee the required level of safety.

For ordinary buildings the safety requirements are lower and their use after strong earthquakes is usually not a matter. So seismic codes allow to design them taking into account their energy dissipation capacity, and structural damages under strong earthquakes are welcome, the safeguard of human life being the only goal to be pursued. Obviously, in ordinary buildings the increase in construction cost due to base isolation does not encourage its use.

Therefore, it is worth to analyze in detail the design criteria and the cost of an isolation system, in the optic of its optimum design. It is worth to remind that seismic isolation is economically more convenient in a long term analysis. In fact any building will be subject during its life time at least to one strong earthquake, which will certainly cause important damages so that heavy repairing works will be needed. Instead, a well designed isolated building will not suffer any important damages even under strong earthquakes and so no repairing works will be needed.

2. Reduction of the seismic actions

As well known seismic isolation is based on the terrific reduction of the energy that the soil transmits to the building, which is pursued by increasing the fundamental period of the structure. With reference to the usual spectrum relations, such as those suggested by the Italian code [MinInfra 2008], the spectral
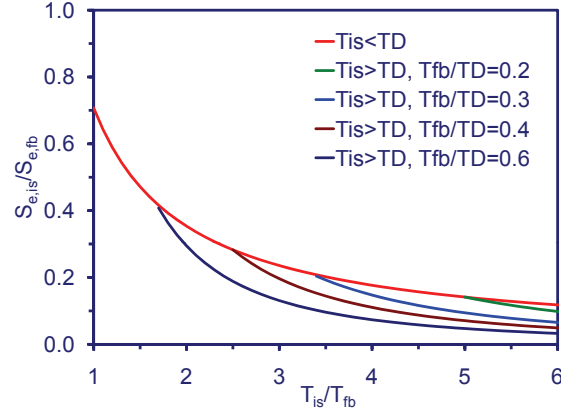
Figure 1. Elastic spectra ratios $S_{e,is}/S_{e,fb}$ $(\eta_{is}/\eta_{fb} = 0.707)$.

acceleration reductions related to the use of seismic isolation are plotted in Figure 1 versus the ratio T_{is}/T_{fb} between the fundamental period of the building designed with a base isolation system and the fundamental period of the same building designed without isolation system (fixed base building), for $T_{is} \in [T_C, T_D]$ and $T_{is} \in [T_D, 4.0]$, respectively [Buffarini et al. 2007]:

$$\frac{S_{e,is\,3}}{S_{e,fb}} = \frac{\eta_{is}}{\eta_{fb}} \cdot \frac{T_{fb}}{T_{is}}, \qquad \frac{S_{e,is\,4}}{S_{e,fb}} = \frac{\eta_{is}}{\eta_{fb}} \cdot \left(\frac{T_D}{T_{fb}}\right) \cdot \left(\frac{T_{fb}}{T_{is}}\right)^2.$$

The first curve ($T_{is} < T_D$, upper line) is unique if we assume $T_{fb} = T_C$ for $T_{fb} < T_C$. For the second relation ($T_{is} > T_D$), different curves relative to different values of T_{fb}/T_D are plotted. These start from the first upper curve at the abscissa for which $T_{is} = T_D$. In the "isolated spectrum" the value of damping $\xi = 15\%$ ($\eta_{is} = 0.707$) has been considered, while as usual $\xi = 5\%$ for nonisolated buildings ($\eta_{fb} = 1$).

The design spectrum ratios, corresponding to the ultimate limit state analysis, are plotted in Figure 2, for $q_{fb}/q_{is} = 2.7$, which is usual value for regular frames. These ratios are given by the following relations,
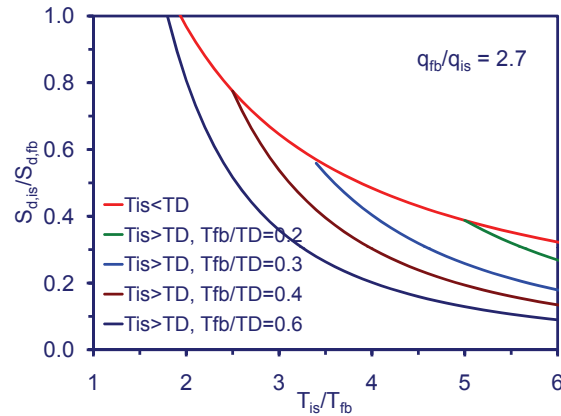

Figure 2. Limit state spectrum ratios $S_{d,is}/S_{d,fb}$ $(\eta_{is}/\eta_{fb} = 0.707)$.

valid for $T_{is} \in [T_C, T_D]$ and $T_{is} \in [T_D, 4.0]$, respectively:

$$\frac{S_{d,is\,3}}{S_{d,fb}} = \eta_{is} \cdot \frac{q_{fb}}{q_{is}} \cdot \frac{T_{fb}}{T_{is}}, \quad \frac{S_{d,is\,4}}{S_{d,fb}} = \eta_{is} \cdot \frac{q_{fb}}{q_{is}} \cdot \left(\frac{T_{fb}}{T_{is}}\right)^2 \cdot \left(\frac{T_D}{T_{fb}}\right).$$

The economical comparison between isolated and nonisolated buildings depends on the design spectra reduction. It is worth reminding that for a good decoupling of the building motion, with reference to the soil motion, the ratio T_{is}/T_{fb} should be high enough. In the following the minimum value $(T_{is}/T_{fb})_{min} = 3$ has been assumed.

3. Cost of fixed base buildings in seismic area

Preliminary considerations. The economic suitability of seismic isolation depends on several factors, among these [Clemente and Buffarini 2008]:

  – the earthquake intensity: for very low seismic input also a traditional building could be able to absorb the seismic actions in the elastic range and no damages should occur during the design earthquake;

  – the soil characteristics: as well known, earthquake spectra on soft soils present a wider range in which the acceleration is constant at its maximum value; as a result the period of the isolated building should be higher enough and consequently the displacement will get higher;

  – the shape of the building both in plan and elevation: design a seismic resistant structure in irregular buildings could be quite hard with traditional systems;

  – the size of the building: the percentage cost of the isolation system is lowered in higher and larger buildings.

It is clear that it is impossible to find out general results that can be valid for all the structures. So, in order to point out the main aspects of the comparison, consider the building in Figure 3. It is a five plus one underground level building, having size in plan equal to $L_x = 17.50\,\text{m}$ and $L_y = 12.00\,\text{m}$ (Figure 4). Due to its very regular shape it is not difficult to design a traditional seismic resistant structure.
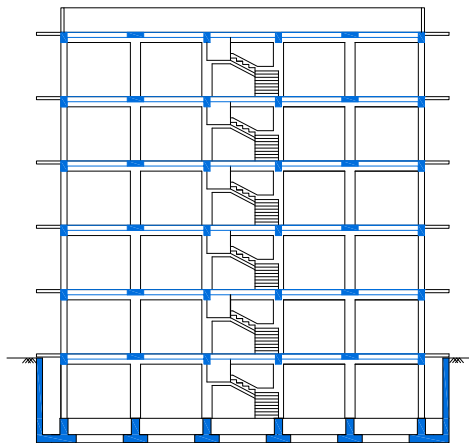

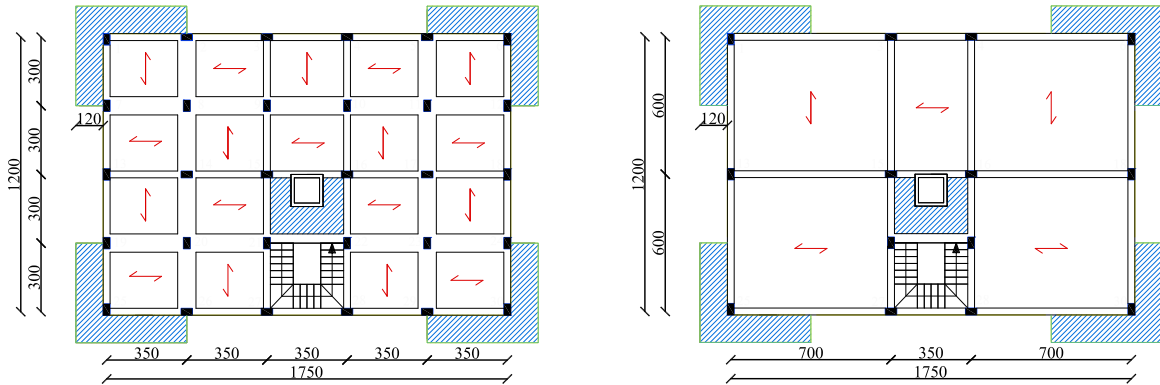**Figure 3.** Longitudinal vertical section of the building.

Figure 4. The two structural solutions: $i_x = 3.5$, $i_y = 3.0$ m (left), and $i_x = 7.0 - 3.5 - 7.0$, $i_y = 6.0$ m (right).

An effective comparison between a base-isolated building and the corresponding traditional one is quite hard. It is important to state that the architectural results should be very similar, otherwise the economic values of the two buildings could be very different. This preliminary consideration resulted in choosing the same solution for the underground level, where the isolators have been placed at the top of the pillars and the same sustaining concrete wall in both cases has been considered around the structure (Figure 3).

For the same reason, the same locations for the pillars have been assumed. Of course, the pillars of the isolated building will have cross-sections and reinforcing steel area different from the nonisolated one. Two different solutions have been considered for the number of pillars, and therefore for the space between the pillars:

(a) $i_x = 3.5$ and $i_y = 3.0$ m, which should be the best solution for the fixed base building (Figure 4, left);

(b) $i_x = 7.0 - 3.5 - 7.0$ and $i_y = 6.0$ m, which should be a better solution for the base-isolated building (the central span contains the stairs and the elevator, Figure 4, right).

In all the cases the same materials have been used for all the structural elements:

– the concrete has a characteristic compression strength $R_{ck} = 30$ N/mm^2; the compression design strength at the ultimate limit state is $f_{cd} = 14$ N/mm^2;

– the steel of the reinforcing bars has a tensile characteristic strength $f_{yk} = 450$ N/mm^2; the tensile design strength at the ultimate limit state is $f_{yd} = 390$ N/mm^2.

The decks have always a thickness equal to 25 cm $(20 + 5)$. The buildings have been designed following the same design criteria both for the concrete sections and for the reinforcing steel area, both for the superstructure and the foundation. The structural analysis and the design have been carried out according to the Italian seismic code [MinInfra 2008; MinInfra 2009]. The structure is subject to the usual permanent loads (self weight and other permanent loads) and to the typical variable loads of the residential buildings (2.0 kN/m^2).

The seismic analysis has been performed by means of the response spectrum analysis. The fixed base building (denoted by a subscript "fb") has been designed considering several values of the spectrum amplitude at T_{fb}, ranging up to $1.50g$. In practice, with the purpose of evaluating the internal forces, the analysis has been performed by referring to a structure with pillars and beams having the same concrete cross-sections constant at all the levels (30×50 cm) and imposing a spectral amplitude, independent of the actual fundamental period of the building. Due to the rules assumed for the design of the pillars and beams, which will be specified later, this turns to have no significant influence on the results.

The set of cross-sections. On the basis of the resulting internal forces, the effective concrete cross-section of each structural element has been designed. A selected set of cross-sections has been chosen for the beams. In more detail, the following concrete cross-sections have been considered:

$$\boxed{A_c = b_t \times H \text{ (cm)} \quad 30 \times 40 \quad 30 \times 50 \quad 30 \times 60 \quad 40 \times 60 \quad 40 \times 70 \quad 40 \times 80}$$

Some internal beams have the same height as the floor (25 cm); these beams have always the same width of 80 cm. For each concrete cross-section, we have considered all the values of bending reinforcing steel area in the allowable range $[A_{s,\min}, A_{s,\max}]$, where

$$A_{s,\min} = 0.26 \cdot b_t \cdot d \cdot \frac{f_{ctm}}{f_{yk}} \geq 0.0013 \cdot b_t \cdot d, \quad A_{s,\max} = 0.04 \cdot A_c$$

($d = H - 4$ cm, $f_{ctm} = 2.6$ MPa, $f_{yk} = 450$ MPa), with a step equal to the area of a bar of 10 mm diameter. Stirrups of diameter 8 mm have been considered with a space ranging from 5 to 25 cm. Each span has been divided into three parts, the central half span and the side quarter spans, in which the reinforced steel area has been kept constant (Figure 5, left).
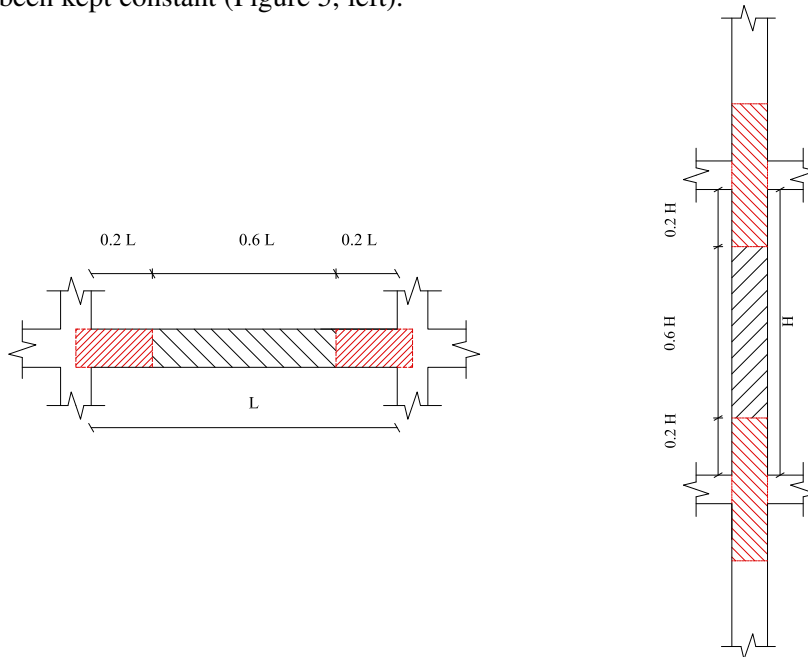

Figure 5. Parts of a beam (left) and a pillar (right) in which the steel reinforcement has been kept constant.
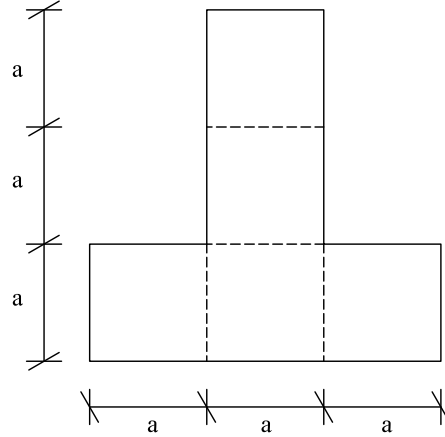
Figure 6. Cross-section of foundation beams.

For the pillars a certain (high) number of cross-sections have been considered having the same concrete cross-sections of the beams and with reinforced steel area varying in the range $[A_{\text{s,min}}, A_{\text{s,max}}]$, where

$$A_{\text{s,min}} = 0.10 \cdot \frac{N_{\text{Ed}}}{f_{\text{yd}}} \geq 0.003 \cdot A_{\text{c}}, \quad A_{\text{s,max}} = 0.04 \cdot A_{\text{rmc}}$$

(N_{Ed} = design axial force, $f_{\text{yd}} = 390$ MPa) by a step equal to the area of a 14 mm diameter bar. Stirrups of diameter 8 mm have been considered with a space ranging from 5 to 25 cm. Pillars have constant steel area along their height between two consecutive decks. Instead, their height has been divided into three parts, the central half and the side quarter, for the deployment of the steel stirrups, which are obviously less spaced near the joints (Figure 5, right).

The foundation beams have T cross-sections (Figure 6), composed by five equal squares of size a, ranging from 30 to 50 cm, and steel area increasing by a step equal to the area of a 14 mm diameter bar. In this case, stirrups of diameter 10 mm have been considered with a distance ranging from 5 to 25 cm. Also for the foundation beams, each span has been divided into three parts, the central half span and the side quarter spans, in which the reinforced steel area has been kept constant.

The cost analysis has been carried out by referring to the official prize list of the Molise region in Italy [Molise 2005].

Cost analysis of a fixed base building. As already said, with the purpose of evaluating the internal forces only one model has been considered, in which all the pillars and the beams have the same constant concrete cross-section in the entire building. First of all the internal forces due to the vertical loads have been calculated both for their maximum values (ultimate limit state) and for the values of them, which are supposed to act contemporarily to seismic actions (as usual, the variable actions are reduced with reference to their maximum value). Then the response spectrum analysis has been performed by referring to a design spectral amplitude S_d deduced from the elastic spectral amplitude S_e by means of a structural factor $q_{\text{fb}} = 4.1$, which is typical for concrete buildings with regular frame structure.

Then for the significant sections of all the beams (end-span and half-span sections) the internal forces (shear and bending moment) have been evaluated as a function of the spectral amplitude S_e. For example,
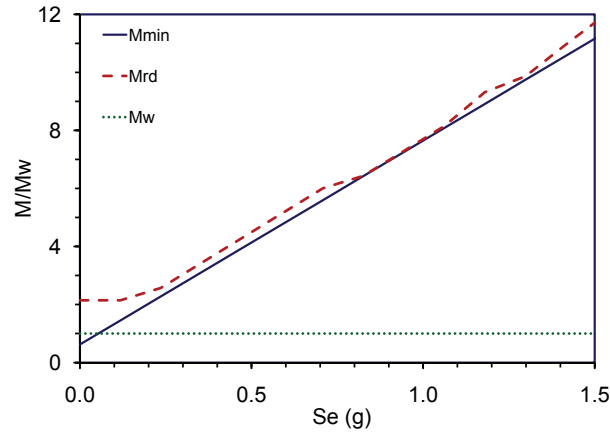
Figure 7. Minimum bending moment ($M_{\min}$), resistant bending moment (M_{rd}) and bending moment due to vertical loads (M_w) versus S_e for the end-section of a beam.

in Figure 7 a typical diagram of the bending moment versus S_e is plotted for a end-span section (continuous line). The bending moment at $S_e = 0$ is relative to the vertical loads acting contemporarily to seismic actions. The horizontal dotted line represents the bending moment due to the maximum vertical loads. The values of the bending moment have been compared with the ultimate resistant moments of the previously defined set of cross-sections and the cross-sections of minimum cost have been chosen. The same procedure of the beams has been used for the foundations.

Analogously, for the end sections of all the pillars, the M-N values have been evaluated as a function of the spectral amplitude S_e and have been compared with the M-N domains of the defined cross-sections; see the left part of Figure 8. The right part of Figure 8 plots the cost per unit length versus S_e, both for a beam and a pillar.
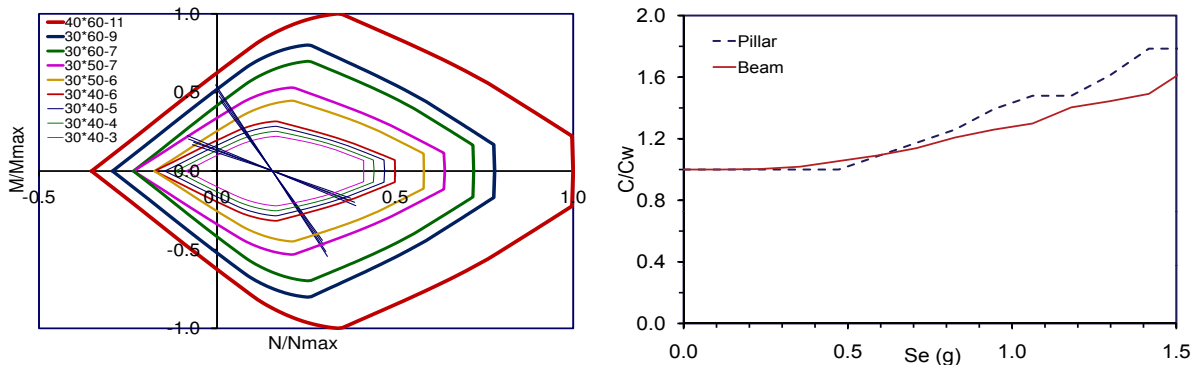

Figure 8. Left: M-N pairs in a pillar cross-section and domain of the cross-sections selected (individualized by "$b \times H$-number of $\phi 14$ bars"; the values are normalized with reference to the maximum N and M of the larger domain in the figure). Right: cost of pillar and beam, both normalized with reference to the cost for nonseismic design.

After this step the cross-section of beam and pillar can be very different at the same deck and also along the same span. So a suitable homogenization should be done. The final cross-sections have been selected under the following conditions:

- the pillars at each level have the same concrete cross-section but can have different reinforcement steel area; obviously, from one level to the other also the concrete cross-sections can be different;

- the beams of each deck have the same concrete cross-section but can have different reinforcement steel area; from one deck to the other also concrete cross-sections can be different;

- as already said, some internal beams have the same height of the floor and their cross-section is 80×25;

- the foundation beams have the same concrete cross-section but can have different reinforcement steel area.

With this assumption, in order to perform an economic comparison, the seismic analysis carried out on the building having a unique constant cross-section for beams and pillars can be supposed to be sufficiently approximated. Table 1 summarizes the concrete cross-sections of pillars and beams for the fixed base building, for both pillar locations a and b. Note that for $S_e = 1.50g$ the cross-sections of the pillars at the lower levels, for case b, are out of the defined set.

The total cost has finally been evaluated by the summation of the local costs. In Figure 9 the cost of the structure of the building is plotted versus S_e, with reference to the two solution adopted for the pillar spacing (cases a and b). The contributions of the superstructure and the foundation are distinguished. As already pointed out, the solution b is not suitable for the fixed base building in areas of high seismicity.

$S_e =$		0.50g		1.00g		1.50g	
Level	case =	a	b	a	b	a	b
5		30×40	30×50	30×40	30×60	30×50	—
4		30×40	30×50	30×50	30×60	30×60	—
3		30×40	30×50	30×50	40×70	30×60	—
2		30×40	30×60	30×50	40×80	40×70	—
1		30×40	30×60	30×60	40×80	40×80	—
Foundation		30×40	40×60	30×60	40×90	40×80	—

$S_e =$		0.50g		1.00g		1.50g	
Deck	case =	a	b	a	b	a	b
5		30×40	30×40	30×40	30×50	30×40	—
4		30×40	30×50	30×40	40×70	30×50	—
3		30×40	30×60	30×40	40×70	30×60	—
2		30×40	30×60	30×50	40×70	30×60	—
1		30×40	30×60	30×50	40×70	40×70	—
Foundation		30×40	30×60	30×50	40×70	40×70	—

Table 1. Fixed base building: pillar cross-sections (top) and beam cross-sections (bottom) for some values of the spectral amplitude, in the pillar locations a and b.
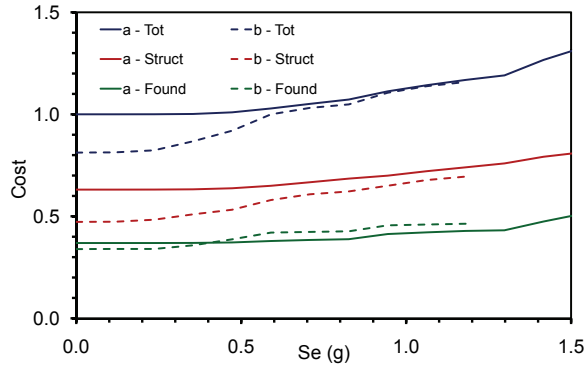
Figure 9. Fixed base building *a* and *b*: cost of the building versus S_e (note that for high values of the seismic input the solution *b* cannot be realized). The values are normalized with referenced to the total cost of the building in absence of seismic actions.

4. The base-isolated building

The same buildings (cases *a* and *b*) have been designed with base isolation (subscript "is"), for several values of the spectrum amplitude at T_{is}, ranging up to $0.30\,g$, which is certainly higher than the maximum suitable value to design structures in the elastic range. In this case, too, the seismic analysis has been performed by referring to a structure with pillars and beams having the same concrete cross-sections constant at all the levels (30×50 cm) and imposing spectral amplitude, independent of the actual fundamental period of the building.

$S_e =$		$0.50\,g$		$1.00\,g$		$1.50\,g$	
Level	case =	*a*	*b*	*a*	*b*	*a*	*b*
5		30×40	30×40	30×40	30×50	30×40	30×50
4		30×40	30×40	30×40	30×50	30×40	30×50
3		30×40	30×40	30×40	30×50	30×50	30×60
2		30×40	30×50	30×40	30×60	30×50	40×70
1		30×40	30×60	30×50	40×60	30×50	40×80
Foundation		80×80	80×80	80×80	80×80	80×80	80×80

$S_e =$		$0.50\,g$		$1.00\,g$		$1.50\,g$	
Deck	case =	*a*	*b*	*a*	*b*	*a*	*b*
5		30×40	30×50	30×40	30×50	30×40	30×50
4		30×40	30×50	30×40	30×60	30×40	30×60
3		30×40	30×50	30×40	30×60	30×40	40×70
2		30×40	30×50	30×40	30×60	30×40	40×70
1		30×40	30×50	30×40	30×60	30×50	40×70
0		30×40	30×50	30×40	30×60	30×50	40×70

Table 2. Base isolated building: pillar cross-sections (top) and beam cross-sections (bottom) for some values of the spectral amplitude, in the pillar locations *a* and *b*.
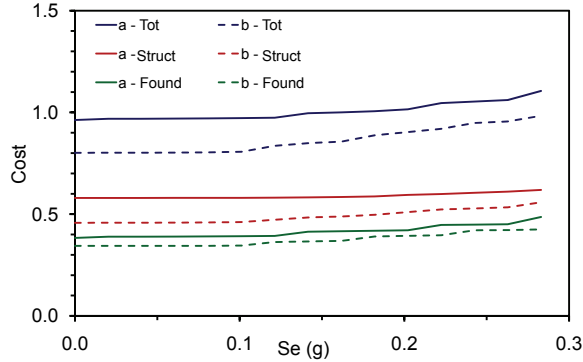
Figure 10. Base isolated building *a* and *b*: cost of the building versus $S_{e,is}$.

The isolation system was placed at the top of the underground level. The same procedure explained before for the fixed base building was used, first evaluating the internal forces due to the vertical loads for their maximum values (ultimate limit state) and for the values of them, which are supposed to act contemporarily to the seismic actions. Then the response spectrum analyzis was carried out by referring to a design spectrum having constant amplitude and reducing the resulting internal forces due to seismic action by means of a structural factor $q_{is} = 1.5$, the maximum value compatible with regular frames structures. Then for each significant section (end-span sections of pillars, end-span and half-span sections of the beams) the internal forces due to the seismic actions were evaluated as functions of the spectral amplitude $S_{e,is}$.

Table 2 summarizes the concrete cross-sections of pillars and beams. The costs of the structure of the building are plotted versus $S_{e,is}$ in Figure 10, for the cases *a* and *b*. As one can see, the increase of the cost is apparent at two values of the spectral amplitude ($S_{e,is} \approx 0.1\,g$ and $S_{e,is} \approx 0.2\,g$). It seems obvious to consider one of these as limit value $S_{e,is,d}$ for the superstructure and to design the isolation systems in order to guarantee the corresponding period T_{is}. In the following $S_{e,is,d} = 0.2\,g$ has been assumed, which turned to be more suitable from the economical point of view. It is worth observing that this value is relative to the studied building and will change for different buildings.

5. The isolation system

The sets of elastomeric isolators and sliders. For the elastomeric isolators, too, a selected set of types was defined. They were designed according to the ISO recommendations [ISO 2007]. For each value of the diameter D_e, all possible values of the thickness t_i of the rubber layers have been considered. Note that for usual buildings the maximum values of t_i are the most suitable, due to the low value of the vertical load V. So for each pair D-t_i, and for each number of rubber layers n_g, the total rubber thickness can be deduced:

$$t_e = n_g \cdot t_i.$$

By setting the shear strain γ_s to the maximum allowable value $\gamma_{s,lim}$,

$$\gamma_s = \frac{d_2}{t_e} = \gamma_{s,lim},$$

and by taking $\gamma_{s,\lim} = 2.0$, according to the Italian code [MinInfra 2009], we deduce the maximum horizontal displacement under seismic action:

$$d_2 = 2 \cdot t_e.$$

If we fix a maximum value for the bending rotation α (usually very low in buildings), the corresponding shear strain γ_α can be deduced:

$$\gamma_\alpha = \frac{3}{8} \cdot \alpha \cdot \frac{D_e^2}{t_i t_e}$$

and then the maximum value of the shear strain due to vertical load:

$$\gamma_c = \gamma_{t,\lim} - (\gamma_s + \gamma_\alpha),$$

where we take $\gamma_{t,\lim} = 5.0$ according to [MinInfra 2009]. The corresponding vertical load

$$V_c = S_1 \cdot G_{din} \cdot A_r \cdot \frac{\gamma_c}{1.5}$$

is to be compared with the critical load

$$V_{cr} = S_1 \cdot G_{din} \cdot A_r \cdot \frac{D_e}{t_e}$$

and the vertical load corresponding to the maximum stress in the steel plates:

$$V_{lam} = f_{yk} \cdot \frac{A_r \cdot t_s}{1.3 \cdot 2t_i}.$$

The maximum load for the chosen isolator, compatible with the displacement d_2, is

$$V = \min(V_c, V_{cr}, V_{lam}).$$

In the following investigation isolators with damping factor $\xi = 15\%$ have been used. Besides $G_{din} = 0.8\,\text{MPa}$ has preferably been used. When $G_{din} = 0.4\,\text{MPa}$ it is specified in the tables. Figure 11 plots K_e and V against d_2 for some isolators. The characteristics of some isolators used in the following are
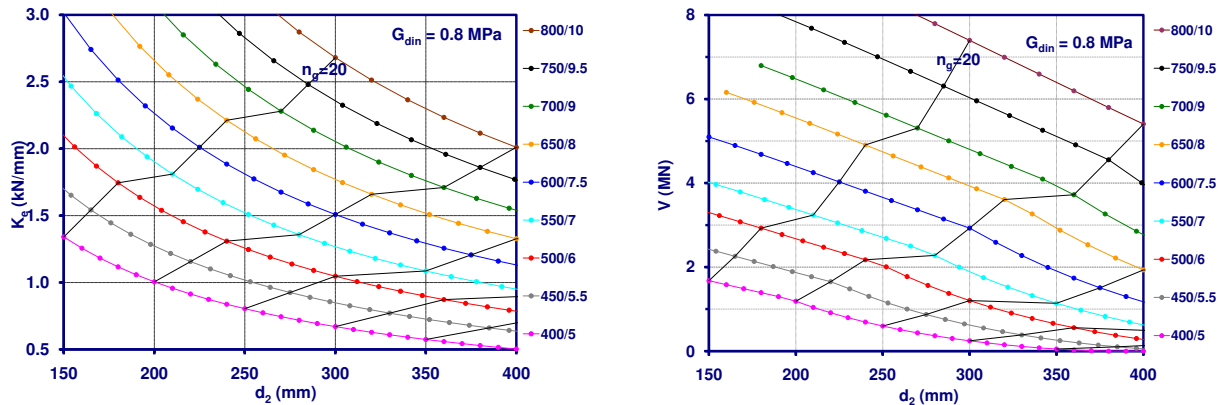

Figure 11. Elastomeric isolators: K_e versus d_2 (left) and V versus d_2 (right).

Elastomeric isolators	G (MPa)	D (mm)	t_i (mm)	t_e (mm)	t_s (mm)
400/5/25	0.8	400	5	125	2
500/6/24	0.8	500	6	144	2
600/7.5/21	0.8	600	7.5	157.5	3
700/9/16	0.8	700	9	144	3

Table 3. Characteristics of some isolation devices used in the investigation.

reported in Table 3. According to a proposal consistent with the official prize list used, the cost per unit volume of the elastomeric isolators has been assumed equal to 570 or 850 times the cost of the concrete (in €/m³), if the total volume of the device is higher or lower than 50 dm³, respectively.

The sliders are individualized by the maximum vertical load and the maximum horizontal displacement in any direction. The costs suggested by the Italian producers have been used.

Design of the isolation system. The isolation system is designed on the basis of the period T_{is}. This is chosen in order to have the maximum allowable acceleration $S_{e,is} = S_{e,is,d}$ (= 0.2 g) in the building. Obviously the choice of T_{is}, for which $S_{e,is} = S_{e,is,d}$ depends on the shape and amplitude of the elastic spectrum. In the analysis the usual shape for the spectrum has been considered, characterized by the following relationships in the ranges of interest:

$$T_B \leq T < T_C \qquad S_e(T) = a_g \cdot S \cdot \eta \cdot F_0,$$
$$T_C \leq T < T_D \qquad S_e(T) = a_g \cdot S \cdot \eta \cdot F_0 \cdot T_C/T,$$
$$T_D \leq T \qquad S_e(T) = a_g \cdot S \cdot \eta \cdot F_0 \cdot T_C T_D/T^2.$$

The following average values of the periods have been assumed as a function of the soil characteristics:

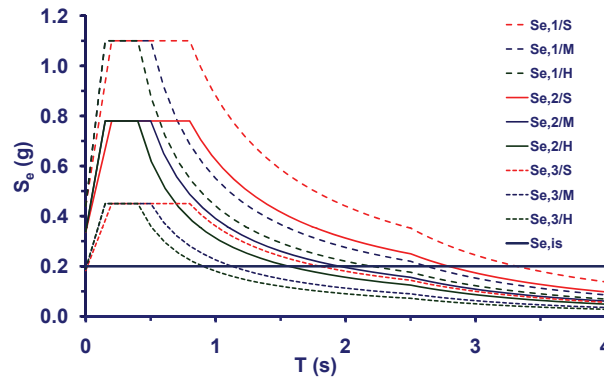| Hard soil (HS)	$T_B = 0.15$	$T_C = 0.40$	$T_D = 2.50$	(sec),
Medium soil (MS)	$T_B = 0.15$	$T_C = 0.50$	$T_D = 2.50$	(sec),
Soft soil (SS)	$T_B = 0.15$	$T_C = 0.80$	$T_D = 2.50$	(sec).

Figure 12. Choice of T_{is} for the different spectra.

With the hypothesis $T_B < T_{fb} < T_C$, three values of the spectral amplitude in the interval $[T_B, T_C]$ have been considered:

$$S_{e,1} = 1.10g, \quad S_{e,2} = 0.78g, \quad S_{e,3} = 0.45g.$$

In the resulting spectra, plotted in Figure 12, the chosen value $S_{e,is,d} = 0.2g$ is obtained at different periods. When the period turned out lower than 2.0 s, it was increased up to this value in order guarantee a suitable decoupling between the soil and the structure vibrations. Obviously, in these cases, the spectral value at $T = 2.0$ s, which is lower than $0.2g$, was used for the design. Finally the assumed periods were:

Hard soil (HS)	$T_{is,1} = 2.0$	$T_{is,2} = 2.0$	$T_{is,3} = 2.16$	(sec),
Medium soil (MS)	$T_{is,1} = 2.0$	$T_{is,2} = 2.0$	$T_{is,3} = 2.60$	(sec),
Soft soil (SS)	$T_{is,1} = 2.0$	$T_{is,2} = 2.8$	$T_{is,3} = 3.32$	(sec).

For any T_{is} found, the total stiffness $K_{e,tot}$ can be evaluated, the total mass of the superstructure being known with sufficient accuracy.

The design of the seismic isolation system was performed according to the usual suggestions. The devices were put under each pillar, at least 8 of them are elastomeric isolators, which have been mainly deployed under the perimeter pillars. Only one type of elastomeric isolator and one type of sliding device have been used.

Several deployments have been considered, which comply with the previous requirements and for which the dynamic behavior is optimum. This is very simple for the building considered and in the case of only one type of elastomeric isolator. Finally, four deployments have been selected, as shown in Figure 13.
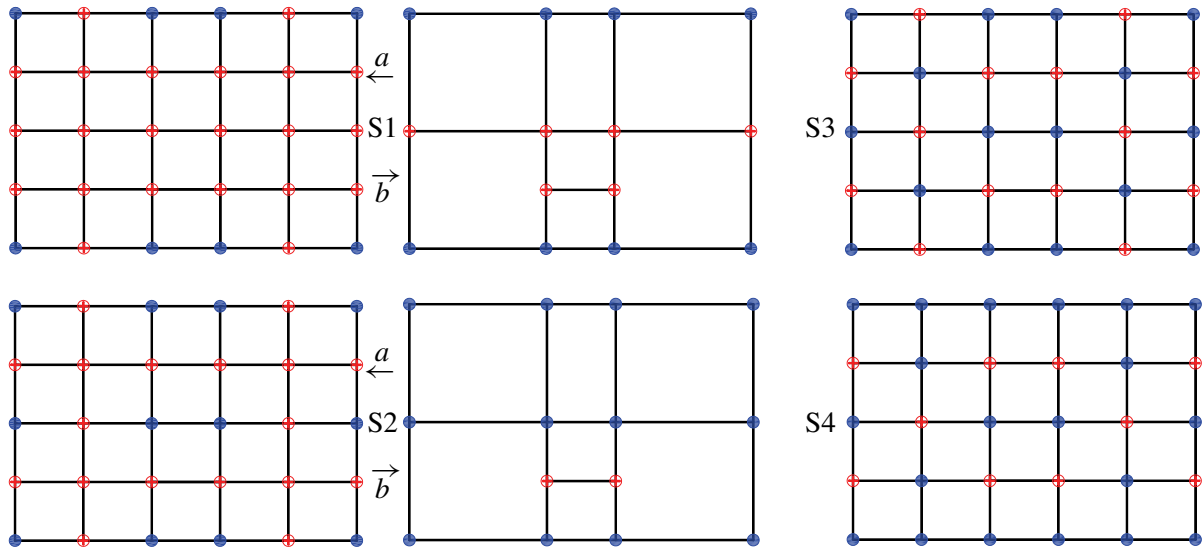

Figure 13. Different deployments of the elastomeric (filled circles) and sliding devices. Note that S3 and S4 are not possible for case b.

Deployment / Case	Elastomeric No.	$D/t_i/n_g$	Sliders No.	V/d_2
S1 / a	8	700/9/16	22	1500/300
S1 / b	8	650/8/22	6	3000/350
S2 / a	12	600/7.5/21	12	1500/300
S2 / b	18	750/9.5/19*	2	3000/350
S3 / a	16	500/6/24	12	1500/300
S4 / a	14	650/8/19*	12	1500/300

Table 4. Isolation systems for $S_{e,1} = 1.10\,g$ and medium soil. Asterisks mark the cases where $G = 0.4\,\text{MPa}$.

For each of them, the following steps were taken:

1. The stiffness K_e of the single device was deduced, by dividing $K_{e,tot}$ for the total number of elastomeric isolators.

2. The building being very regular, a first but good approximation to the value of the design displacement can be deduced on the basis of the spectral displacement and of the rotational stiffness of the isolation system, which influences the displacement due to the additional eccentricity (5% of the corresponding length of the building).

3. With K_e and the value of the design displacement, the isolator to be used can be chosen in the previously defined set, and then the vertical load can be verified.

The characteristics of the elastomeric isolators and the sliding devices corresponding to the selected deployments are summarized in Table 4. The comparison between the different solutions is performed on the basis of economical considerations.

		Fixed Base			Base Isolated
		$S_{e,3} = 0.45\,g$	$S_{e,2} = 0.78\,g$	$S_{e,1} = 1.10\,g$	$S_{e,is} = 0.20\,g$
case a	Excavation	0.088	0.088	0.091	0.088
	Foundations	0.236	0.248	0.277	0.278
	Structure	0.555	0.590	0.632	0.544
	Total	0.879	0.926	1.000	0.910
case b	Excavation	0.094	0.098	0.101	0.094
	Foundations	0.242	0.273	0.300	0.248
	Structure	0.462	0.537	0.594	0.469
	Total	0.799	0.907	0.995	0.812

Table 5. Cost comparison for the structures of a fixed base building (for three typical values of the spectral amplitude) and of a seismic isolated building, for medium soil.

Soil	case =	$S_{e,3} = 0.45\,g$ a	b	$S_{e,2} = 0.78\,g$ a	b	$S_{e,1} = 1.10\,g$ a	b
	Fixed Base	0.88	0.80	0.93	0.91	**1.00**	0.99
	Base Isolated	0.91	0.81	0.91	0.81	0.91	0.81
Hard	isolation system	0.12	0.07	0.14	0.08	0.17	0.13
Hard	total BI	1.03	0.88	1.05	0.89	1.18	0.94
Hard	BI/FB	1.17	1.10	1.13	0.97	1.08	0.94
Medium	isolation system	0.10	0.07	0.20	0.13	0.24	0.21
Medium	total BI	1.01	0.88	1.11	0.94	1.15	1.02
Medium	BI/FB	1.15	1.11	1.20	1.04	1.15	1.02
Soft	isolation system	0.20	0.13	0.42	0.43	-	-
Soft	Total BI	1.11	0.94	1.33	1.24	-	-
Soft	BI/FB	1.26	1.15	1.44	1.34	-	-

Table 6. Comparison between the costs of the structures of the fixed base building and the seismic isolated building.

6. Cost evaluation

The top half of Table 5 compares the costs of the fixed base building for the three values of the spectral amplitude with those of the isolated building (without the cost of the isolation system) for case a. The values have been normalized with reference to the total cost of the fixed base building in high seismicity area. As you can see the construction cost of the isolated building is lower than the cost of the fixed base building for high level seismicity area, while the difference is negligible in the other cases. In more details the superstructure of the isolated building is always cheaper and almost equal to the cost of a fixed base superstructure in low seismicity area. The cost of the substructure of the isolated building is always higher and very close to the cost of the substructure of the fixed base building in the high seismicity area.

Passing to case b, the cost of the fixed base building in the high seismicity area is almost the same of case a, while the cost of the isolated building is much lower, also than the fixed base building in medium seismicity area and very similar to the cost of the building in low seismicity area; see the bottom half of Table 5.

In order to conclude the comparison, the costs of the isolation system have been added to those of the isolated structures. The results are summarized in Table 6 for the three areas and for both case a and b. It is worth noting that the cost of the foundation structure is influenced by the seismic acceleration S_e, but this influence is very low on the structural total cost. The results confirm that solution a is more suitable for fixed base buildings while solution b is more suitable for isolated buildings. Actually, case b appears to be more convenient also for the fixed base building but it is worth pointing out that beams and pillars have very large cross-sections in this case. In areas with low intensity seismicity, the cost of the traditional building is low enough and use of seismic isolation could be expensive. Finally, the use of seismic isolation requires more care in the case of soft soil in high seismicity area also from the economical point of view. In fact, it is very hard to find a suitable solution.

Note that use of different number of pillars turns in different values of usable surface in the building. So taking into account the architectural and functionality requirements and economic value of the usable surface, it appears obvious to chose the solution *a* for a fixed base building and the solution *b* for the base-isolated one. The comparison between these two cases gives negligible differences for all seismic intensities. So we can conclude that use of base isolation does not determine a significant increase in cost.

7. Other investigations

The previous analysis refers to the case of a very regular building, for which it is not difficult and not expensive to realize a traditional structure without seismic isolation. As already said the numerical results are just relative to the case analyzed and cannot be generalized, especially to buildings with less regular geometrical characteristics.

Therefore it is interesting to analyze what happens for different cases. The next few subsections show the results of numerical investigations carried out on a broad selection of cases: buildings having different height, irregular buildings, and structures with particular functions. The soft soil case will not be considered for irregular and special buildings, given what was said about the use of seismic isolation in the presence of soft soil.

Influence of the height. Two buildings with the same plan as the previous one have been considered but having 3+1 and 7+1 levels; for convenience we call them "squat" and "tall".

Squat buildings. In Figure 14 the total costs of the fixed base and the base-isolated buildings having 3+1 levels are shown. In this case the base-isolated building has been designed for a spectral amplitude $S_{\text{e,is}} = 0.23 g$. The minimum value of the period T_{is} has been fixed equal to 1.5 s, compatible with the period of the superstructure.

Table 7 summarizes the total costs. It is apparent that the increase of the cost of the foundation due to the isolation system is not balanced by the reduction of the cost in elevation. Use of seismic isolation determines the increases of the total cost not lower than 10%. The influence of seismic isolation on the total cost becomes very important for low intensity seismicity.
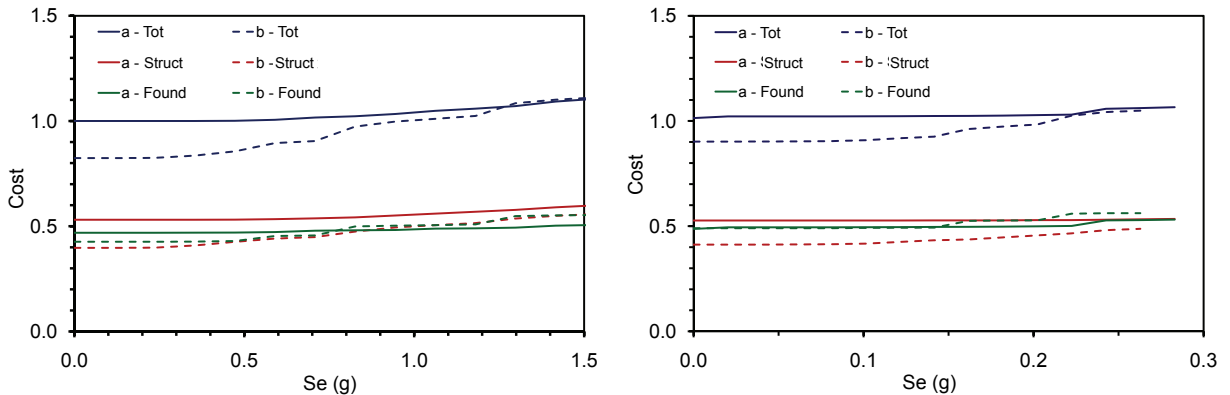

Figure 14. Squat building (3+1 levels): total cost of the building versus S_{e}, in the case of fixed base (left) and base isolation (right).

Soil	case =	$S_{e,3} = 0.45g$		$S_{e,2} = 0.78g$		$S_{e,1} = 1.10g$	
		a	*b*	*a*	*b*	*a*	*b*
	Fixed Base	0.95	0.81	0.97	0.90	**1.00**	0.96
	Base Isolated	0.98	0.94	0.99	0.94	0.99	0.94
Hard	Isolation system	0.15	0.08	0.18	0.09	0.20	0.12
	Total BI	1.14	1.01	1.16	1.02	1.19	1.06
	BI/FB	1.19	1.24	1.20	1.14	1.19	1.10
Medium	Isolation system	0.16	0.09	0.22	0.12	0.25	0.18
	Total BI	1.15	1.03	1.20	1.06	1.24	1.11
	BI/FB	1.21	1.26	1.24	1.18	1.24	1.15
Soft	Isolation system	0.20	0.15	0.44	0.48	—	—
	Total BI	1.19	1.08	1.43	1.42	—	—
	BI/FB	1.25	1.33	1.47	1.58	—	—

Table 7. Squat building (3+1 levels): Comparison between the costs of the structures of the fixed base building and the seismic isolated building.

Tall buildings. In Figure 15 the total costs of the fixed base and the base-isolated buildings having 7+1 levels are shown. In this case the base-isolated building has been designed for a spectral amplitude $S_{e,is} = 0.20g$. The minimum value of the period T_{is} has been fixed equal to 2.5 s, compatible with the period of the superstructure, which is in this case out of the range of constant spectral acceleration.

Table 8 summarizes the total costs. The cost reduction of the building structure is very low in case *a*, and significant in case *b*. But also in this last case this reduction is not sufficient to balance the cost of the seismic isolation except that in the high seismicity area. This is due to the increasing of the period of the superstructures with reference to the 5+1 levels building, which happens not to be at the plateau but in the decreasing zone of the spectrum, and to the consequent increase in the period of the isolated structure, with turns in higher displacements and so in higher cost of the isolation system. We see that,
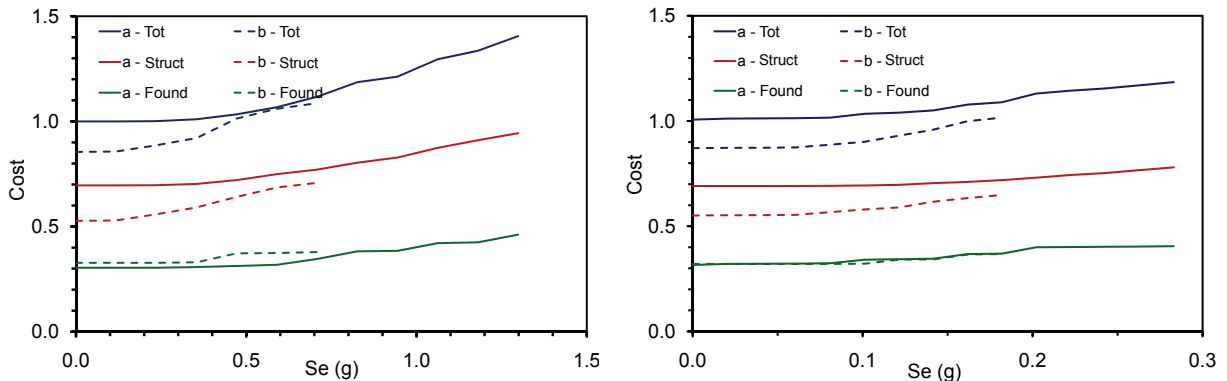

Figure 15. Tall building (7+1 levels): total cost of the building versus S_e, in the case of fixed base (left) and base isolation (right).

Soil	case =	$S_{e,3} = 0.45g$		$S_{e,2} = 0.78g$		$S_{e,1} = 1.10g$	
		a	b	a	b	a	b
	Fixed Base	0.91	0.82	0.94	0.92	**1.00**	0.98
	Base Isolated	0.97	0.87	0.97	0.87	0.97	0.87
Hard	Isolation system	0.11	0.06	0.16	0.10	0.20	0.11
	Total BI	1.07	0.93	1.12	0.97	1.16	0.98
	BI/FB	1.18	1.14	1.20	1.06	1.16	1.00
Medium	Isolation system	0.13	0.10	0.20	0.15	0.28	0.21
	Total BI	1.09	0.97	1.16	1.02	1.25	1.07
	BI/FB	1.20	1.19	1.24	1.11	1.25	1.10
Soft	Isolation system	0.21	0.12	0.39	0.24	—	—
	Total BI	1.17	0.99	1.36	1.11	—	—
	BI/FB	1.29	1.22	1.45	1.20	—	—

Table 8. Tall building (7+1 levels): comparison between the costs of the structures of the fixed base building and the seismic isolated building.

as always, the use of seismic isolation leads to a significant cost increase for buildings in low seismicity area.

Irregular buildings. According to the Italian code, the structural factor used for design fixed base buildings must be reduced by 0.8 if the building is irregular in plan and/or in elevation. In the following both cases of irregularity are considered.

Buildings irregular in plan. The irregularity in plan has been simulated by increasing the mass of half of the decks at each floor and reducing that of the other part, keeping the total mass constant. The distribution of the stiffness has been kept symmetric as in the normal building.

In more detail, the structural configuration of the building in Figure 16 is the same of the previous building, both in plan and in elevation, while vertical loads and masses have been modified in order to move the center of gravity in the longitudinal direction of 5% of the maximum size. In Figure 17 the total cost of the fixed base and base-isolated buildings irregular in plan are plotted. Table 9 summarizes the total costs. Use of seismic isolation is always convenient for case *b*.

Buildings irregular in elevation. The building analyzed is in Figure 18. Only one part of the structure has 7+1 levels, the other just 4+1, the change of size being at the fifth level above the ground.

In Figure 19 the total cost of the fixed base and base-isolated buildings irregular in elevation are plotted. Table 10 summarizes the total costs. In this case the considerations already discussed with reference to tall buildings are still valid. The cost reduction of the building structure is not sufficient to balance the cost of the seismic isolation system except that in the high seismicity area because of the value of the period of the superstructure and because of the consequent increase in the period of the isolated structure, and so of the displacements.

The differences are always low, so we can conclude that seismic isolation is very suitable for irregular buildings.
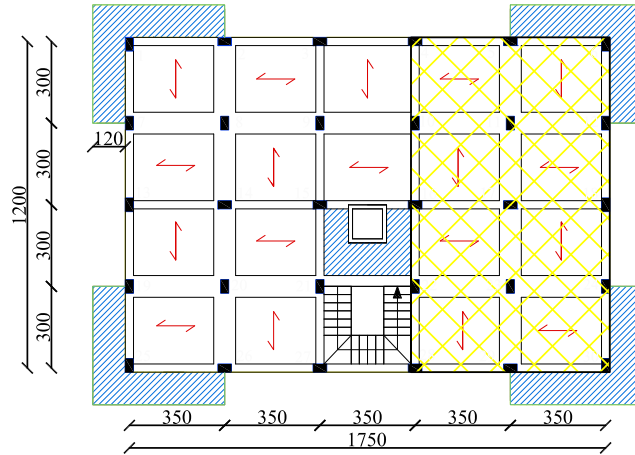
Figure 16. Building irregular in plan.

Figure 17. Building irregular in plan: cost of the building versus S_e, in the case of fixed base (left) and base isolation (right).

Soil	case =	$S_{e,3} = 0.45\,g$		$S_{e,2} = 0.78\,g$		$S_{e,1} = 1.10\,g$	
		a	b	a	b	a	b
	Fixed Base	0.81	0.80	0.89	0.88	**1.00**	1.00
	Base Isolated	0.81	0.71	0.83	0.75	0.87	0.81
Hard	Isolation system	0.12	0.06	0.15	0.08	0.19	0.11
	Total BI	0.92	0.78	0.98	0.83	1.06	0.93
	BI/FB	1.14	0.96	1.10	0.93	1.06	0.93
Medium	Isolation system	0.15	0.08	0.21	0.12	0.28	0.18
	Total BI	0.96	0.79	1.04	0.87	1.15	0.99
	BI/FB	1.18	0.98	1.17	0.97	1.15	0.99

Table 9. Building irregular in plan: comparison between the costs of the structures of the fixed base building and the seismic isolated building.
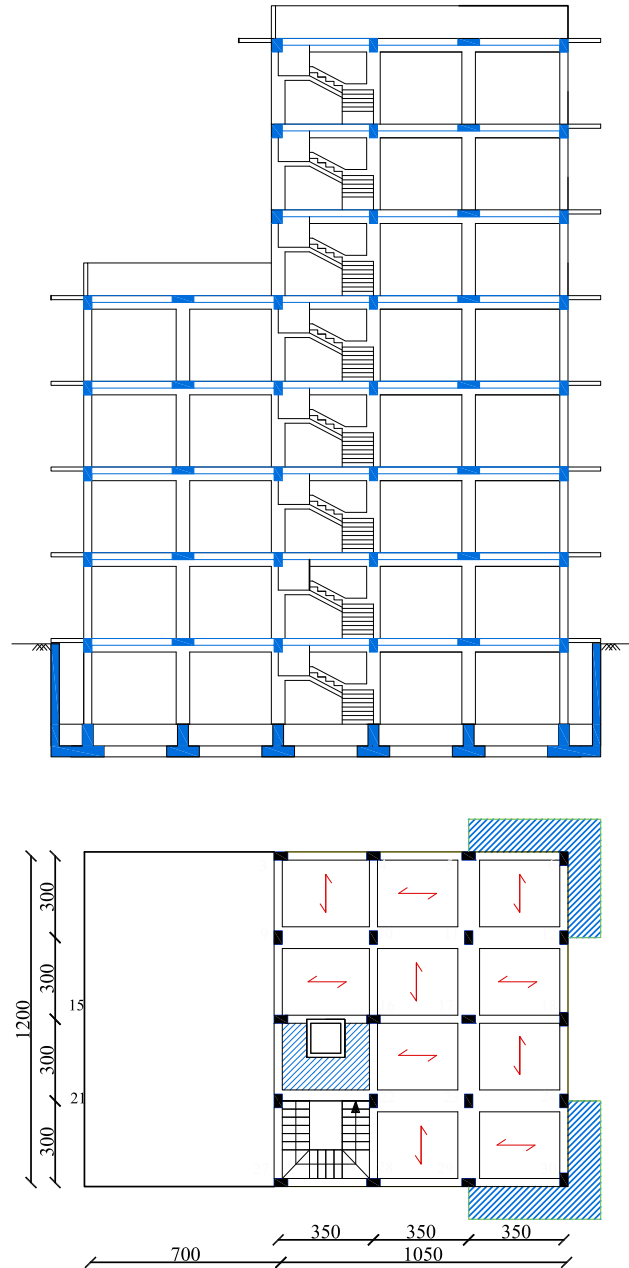
Figure 18. Building irregular in elevation: plan of the taller part and vertical section.

Special-use buildings. The buildings discussed in preceding sections are all characterized by "normal" size and designed for residential use. The structure in Figure 20 is a school building, having size in plan equal to 31.5×18.0 m, and height of 3+1 levels of 4.00 m. The structural system is very easy, with distances between the pillars of $7.0, 7.0, 3.5, 7.0, 7.0$ m in longitudinal direction and $6.0, 6.0, 6.0$ m
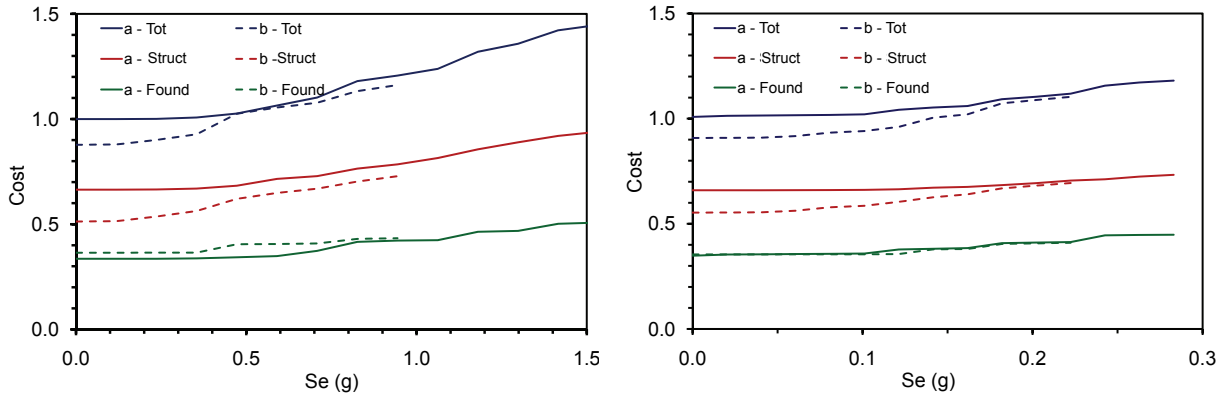
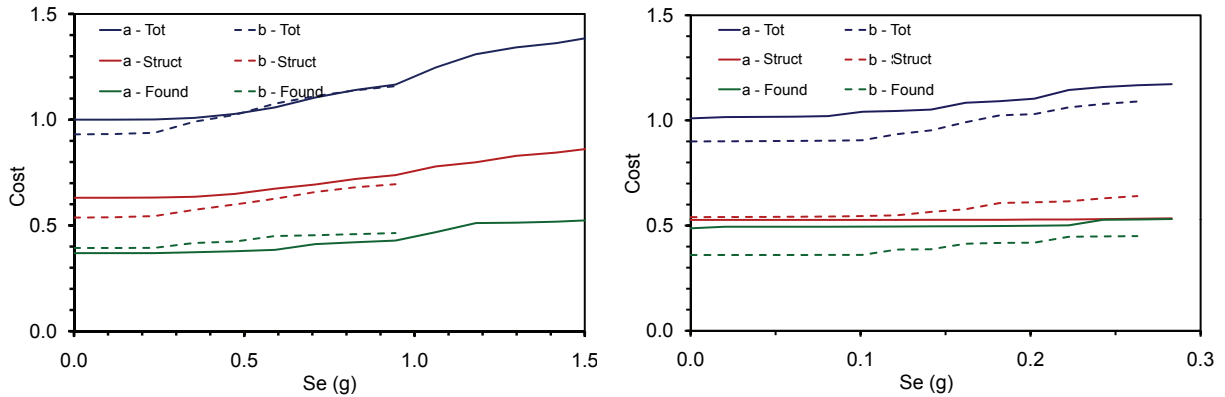**Figure 19.** Building irregular in elevation: cost of the building versus S_e, in the case of fixed base (left) and base isolation (right).

Soil	case =	$S_{e,3} = 0.45\,g$		$S_{e,2} = 0.78\,g$		$S_{e,1} = 1.10\,g$	
		a	*b*	*a*	*b*	*a*	*b*
	Fixed Base	0.84	0.80	0.90	0.88	**1.00**	1.00
	Base Isolated	0.84	0.73	0.85	0.75	0.87	0.80
Hard	Isolation system	0.11	0.11	0.15	0.11	0.20	0.14
	Total BI	0.95	0.84	1.00	0.86	1.07	0.94
	BI/FB	1.14	1.04	1.11	0.97	1.07	0.94
Medium	Isolation system	0.14	0.11	0.21	0.18	0.39	0.27
	Total BI	0.97	0.84	1.06	0.93	1.26	1.06
	BI/FB	1.16	1.04	1.18	1.05	1.26	1.06

Table 10. Building irregular in elevation: comparison between the costs of the structures of the fixed base building and the seismic isolated building.

in transversal direction. The structure is subject to the usual permanent loads (self weight and other permanent loads) and to the typical variable loads of the school buildings ($4.0\,\text{kN/m}^2$). A larger set of cross-sections has been considered. In Figure 21 the total cost of the fixed base and base-isolated special-use buildings are plotted. Table 11 summarizes the total costs. Use of base isolation causes a small increase of the construction cost but this is justified by importance of such buildings, i.e., the seismic risk. Obviously the difference is much lower for taller buildings.

8. Conclusions

In general, the difference between the cost of a building designed with a fixed base and the same building designed with base isolation is very low. Differences are certainly negligible for buildings designed to support very high level earthquakes, but also for low intensity earthquakes the choice of base isolation is obviously justified, especially for irregular and special-use buildings. In this last case, the solution with base isolation could be even less expensive. Besides, we should accounting for the different useful areas
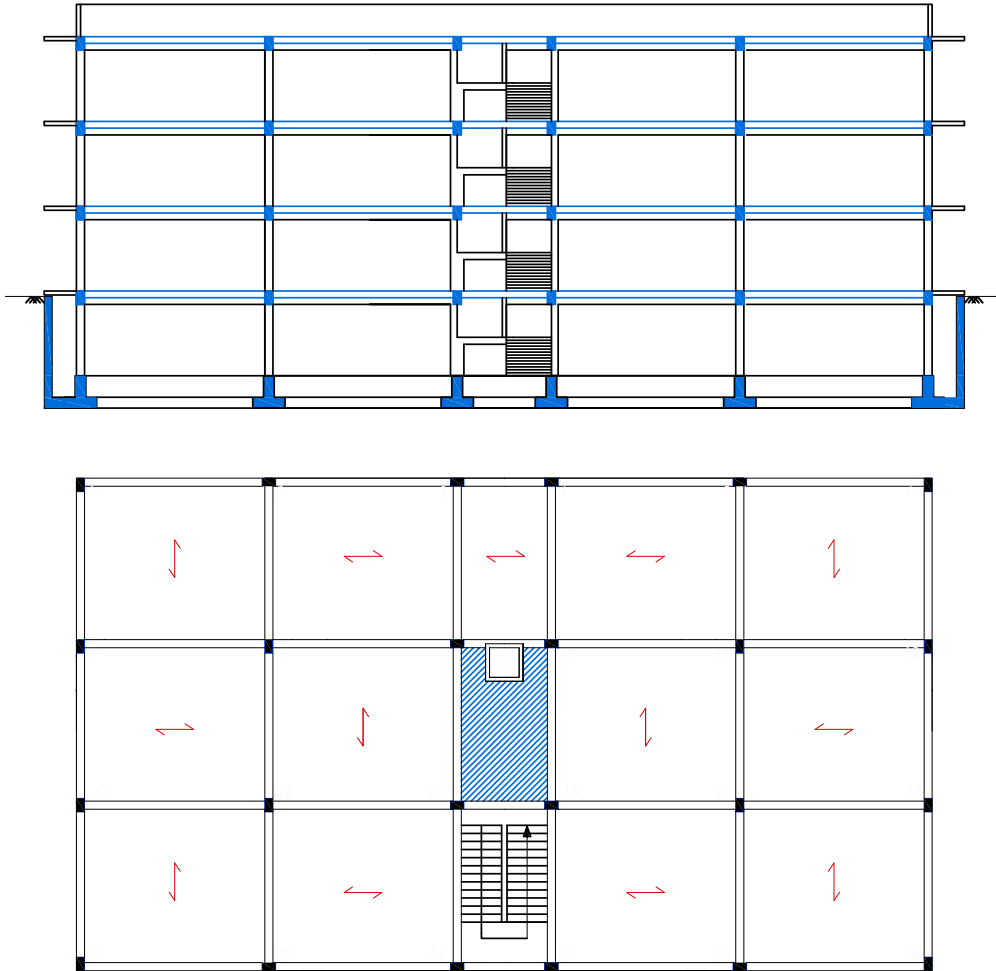
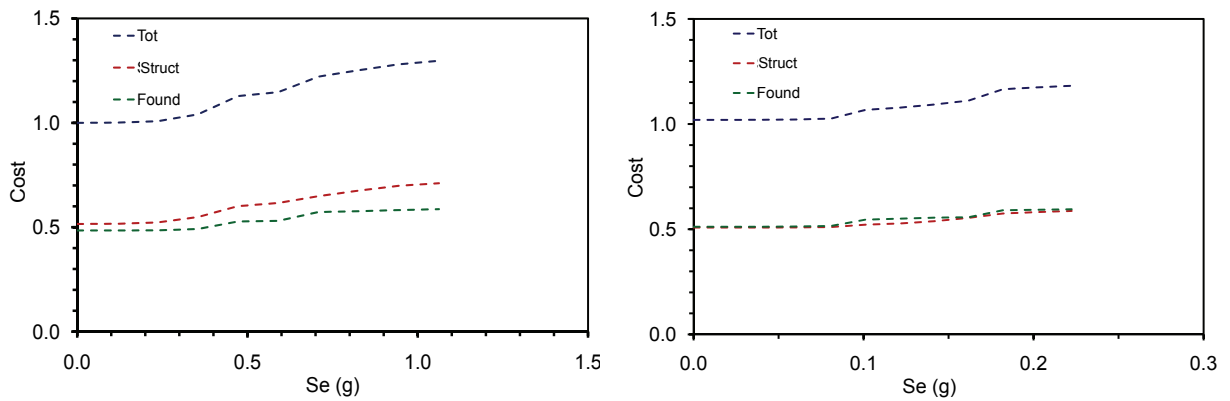**Figure 20.** Nonresidential building (3+1 levels).

Figure 21. Nonresidential building: cost of the building versus S_e, in the case of fixed base (left) and base isolation (right).

Soil	case =	$S_{e,3} = 0.45\,g$ b	$S_{e,2} = 0.78\,g$ b	$S_{e,1} = 1.10\,g$ b
	Fixed Base	0.86	0.95	**1.00**
	Base Isolated	0.79	0.83	0.85
Hard	Isolation system	0.11	0.13	0.16
	Total BI	0.90	0.96	1.01
	BI/FB	1.05	1.01	1.01
Medium	Isolation system	0.12	0.17	0.20
	Total BI	0.91	1.00	1.05
	BI/FB	1.06	1.05	1.05

Table 11. Nonresidential building: comparison between the costs of the structures of the fixed base building and the seismic isolated building.

due to the smaller size of pillars in the solution with base isolation, which translates to a different value of the building. Finally, the use of seismic isolation is certainly suitable if we frame the comparison in the context of the building's life time. In fact, seismic isolated building will not need reparation works, even after strong earthquakes.

The analysis also pointed out that, in order to improve our prevention activities in the seismic field, we should change our way of designing structures in seismic areas. In fact, buildings can be designed to support seismic action in the elastic range up to a certain value of seismic input (for example $S_e = 0.3\,g$). Therefore for buildings in low seismicity areas the assumption of a very low structural factor should guarantee their good performance and the absence of important damages. For energy input higher than that value use of new antiseismic technologies should be compulsory, instead of entrusting the safety against collapse to ductility, which will turn into lots of expenses for structural repairing. It is worth recalling that current codes allow the use of the same structural factors in low and high seismicity areas.

Acknowledgments

References

[Buffarini et al. 2007] G. Buffarini, P. Clemente, and A. Satta, "Isolamento sismico: valutazioni economiche", in *L'Ingegneria sismica in Italia: XII Convegno ANIDIS 2007* (Pisa, 2007), edited by F. Braga and W. Salvatore, Edizioni Plus, Pisa, 2007. In Italian.

[Clemente and Buffarini 2008] P. Clemente and G. Buffarini, "Optimization criteria in design of seismic isolated building", *AIP Conf. Proc.* **1020**:1 (2008), 1366–1373.

[ISO 2007] "Elastomeric seismic-protection isolators – Part 3: Applications for buildings – Specifications", ISO 22762-3:2005, International Organization for Standardization, 2007, Available at http://www.tinyurl.com/ISO-36981. Revised by ISO/FDIS 22762-3:2010.

[MinInfra 2008] Ministero delle Infrastrutture, "Nuove norme tecniche per le costruzioni", *Gazz. Uff.* **29**:Suppl. Ordinario n. 30 (2008). Decreto ministeriale 14 gennaio 2008.

[MinInfra 2009] Ministero delle Infrastrutture, "Istruzioni per l'applicazione delle 'Nuove norme tecniche per le costruzioni' di cui al D.M. 14 gennaio 2008", *Gazz. Uff.* **47**:Suppl. Ordinario n. 27 (2009). Circolare 2 febbraio 2009, n. 617.

[Molise 2005] Regione Molise, *Listino prezzi opere edili della regione Molise*, 5th edition, Campobasso, 2005, Available at http://www.prezziario.molise.it.

PAOLO CLEMENTE: paolo.clemente@enea.it
ENEA Casaccia Research Centre, Via Anguillarese 301, I-00123 Rome, Italy

GIACOMO BUFFARINI: giacomo.buffarini@enea.it
ENEA Casaccia Research Centre, Via Anguillarese 301, I-00123 Rome, Italy

STABILITY AND POST-BUCKLING BEHAVIOR
IN NONBOLTED ELASTOMERIC ISOLATORS

JAMES M. KELLY AND MARIA ROSARIA MARSICO

This paper is a theoretical and numerical study of the stability of light-weight low-cost elastomeric isolators for application to housing, schools and other public buildings in highly seismic areas of the developing world. The theoretical analysis covers the buckling of multilayer elastomeric isolation bearings where the reinforcing elements, normally thick and inflexible steel plates, are replaced by thin flexible reinforcement. The reinforcement in these bearings, in contrast to the steel in the conventional isolator (which is assumed to be rigid both in extension and flexure), is assumed to be completely without flexural rigidity. This is of course not completely accurate but allows the determination of a lower bound to the ultimate buckling load of the isolator. In addition, there are fewer reinforcing layers than in conventional isolators which makes them lighter but the most important aspect of these bearings is that they do not have end plates again reducing the weight but also they are not bonded to the upper and lower support surfaces. The intention of the research program of which this study is a part is to provide a low-cost light-weight isolation system for housing and public buildings in developing countries.

1. Introduction

The recent earthquakes in India, Turkey and South America have again emphasized the fact that the major loss of life in earthquakes happens when the event occurs in developing countries. Even in relatively moderate earthquakes in areas with poor housing many people are killed by the collapse of brittle heavy unreinforced masonry or poorly constructed concrete buildings. Modern structural control technologies such as active control or energy dissipation devices can do little to alleviate this but it is possible that seismic isolation could be adapted to improve the seismic resistance of poor housing and other buildings such as schools and hospitals in developing countries [Kelly 2002].

The theoretical basis of seismic isolation [Kelly 1997] shows that the reduction of seismic loading produced by the isolation systems depends primarily on the ratio of the isolation period to the fixed base period. Since the fixed base period of a masonry block or brick building may be of the order of 0.1 second, an isolation period of 1 sec. or longer would provide a significant reduction in the seismic loads on the building and would not require a large isolation displacement. For example, the current UBC code for seismic isolation [UBC 2007, Chapters 16, 17] has a formula for minimum isolator displacement which, for a 1.5 second system, would be around 15 cm (6 inches).

The problem with adapting isolation to developing countries is that conventional isolators are large, expensive, and heavy. An individual isolator can weight one ton or more and cost as much as $10,000 for each isolator. To extend this valuable earthquake-resistant strategy to housing and commercial buildings, it is necessary to reduce the cost and weight of the isolators.

The primary weight in an isolator is due to the steel reinforcing plates, which are used to provide the vertical stiffness of the rubber-steel composite element. A typical rubber isolator has two large end-plates (25 mm) and 20 thin reinforcing plates (3 mm). The high cost of producing the isolators results from the labor involved in preparing the steel plates and the laying-up of the rubber sheets and steel plates for vulcanization bonding in a mold. The steel plates are cut, sand-blasted, acid cleaned, and then coated with bonding compound. Next, the compounded rubber sheets with the interleaved steel plates are put into a mold and heated under pressure for several hours to complete the manufacturing process. The purpose of this program of the research of which this is a part is to suggest that both the weight and the cost of isolators can be reduced by using fiber reinforcing sheets [Kelly 1999], no end plates and no bonding to the support surfaces. Since the demands on the bonding between the rubber and the reinforcing plates are reduced, a simpler and less expensive manufacturing process can be used.

The manufacturing process for conventional isolators has to be done very carefully because the testing requirements in the current codes for seismic isolation require that the isolators be tested prior to use for very extreme loading conditions. The bond between the rubber and the steel reinforcement and between the rubber and the end plates must be very good for the bearing to survive these tests [Gent and Meinecke 1970]. The effect of a large shear displacement of the isolator is to generate an unbalanced moment that must be balanced by tensile stresses. The compression load is carried through the overlap region between top and bottom surfaces and the unbalanced moment is carried by tension stresses in the regions outside the overlap as shown in the diagram in Figure 1.

The bearings being studied here do not have these tension stresses. The primary reason for this is the fact that the top and bottom surfaces can roll off the support surfaces and no tension stresses are produced. The unbalanced moments are resisted by the vertical load through offset of the force resultants on the top and bottom surfaces.

While these isolators can undergo large displacements there is a concern with their stability. The conventional analysis for the buckling of isolators has focused only on isolators that are bolted at each end to rigid surfaces [Imbimbo and Kelly 1997]. The analysis is also based on the assumption that the steel reinforcing plates are essentially rigid but here the shims are very thin and bending of the shims could have an effect on the stability of these bearings [UBC 2007]. In this paper we will study the
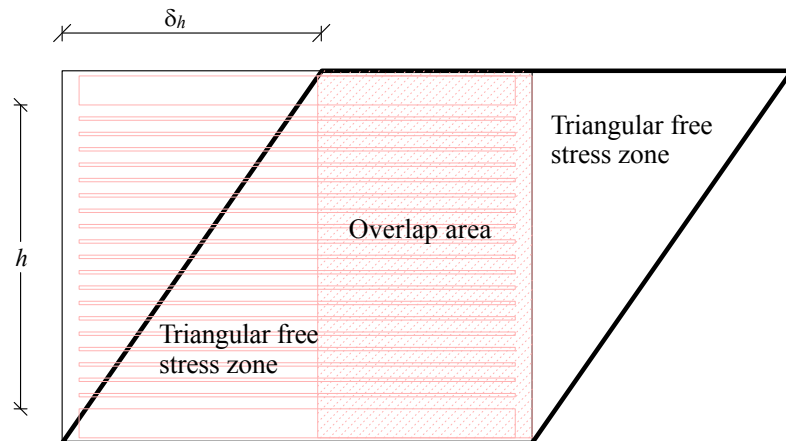

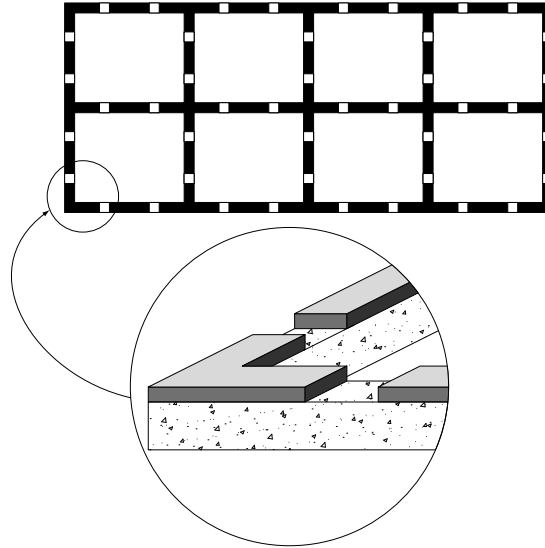**Figure 1.** Overlap area between the top and bottom of the bearing.

Figure 2. System of strip isolators in wall building.

buckling of such a bearing and attempt to clarify the post-buckling behavior based on the postulate that the vertical load in the buckled configuration is carried through the overlap area between top and bottom and that the triangular areas outside the overlap area are free of stresses. The approach will be done first for a bearing in the form of an infinite strip and then will be applied to a circular bearing. One reason for studying the strip is that the solution can be easily checked by a two-dimensional numerical model which might be considered as an experimental test.

Another benefit to using fiber reinforcement is that it would then be possible to build isolators in long rectangular strips, whereby individual isolators could be cut to the required size [Kelly and Takhirov 2002]. All isolators are currently manufactured as either circular or square. Rectangular isolators in the form of long strips would have distinct advantages over square or circular isolators when applied to buildings where the lateral resisting system is walls. When isolation is applied to buildings with structural walls, additional wall beams are needed to carry the wall from isolator to isolator. A strip isolator would have a distinct advantage for retrofitting masonry structures and for isolating residential housing constructed from concrete or masonry blocks. A possible layout of a complete system of strip isolators is shown in Figure 2.

2. Theoretical underpinnings of the stability analysis

The theoretical analysis is concerned with the buckling of a long strip bearing in which the stress state is essentially plain strain as shown in Figure 4; see [Kelly 2003]. When the bearing is displaced horizontally the material begins to roll-off the supports and the vertical load is carried through the overlap area between the top and bottom of the bearing as shown in Figure 3 and Figure 1. Thus the effective column cross-sectional area is reduced and the buckling load and the vertical stiffness are reduced also. The bearing shown in Figure 4 is a long strip fiber-reinforced bearing under vertical load and displaced horizontally to a shear deformation of 100% shear strain in its short direction [Tsai and Kelly 2002]. The fiber sheets

Figure 3. Fiber-reinforced strip bearing under vertical load and horizontal displacement test.
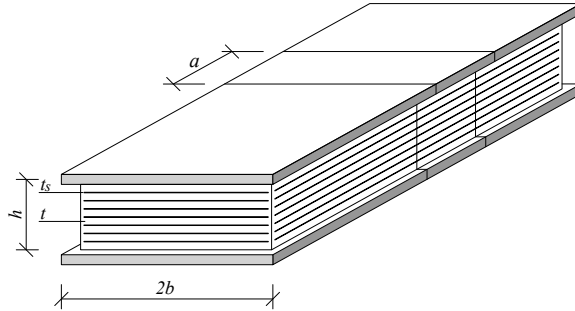
Figure 4. An infinite strip pad of width 2*b*.

are distinctly shown in the figure and it is clear that they are flat in the region of overlap between top and bottom. It is the postulate of this analysis that the vertical load is carried through the overlap area in the same way as a conventionally reinforced bearing and that the two triangular regions under the roll-off are stress free.

The process can be visualized as being conducted in a displacement controlled test machine where a steadily increasing vertical displacement is imposed on the bearing. At the first stage the vertical force needed to produce the displacement rises until the load reaches the buckling load whereupon the bearing begins to buckle sideways and to roll-off at the ends, thus reducing the effective area.

To determine the relationship between the imposed vertical displacement and the resulting horizontal displacement we use a relationship developed to analyze the interaction between the vertical stiffness and the horizontal displacement of a bearing using the linear elastic equations for a multilayer elastomer bearing. This result from [Tsai and Kelly 2005a]. provides the vertical displacement resulting from a horizontal displacement of the top of a bearing, this being in addition to that caused directly by vertical compression due to the axial load. This additional vertical displacement we will call the geometric part of displacement and denote it by δ_v^G and the connection between this and the horizontal displacement is given in [UBC 2007] as

$$\delta_v^G = \frac{\pi G A_s}{4 P_{\text{crit}}} \left(\frac{\pi p - \sin \pi p}{1 - \cos \pi p} \right) \frac{\delta_h^2}{h}, \tag{2-1}$$

where $p = P/P_{\text{crit}}$, with P the applied vertical load and $P_{\text{crit}} = (\pi/h)(EI_sGA_s)^{1/2}$, leading to

$$\delta_v^G = \frac{1}{4}\left(\frac{GA_s}{EI_s}\right)^{1/2}\left(\frac{\pi p - \sin \pi p}{1 - \cos \pi p}\right)\delta_h^2. \tag{2-2}$$

In the first instance to model the two-dimensional numerical experiment the analysis will be based on an infinite strip with width $2b$, rubber layer thickness t and n rubber layers for a total height $h = nt + (n-1)t_s$, where t_s is the thickness of the reinforcing elements (Figure 4).

The compression modulus of a single pad in the form of a long strip is

$$E_c = 4GS^2, \tag{2-3}$$

where the shape factor is $S = b/t$ and the vertical stiffness of the whole bearing is

$$K_v = \frac{4GS^2(2b)}{nt}. \tag{2-4}$$

The two quantities GA_s and EI_s are the effective shear stiffness per unit length and the effective bending stiffness per unit length of the bearing modeled as a continuous homogeneous beam and are given by $GA_s = G(2b)h/nt$ and

$$EI_s = 4GS^2\frac{1}{5}\left(\frac{2}{3}b^2\right)\frac{h}{nt};$$

see [Kelly and Takhirov 2004]. This leads to the buckling load in the undeflected configuration as

$$P_{\text{crit}} = \frac{4\pi Gb^3}{\sqrt{15}\,nt^2}. \tag{2-5}$$

The vertical displacement due to pure compression of the bearing in the undeflected configuration, denoted by δ_v^C, corresponding to this load is

$$\delta_v^C = \frac{P_{\text{crit}}}{K_v} = \frac{\pi}{2\sqrt{15}}t. \tag{2-6}$$

It is quite unexpected that this displacement depends only on the thickness of a single layer. Since the dimension b cancels in this calculation, this means that if the width $2b$ is replaced by the overlap area when the bearing displaces sideways, namely $2b - \delta_h$, the compressive part of the vertical displacement remains unchanged. When the imposed vertical displacement is increased beyond $\pi t/(2\sqrt{15})$, the additional vertical displacement must be accommodated by a geometric displacement related to the horizontal deformation of the column as a whole [Marsico 2008]. The relation between the horizontal displacement and the geometrical part of the vertical displacement in terms of the stiffness quantities for the long strip reduces to

$$\delta_v^G = \frac{\pi\sqrt{15}}{16}\frac{t}{b^2}\delta_h^2. \tag{2-7}$$

This result is the geometric part of the vertical deflection of the bearing when it is displaced horizontally at the buckling load but it can be used to provide the horizontal displacement due to increased vertical displacement in the test machine by replacing $2b$ by the reduced area $2b - \delta_h$, giving

$$\frac{\delta_h^2}{(b - \delta_h/2)^2} = \frac{16}{\pi\sqrt{15}t}\left(\delta_v - \frac{\pi}{2\sqrt{15}}t\right). \tag{2-8}$$

The solution for $\delta_h/(2b)$ is

$$\frac{\delta_h}{2b} = \frac{\sqrt{\frac{2}{15}}(x-1)^{1/2}}{1+\sqrt{\frac{2}{15}}(x-1)^{1/2}}, \tag{2-9}$$

where

$$x = \frac{\delta_v}{\pi t/2\sqrt{15}}. \tag{2-10}$$

Substitution of this result back into the expression for P_{crit} based on the reduced area, denoted by $P_{\text{crit}}(\delta_h)$, and normalization by the value of P_{crit} based on the original area P_{crit}^0 leads to

$$\frac{P_{\text{crit}}(\delta_h)}{P_{\text{crit}}} = p(\delta_h) = \left(1 - \frac{\delta_h}{2b}\right)^3, \tag{2-11}$$

which, after substitution of the result for $\delta_h/(2b)$, reduces to

$$p(\delta_h) = \left(1 + \sqrt{\frac{2}{15}}(x-1)^{1/2}\right)^{-3}. \tag{2-12}$$

The interesting point about this result is that it suggests that the buckling of the unbonded isolator is an example of classical imperfection sensitive buckling. The slope of the force displacement curve at the point of instability is negative infinity. The approximation of the post-buckling load immediately after buckling is

$$p(\delta_h) = 1 - 3\sqrt{\frac{2}{15}}(x-1)^{1/2}. \tag{2-13}$$

The post-buckling load, due the negatively infinite derivative just after buckling, drops very aggressively.

3. Numerical experiment

The analysis given in the previous section was based on the idea that the isolator is placed in a displacement controlled test machine and subjected to a steadily increasing vertical displacement which was denoted there by δ_v. This displacement manifests itself in the bearing in two parts, the first which is due to the axial shortening of the bearing due to pure compression and denoted by δ_v^C and the second due to the end shortening when the load reaches the critical load denoted by δ_v^G. When the displacement at which the load reaches the critical load is further increased the bearing can accommodate the increased vertical displacement by lateral displacement and this lateral displacement denoted there by δ_h can be calculated from the end shortening part of the total vertical displacement. To verify that this approach is at least qualitatively correct a finite element analysis was carried out on a simple model of a long strip isolator.

The numerical experiment was done using the finite element program MARC [1988]. The model is two-dimensional, corresponding to a long strip isolator and the reinforcing plates are modeled by rebar elements which have an axial stiffness but no bending resistance. This is an extreme case of plate flexibility but it is used to simplify the numerical analysis. The model has contact elements at the top and bottom surfaces that allow it roll off the rigid supports and a small horizontal load is applied at the

top to act as an imperfection and cause it to displace to one side when the load gets close to the buckling load [Tsai and Kelly 2005b].

The result is shown in the sequence of diagrams in Figure 5. The zone at the top where the surface has lost contact is directly above the bottom corner and the same in reverse at the bottom. The two triangular regions below and above the two roll out areas are free of stresses. When the vertical load is plotted against the vertical displacement as shown in Figure 6 the load rises linearly until it gets close to the buckling load then levels and then as the increased vertical displacement causes lateral displacement to develop the vertical load decreases with the reduction in the overlap area between the top and the bottom of the bearing. In effect the column is buckling with a steadily decreasing cross-sectional area. This then is, at least qualitatively, the behavior that we will attempt to reproduce analytically for a strip bearing and a circular bearing in the next two sections.

4. Vertical displacement of the top of a bearing for an infinite strip

The total vertical displacement on the top of the bearing is equal to the sum of the vertical displacement depending on the geometry and the one depending on the applied load as $\delta_v^t = \delta_v^G + \delta_v^0$. In particular the value of $\delta_v^0 = Ph/EA_s$ for an infinite strip is

$$\delta_v^0 = \frac{Pt_r t^2}{8Gb^3}. \tag{4-1}$$

The analysis of the experimental behavior of the bearing can be subdivided into three steps. First the lateral displacement, δ_h, is not present and the vertical load, P, with $0 \le P < P_{\text{crit}}$, is applied (Figure 7, left). As P grows it becomes equal to the critical load on the total area (Figure 7, middle); at this point the horizontal displacement, δ_h, begins to develop and the vertical load, P, is then the critical load calculated on the reduced area (Figure 7, right). See [Marsico and Kelly 2009].

When the horizontal displacement is not applied, the vertical displacement depending on the geometry (as in steps 1 and 2) is equal to 0; then the total vertical displacement is

$$\delta_v^t = 0 + \frac{Pt_r t^2}{8Gb^3} = \frac{Pt_r t^2}{8Gb^3}. \tag{4-2}$$

However, the displacement depending on the load changes from step 1 to step 2, because of the increasing load. Thus the total vertical displacement in step 2 is

$$\delta_v^t = 0 + \frac{\pi t}{2\sqrt{15}} = \frac{\pi t}{2\sqrt{15}}. \tag{4-3}$$

In step 3, the shortening on the top of the bearing will depend on the horizontal displacement and on the reduced area and will be

$$\delta_v^t = \frac{\pi}{16} \frac{t}{(b - \delta_h/2)^2} \sqrt{15}\delta_h^2 + \frac{\pi t}{2\sqrt{15}}. \tag{4-4}$$

Introducing

$$x = \frac{\delta_h}{2b} \quad \text{and} \quad \frac{P_{\text{crit}(Ar)}}{P_{\text{crit}}} = \left(1 - \frac{\delta_h}{2b}\right)^3 = (1 - x)^3 = y_2,$$

for $x \geq 0$ and $\delta = \pi t / 2\sqrt{15}$, we can plot $y_1 = \delta_v^t/(2b) = \delta\left(1 + \frac{15}{4}x^2(1-x)^2\right)$ versus y_2 and $y_1 = \delta_v^t/(2b)$ versus x. The behavior of the bearing is clarified in Figure 8, where the solid line represents the critical load increasing versus the vertical displacement produced while the dash line plots the horizontal displacement causing the critical load to decrease because the reduction of the area. The ratio w_c is defined as the critical load applied on the reduced area normalized with respect to the critical load on the total area.
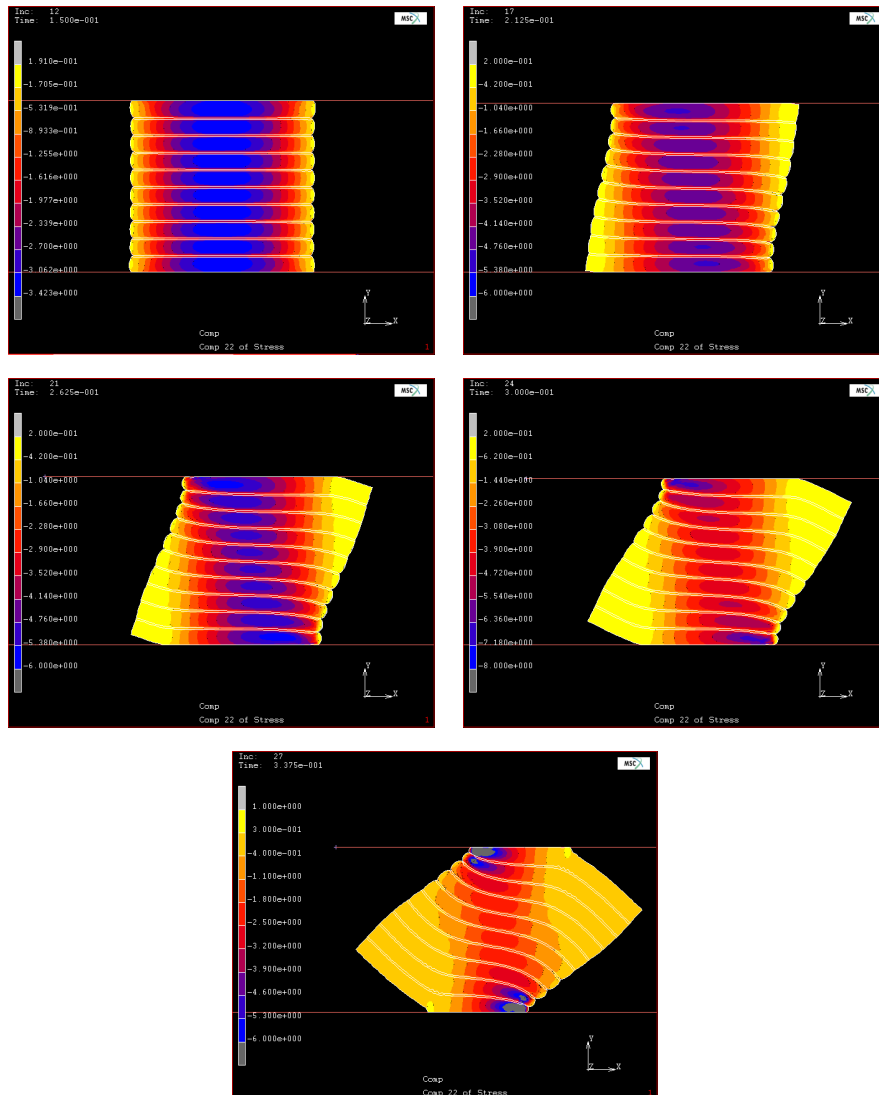
Figure 5. Sequence of buckling and post-buckling configurations showing stress-free triangular zones.
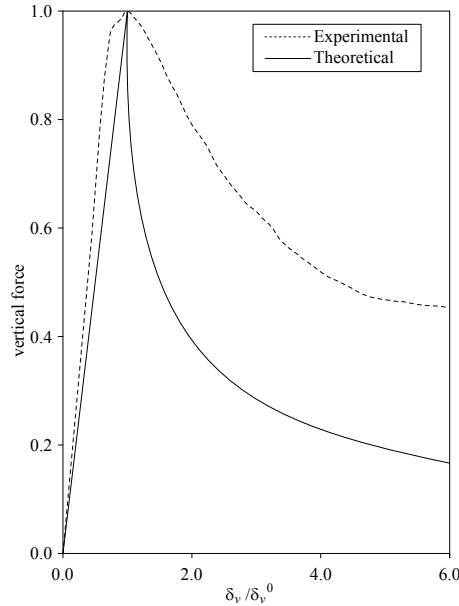
Figure 6. Normalized vertical force versus normalized vertical displacement from numerical experiment and analytical model.

5. Application of post-buckling analysis to circular bearing

Although the strip isolator has been suggested as the preferred form use with low-cost housing in developing countries there may be cases where it may be more convenient to use a circular isolator. For a circular bearing of radius R the parameters that differ from those of the strip bearing are the compression modulus E_c, the shape factor S and the effective moment of inertia I_{eff}. The modulus is

$$E_c = 6GS^2, \tag{5-1}$$

where the shape factor S is $R/(2t)$. The bending stiffness EI_{eff} in this case is

$$EI_{\text{eff}} = E_c\left(\tfrac{1}{3}I\right), \tag{5-2}$$
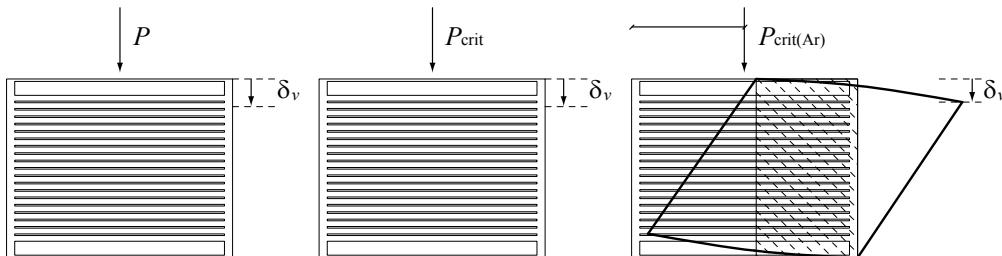
Figure 7. Behavior of the bearing under increasing load. From left to right, steps 1, 2 and 3.
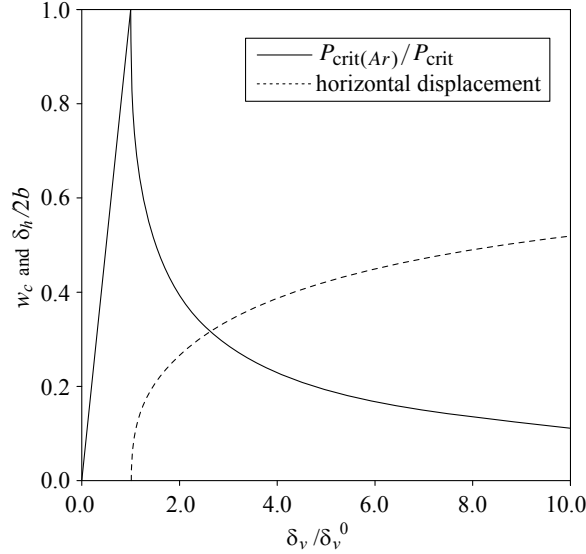
Figure 8. Critical load, horizontal and vertical displacement for an infinite strip bearing.

where I is the actual moment of inertia. The critical load in the undeformed configuration is given by

$$P_{\text{crit}}^0 = \frac{\sqrt{2}}{nt} \pi G A S r, \tag{5-3}$$

where the radius of gyration r equals $R/2$. The vertical stiffness of the bearing in the undeflected position is

$$K_v = \frac{E_c A}{nt}, \tag{5-4}$$

so the vertical displacement at the point of buckling is

$$\delta_v = \frac{\pi t}{3\sqrt{2}}. \tag{5-5}$$

As in the case of the strip, this depends only on the thickness of a single layer.

We can assume that (2-2) continues to hold for the circular bearing under lateral displacement and thus the connection between the geometric part of the vertical displacement and the horizontal deformation after buckling will be

$$\delta_v^G = \frac{\pi}{2\sqrt{2}} \frac{t}{R^2} \delta_h^2. \tag{5-6}$$

This is the form the relationship would take if the full circle is taken as the overlap area. When we apply (2-2) to the actual overlap area we need to assume that the horizontal displacement is large enough that some of the parameters of the circular area will need to be modified. For example the factor 6 in the expression for the compression modulus and the one third factor in the effective moment of inertia must be estimated and although we will use the correct shape factor of overlap area, we observe that the shape of the overlap area is intermediate between a strip and a circle and the two corresponding factors for the strip are 4 and 0.2, respectively. In this case then we will use 5 in the estimate of the compression modulus and 0.25 for the effective moment of inertia.
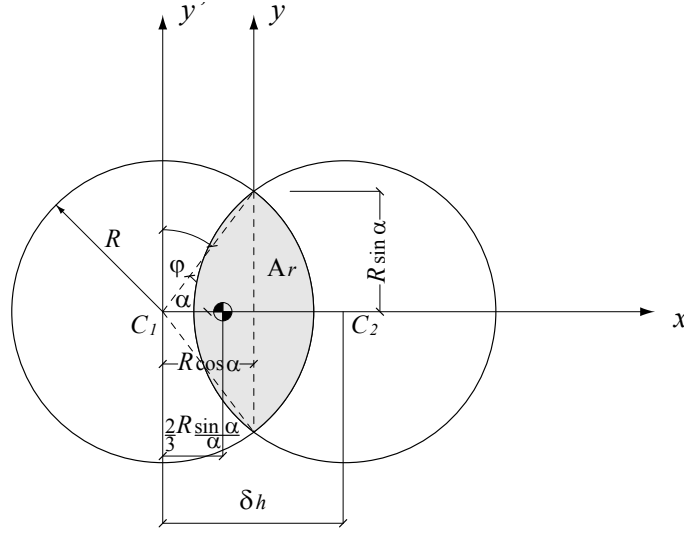
Figure 9. Exact calculation for the overlap area for circular bearing.

5.1. *Geometrical properties of overlap area.* The overlap area is given by twice the circular sector centered in the center of the circular bearing subtracted of a triangle as shown in Figure 9 and it is equal to $A_r = 2R^2(\alpha - \sin\alpha\cos\alpha)$. The horizontal displacement of the bearing, d_h, can be expressed as a function of α, in the form $2R\cos\alpha = \delta_h$, giving $\alpha = \arccos(\delta_h/2R)$, and since $\sin\alpha = \sqrt{1 - \cos^2\alpha}$, the overlap area becomes

$$A_r = 2R^2\left(\arccos x - x\sqrt{1-x^2}\right), \tag{5-7}$$

with $x = \delta_h/2R$, as plotted in Figure 10, left. In the absence of horizontal displacement ($\delta_h = 0$), we have $\arccos x = \pi/2$, and therefore it is useful to write

$$A_r = \pi R^2\left(\frac{2}{\pi}\arccos x - \frac{2}{\pi}x\sqrt{1-x^2}\right).$$

The overlap area length, l_r, is equal to twice $2R\arccos x$, so we can obtain the first shape factor S_r plotted in Figure 10, right, as the ratio between the loaded area and the forced-free area, given by

$$S_r = \frac{2R^2(\alpha - \sin\alpha\cos\alpha)}{4R\alpha t} = \frac{R}{2t}\left(1 - \frac{x\sqrt{1-x^2}}{\arccos x}\right). \tag{5-8}$$

5.2. *Moment of inertia.* The moment of inertia for a circular sector with area $R^2\alpha$ is

$$I_{\dot{y}\dot{y}} = \int_0^R \int_{-\alpha}^{\alpha} r\, dr\, d\theta\, (r\cos\theta)^2 = \tfrac{1}{4}R^4\left(\alpha + \tfrac{1}{2}\sin 2\alpha\right). \tag{5-9}$$

Transporting to the centroidal axis, this becomes

$$I_{yy} = \tfrac{1}{4}R^4\left(\alpha + \tfrac{1}{2}\sin 2\alpha\right) - R^2\alpha\left(\tfrac{2}{3}R\frac{\sin\alpha}{\alpha}\right)^2, \tag{5-10}$$

and then shifting to the center of the overlap area it becomes

$$I_{yy} = \frac{R^4}{4}\left(\arccos\left(\frac{\delta_h}{2R}\right)\left(1 + 4\cos^2\frac{\delta_h^2}{4R^2}\right) - \left(1 - \frac{\delta_h^2}{4R^2}\right)^{1/2}\frac{\delta_h}{2R}\right). \tag{5-11}$$

Now we take the moment of inertia of a triangle with base $2R\sin\alpha$ and height $R\cos\alpha$ (Figure 9), which is given by $I_{yy}^T = \frac{1}{6}R^4\sin\alpha\cos^3\alpha$, and we subtract it from I_{yy}. This leads to the moment of inertia for the overlap area A_r, given as a function of the lateral displacement by

$$I_{yy(\text{overlap})} = \frac{R^2}{2}\left(\arccos x(1 + 4x^2) - (1 - x^2)^{1/2}x\left(\tfrac{13}{3} + \tfrac{2}{3}x^2\right)\right). \tag{5-12}$$
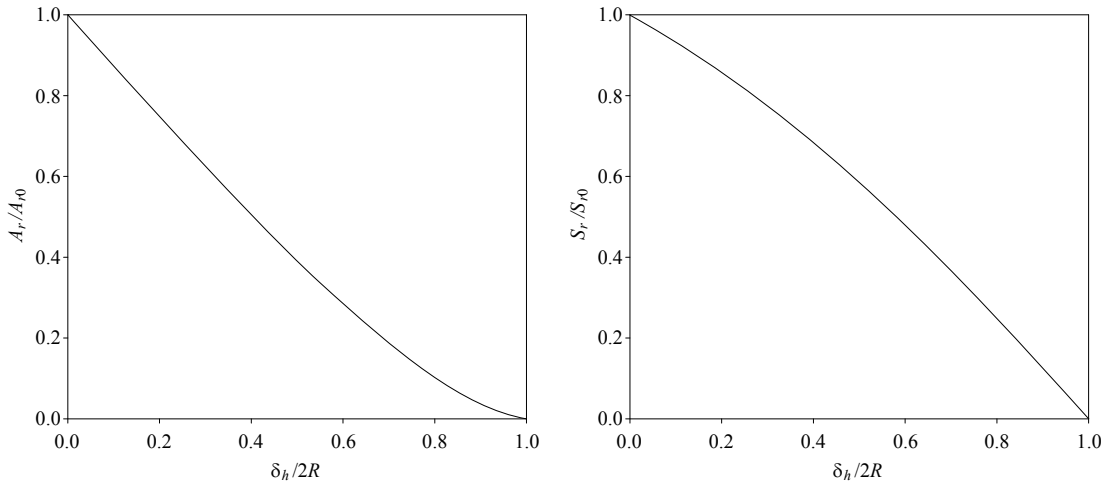

Figure 10. Left: overlap area for increasing lateral displacement. Right: first shape factor for the overlap area.
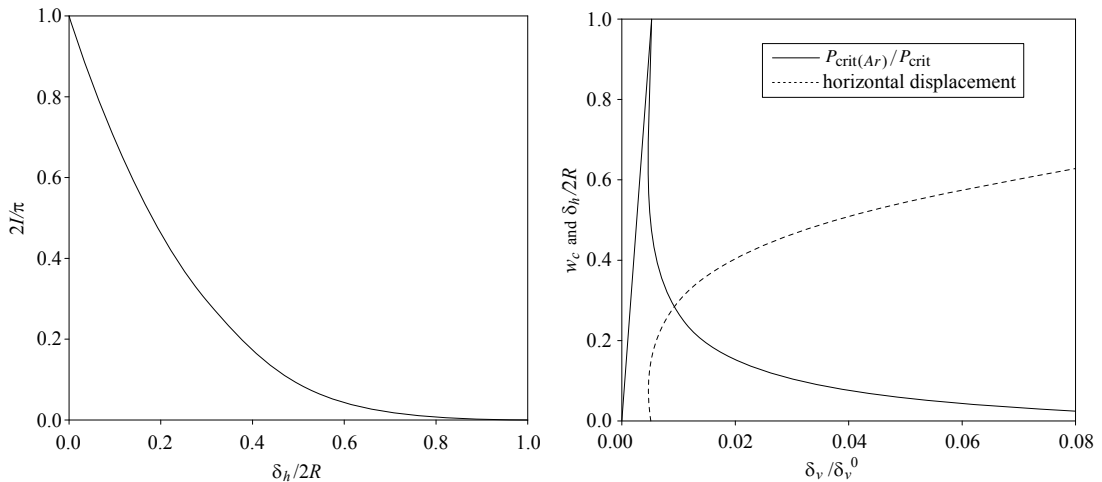

Figure 11. Left: moment of inertia of the overlap area against normalized horizontal displacement. Right: behavior of the bearing with real overlap area.

When the displacement is zero, the bearing is in the undeformed position, so $x = 0$ and $\alpha = \pi/2$, and the moment of inertia is that of a complete circle. On the other hand, when the bearing reaches its maximum horizontal displacement, equal to the diameter $2R$, we have $x = 1$ and $\alpha = 0$. Figure 11, left, shows the function $f(x) = 2I_{yy(\text{overlap})}/\pi$ for $0 < x < 1$.

5.3. *Vertical displacement.* The compression modulus can be approximated to $E_c = 5GS^2$ and the effective inertia to $I_{\text{eff}} = \frac{1}{4}I_{yy(\text{overlap})}$, so substituting the values in (2-2), the vertical displacement δ_v^G will be

$$\delta_v^G = R\alpha t\pi \sqrt{\frac{t_r}{5A_r I_{yy(\text{overlap})}h}}\, \delta_h^2. \tag{5-13}$$

To obtain the vertical displacement depending on the load when the bearing moves, we need the critical load on the reduced area, which is $P_{\text{crit}(A_r)} = (G\pi S/2t_r)\sqrt{5A_r I_{yy(\text{overlap})}}$. Thus

$$\delta_v^0 = \frac{P_{\text{crit}(A_r)}t_r}{E_c A_s} = \frac{\pi}{2}\frac{\sqrt{5A_r I_{yy(\text{overlap})}}\, t_r}{5SA_r h}. \tag{5-14}$$

Adding the two terms and simplifying, we get for the total vertical displacement the value

$$\delta_v^t = \delta_v^G + \delta_v^0 = \frac{\pi}{\sqrt{5A_r}}\left(R\alpha t\sqrt{\frac{t_r}{I_{yy(\text{overlap})}h}}\delta_h^2 + \frac{\sqrt{I_{yy(\text{overlap})}}\, t_r}{2h}\right). \tag{5-15}$$

The buckling and post-buckling behavior for the circular bearing with the properties of the overlap area exactly calculated is shown in Figure 11, right.

6. Conclusions

The theoretical analysis has provided estimates of the buckling behavior of bearings that are reinforced with a flexible fiber reinforcement and not bonded to the structure or the foundation. We have shown that the instability of this type of bearing is similar to that of classical imperfection sensitive instability with a buckling load that decreases very rapidly due to the negative infinity of the force displacement curve just after the buckling load is reached.

For example if the vertical displacement is increased to five times that at the point of buckling, the post-buckling load is only 20% of the buckling load. This suggests that this kind of bearing will have to be designed very conservatively. In real terms a bearing made of a rubber compound with a shear modulus $G = 0.70\,\text{MPa}$ (100 psi), a shape factor $S = b/t = 10$ and a second shape factor $S_2 = 2b/(nt) = 2$, the pressure at buckling according to (2-5) is $p_{\text{crit}} = P_{\text{crit}}/(2b) = 2\pi GS^2/(\sqrt{15}\,n)$, which equals $11.2\,\text{MPa}$ (1622 psi); this in turn means that the design pressure should be no more than $2.23\,\text{MPa}$ (325 psi). This is somewhat less than is used in steel reinforced bearings for large modern isolated buildings but will adequate for low-cost housing and especially for strip bearings supporting masonry wall buildings. We also note that the strip bearings will be arranged in orthogonal directions in the isolation layout as shown in Figure 2 and that only those bearings with their narrow direction in the direction of movement will buckle. In the long direction the bearings are very stable.

References

[Gent and Meinecke 1970] A. N. Gent and E. A. Meinecke, "Compression, bending and shear of bonded rubber blocks", *Polym. Eng. Sci.* **10** (1970), 48–53.

[Imbimbo and Kelly 1997] M. Imbimbo and J. M. Kelly, "Stability aspects of elastomeric isolators", *J. Earthquake Spectra* **13** (1997), 431–449.

[Kelly 1997] J. M. Kelly, *Buckling behaviour of elastomeric bearings in earthquake-resistant design with rubber*, 2nd ed., Springer, London, 1997.

[Kelly 1999] J. M. Kelly, "Analysis of fiber-reinforced elastomeric isolators", *J. Earthquake Eng.* **2** (1999), 19–34.

[Kelly 2002] J. M. Kelly, "Seismic isolation systems for developing countries", *J. Earthquake Spectra* **18** (2002), 1150–1157.

[Kelly 2003] J. M. Kelly, "Tension buckling in multilayer elastomeric bearings", *J. Eng. Mech.* **129** (2003), 1363–1368.

[Kelly and Takhirov 2002] J. M. Kelly and S. M. Takhirov, "Analytical and experimental study of fiber-reinforced strip isolators", Report 2002-11, Earthquake Engineering Research Center, University of California, Berkeley, 2002, available at http://nisee.berkeley.edu/elibrary/Text/1278634.

[Kelly and Takhirov 2004] J. M. Kelly and S. M. Takhirov, "Analytical and numerical study on buckling of elastomeric bearings with various shape factors", Report 2004-03, Earthquake Engineering Research Center, University of California, Berkeley, 2004, available at http://nisee.berkeley.edu/elibrary/Text/1293197.

[MARC 1988] *MARC General-purpose finite element program*, MARC Analysis Research Corporation, Palo Alto, CA, 1988.

[Marsico 2008] M. R. Marsico, *Seismic isolation and energy dissipation: theoretical basis and applications*, Ph.D. thesis, Università di Napoli Federico II, Napoli, 2008, available at http://tinyurl.com/MarsicoThesis-pdf.

[Marsico and Kelly 2009] M. R. Marsico and J. M. Kelly, "Stability and post-buckling behaviour in non-bolted elastomeric isolators", pp. no. 226 in *Proceedings of the XIII Italian Conference on Earthquake Engineering* (ANIDIS) (Bologna, 2009), 2009. On CD.

[Tsai and Kelly 2002] H. C. Tsai and J. M. Kelly, "Stiffness analysis of fiber-reinforced rectangular isolators", *J. Eng. Mech.* **128** (2002), 462–470.

[Tsai and Kelly 2005a] H. C. Tsai and J. M. Kelly, "Buckling load of seismic isolators affected by flexibility of reinforcement", *Int. J. Solids Struct.* **42** (2005), 255–269.

[Tsai and Kelly 2005b] H. C. Tsai and J. M. Kelly, "Buckling of short beams with warping effect included", *Int. J. Solids Struct.* **42** (2005), 239–253.

[UBC 2007] *Uniform Building Code*, International Code Council, 2007.

JAMES M. KELLY: jmkelly@berkeley.edu
Pacific Earthquake Engineering Research Center, University of California, Berkeley, 1301 South 46th Street Building 452, Richmond, CA 94804-4698, United States

MARIA ROSARIA MARSICO: m.r.marsico@bristol.ac.uk
Department of Mechanical Engineering, University of Bristol, Bristol, BS8 1TH, United Kingdom

DESIGN CRITERIA FOR ADDED DAMPERS AND SUPPORTING BRACES

GIUSEPPE LOMIENTO, NOEMI BONESSIO AND FRANCO BRAGA

The papers deals with the use of dissipative braces as retrofit solutions for existing moment resisting frame buildings. Braces are widely used in order to enhance performances of existing buildings under seismic loads, by adding stiffness and strength against inertial forces induced by earthquake ground motions. The braces can be equipped with supplemental dissipators in order to increase the overall energy dissipation capacity of the system and reduce stresses in the existing structures. In the present work, general design criteria for dampers and supporting braces are given and a simple design procedure based on the actual mechanical interaction between dampers and braces has been carried out. A number of design procedures have been proposed for dissipative bracing systems in frame structures. The procedures are often based on simplifying assumptions, due to the complexity of mechanical behavior of systems equipped with dissipative braces. Those assumptions make the procedures easier to use, but at the same time, less reliable in predicting the behavior of complex structures. In the present work, results are obtained without using two of the most common simplifying assumptions that neglect interaction between frame and braces: the use of the floor stiffness in order to characterize the frame behavior, and the use of equivalent systems with a single degree of freedom. The proposed design procedure has been tested on a moment resisting frame building and appears feasible for implementation on real structures.

1. Introduction

In recent years, many important changes in seismic codes are occurred. Most of the changes in the seismic design area derive from greater comprehension of actual poor buildings performances in recent earthquakes. Due to the renewed knowledge of the existing buildings behavior, retrofit of buildings is a paramount task in reducing seismic risk. New techniques for protecting buildings against earthquake have been developed with the aim of improving their capacity. Seismic isolation and energy dissipation are widely recognized as effective protection techniques for reaching the performance objectives of modern codes. However, many codes include design specifications for seismically isolated buildings, while there is still need of improved rules for energy dissipation protective systems. FEMA 356 [FEMA 2000] is one of the first prestandards that gives general criteria for the design of dissipative braces. According to this document, dissipative braces, added in a structure, should be able to ensure the necessary increment in stiffness for the protection in the Immediate Occupancy Performance and the necessary supplemental damping for the protection in the Life Safety Performance. However, design rules for specific devices (viscous, friction, steel devices) are still missing.

A large amount of research has been concerned with development of these innovative earthquake resistant systems. In many studies involving parametric analyses [Choi et al. 2003; Phocas and Pocanschi 2003; Whittaker et al. 2003a; 2003b; Wu and Ou 2003; Lin and Chopra 2002; Goel 2000; 2001; Singh

and Moreschi 2001; Pekcan and Chen 1999; Shukla and Datta 1999; Fu and Kasai 1998] and design procedures [Park and Min 2004; Lee et al. 2004; Moreschi and Singh 2003; Singh and Moreschi 2002; Garcia 2001; Levy et al. 2000; Fu and Cherry 2000; Yamada 2000; Takewaki 1999; Gluck et al. 1997; Ciampi 1993; Filiatrault and Cherry 1990], the structure, equipped with braces and dampers, is modeled as a simple mechanical system. This approach leads to a significant reduction of the complexity of the problem that has to be solved for evaluating the response of the system, but at the same time it leads to approximations, in some cases not acceptable, in the assessment of the behavior of the actual system.

In this paper, two of the most common simplifications that neglect interaction between frame and braces have been analyzed and their effects on the evaluation of the actual behavior of structural systems have been quantified. The study has been conducted on systems that can be modeled as viscoelastic components according to FEMA 356. The proposed design procedure for dissipative braces uses the results of a parametric study considering the actual interaction between frame and different types of dissipative braces and has been validated on a seven-storey frame building through non linear numerical analyses.

2. Problem statement

The analyzed structural systems are the moment resisting frames that are typical systems for the modern building and well suited to be protected with braces equipped with dissipative braces. Only limited damages are tolerated on the frames so the structures are expected to remain in the elastic range. For this reason the frames are modeled in order to perform with a linear-viscous-elastic behavior.

2A. *Frame without braces.* The dynamic characteristic of the frames, subjected to external forces, is formulated for structures discretized with a finite number of degrees of freedom (DOFs) and defined in term of generalized displacements of the nodes. The equation of the motion for a generic elastic multiple degree of freedom (MDOF) frame structure is

$$m_s \ddot{u}(t) + c_s \dot{u}(t) + k_s u(t) = p(t) \tag{2-1}$$

where m_s, c_s and k_s are the mass, damping and stiffness matrices of the frame structure without braces, respectively, u is the displacement vector, t is the time variable and p is the external force vector.

The following assumptions are generally accepted in design of frames subjected to seismic forces:

  (i) Each floor is assumed to be rigid in its own plane.

 (ii) A mass lumped matrix is used to describe inertial effects.

(iii) Structural damping is expressed as a function of the mass and stiffness matrices (*classical damping*).

Assumption (i) is generally appropriate for reinforced concrete buildings with floor slabs or in steel frame buildings with steel floor bracings; assumption (ii) is generally accepted for multi-storey buildings, in which the greater amount of mass is at the floor levels; assumption (iii) permits to neglect the terms related to the viscous forces and to consider only mass and stiffness proportional terms. Under those assumptions, the dynamic problem can be reduced to a smaller one by relating certain degrees of freedom to certain others by means of constraint equations and considering only the mass and stiffness terms. With

this aim in mind, (2-1) can be written as

$$\begin{bmatrix} m_{s,tt} & 0 \\ 0 & 0 \end{bmatrix} \begin{bmatrix} \ddot{u}_t(t) \\ \ddot{u}_0(t) \end{bmatrix} + \begin{bmatrix} k_{s,tt} & k_{s,t0} \\ k_{s,0t} & k_{s,00} \end{bmatrix} \begin{bmatrix} u_t(t) \\ u_0(t) \end{bmatrix} = \begin{bmatrix} p_t(t) \\ 0 \end{bmatrix}, \tag{2-2}$$

where u_t and u_0 denote the displacements along DOFs with mass (dynamic DOFs) and with zero mass, respectively, and p_t are the external dynamic forces acting on the frame.

The displacement vector partition introduced in (2-2) leads to the equation

$$m_{s,tt}\ddot{u}_t(t) + \hat{k}_{s,tt}u_t(t) = p_t(t), \tag{2-3}$$

where $\hat{k}_{s,tt}$ is the condensed stiffness matrix of the frame defined as

$$\hat{k}_{s,tt} = k_{s,tt} - k_{s,0t}^T k_{s,00}^{-1} k_{s,0t}. \tag{2-4}$$

2B. *Frame with braces.* Following the same approach presented in the previous section, for the system composed by frame and braces the equation of motion could be expressed as

$$\begin{bmatrix} m_{s+b,tt} & 0 \\ 0 & 0 \end{bmatrix} \begin{bmatrix} \ddot{u}_t(t) \\ \ddot{u}_0(t) \end{bmatrix} + \begin{bmatrix} k_{s+b,tt} & k_{s+b,t0} \\ k_{s+b,0t} & k_{s+b,00} \end{bmatrix} \begin{bmatrix} u_t(t) \\ u_0(t) \end{bmatrix} = \begin{bmatrix} p_t(t) \\ 0 \end{bmatrix}, \tag{2-5}$$

where $m_{s+b} = m_s + m_b$ is the system mass matrix given by the sum of the frame mass matrix m_s and the braces mass matrix m_b, and $k_{s+b} = k_s + k_b$ is the system stiffness matrix given by the sum of the frame stiffness matrix k_s and the braces stiffness matrix k_b.

Considering (2-5), the static condensation of this system leads to the equation

$$m_{s+b,tt}\ddot{u}_t(t) + \hat{k}_{s+b,tt}u_t(t) = p_t(t), \tag{2-6}$$

where $\hat{k}_{s+b,tt}$ is the condensed stiffness matrix of the frame defined as

$$\hat{k}_{s+b,tt} = k_{s+b,tt} - k_{s+b,0t}^T k_{s+b,00}^{-1} k_{s+b,0t}. \tag{2-7}$$

From (2-5), the displacement vector associated to the DOFs with zero mass can be evaluated through the expression

$$u_0(t) = -k_{s+b,00}^{-1} k_{s+b,0t} u_t(t). \tag{2-8}$$

3. Interaction between frame and braces

Two of the most common assumptions used in design procedures and parametric studies of braces systems assume that (1) each floor of the frame is characterized by a floor stiffness, and (2) the frame can be reduced to an equivalent system with a single degree of freedom. According to the first assumption, the storey drift is function of the shear forces induced by horizontal seismic loads. Generally, this assumption leads to two possible model simplifications:

(1a) The shear-type floor stiffness is obtained imposing that flexural and shear deformations of the beams and axial deformations of the columns are null. This case will be referred as "shear-type" floor stiffness $k_{s,st}$.

(1b) The shear-type floor stiffness is obtained as the ratio between shear forces and storey drift displacements computed on the frame under known horizontal forces, without imposing null deformations. This case will be referred as "equivalent shear-type" floor stiffness, related to the condensed stiffness matrix of the frame without braces $\hat{k}_s$.

For the second assumption, the fundamental mode shape is used in order to reduce the multiple degree of freedom (MDOF) model to a single degree of freedom (SDOF) model. Both assumptions are not able to describe the actual interaction between the frame and braces but are commonly used to reduce the complexity of the problem to be solved and generally accepted for analyzing frames equipped with dissipative braces. Their validity is questionable when the actual system behavior becomes more complex, i.e., when the braces have a stiffness comparable to the frame elements stiffness and the building modifies the shape of its fundamental vibration modes after the insertion of the braces.

3A. *Floor stiffness assumption.* The use of the floor stiffness instead of the whole stiffness matrix is based on the assumption that the braces have no effects on the stiffness of the storey in which they are installed. In this case the floor stiffness of the frame can be added to the stiffness of the braces to evaluate the whole floor stiffness. It is clear, however, that the interaction between frame and braces modifies the frame behavior. The stiffness of each floor is, in fact, influenced by the braces as a function of k_b and k_s. The force vector $p_s(t)$, carried only by the frame for a given displacement vector $u(t)$, can be obtained as

$$\begin{bmatrix} k_{s,tt} & k_{s,t0} \\ k_{s,0t} & k_{s,00} \end{bmatrix} \begin{bmatrix} u_t(t) \\ u_0(t) \end{bmatrix} = \begin{bmatrix} p_{s,t}(t) \\ p_{s,t}(t) \end{bmatrix}. \tag{3-1}$$

Considering that $u_0(t)$ is given by (2-8), this equation can be replaced by

$$\hat{k}_{s*,tt} u_t(t) = p_{s,t}. \tag{3-2}$$

where the condensed stiffness matrix of the frame when the braces are installed is defined as

$$\hat{k}_{s*,tt} = k_{s,tt} - k_{s,0t}^T k_{s+b,00}^{-1} k_{s+b,0t}. \tag{3-3}$$

Similarly, the force vector $p_b(t)$, carried only by the braces for a given displacement vector $u(t)$, can be obtained as

$$\begin{bmatrix} k_{b,tt} & k_{b,t0} \\ k_{b,0t} & k_{b,00} \end{bmatrix} \begin{bmatrix} u_t(t) \\ u_0(t) \end{bmatrix} = \begin{bmatrix} p_{b,t}(t) \\ p_{b,t}(t) \end{bmatrix}, \tag{3-4}$$

where the condensed stiffness matrix of the braces is defined as

$$\hat{k}_{b,tt} = k_{b,tt} - k_{b,0t}^T k_{s+b,00}^{-1} k_{s+b,0t}. \tag{3-5}$$

The condensed stiffness matrices given by (2-4) and (3-3) represent the stiffness of the same frame when no braces are installed and when the braces are installed, respectively. A comparison between those equations indicates that the presence of braces provides a variation in the condensed stiffness matrix of the frame. The variation is expressed as

$$\Delta\hat{k}_{s,tt} = \hat{k}_{s*,tt} - \hat{k}_{s,tt} = k_{s,0t}^T \left(k_{s,00}^{-1} k_{s,0t} - k_{s+b,00}^{-1} k_{s+b,0t} \right). \tag{3-6}$$

In addition, the condensed stiffness matrix of the braces, given by (3-5), includes the terms $k_{s+b,00}$ and $k_{s+b,0t}$ function of the frame stiffness. The interaction between frame stiffness and brace performance is
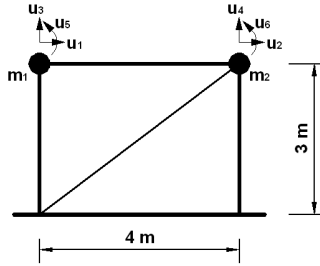
Figure 1. One-bay frame case study.

	EA	EI	GA_s
Beam	4.50×10^6 kN	1.13×10^6 kNm²	1.44×10^6 kN
Columns	2.70×10^6 kN	2.43×10^5 kNm²	8.64×10^5 kN
Brace	8.64×10^5 kN		

Table 1. Mechanical characteristics of the one-bay frame case study.

then to be expected. The floor and brace stiffnesses, computed separately, can be added only accepting an error in the final estimate of the whole floor-stiffness. In the following example, the interaction between the frame and brace stiffnesses has been studied for a simple one bay frame with a diagonal brace. A planar frame, with masses lumped at the column-beam joints and a steel brace with circular section pinned to the frame, was analyzed as first case study (Figure 1).

The mass of the brace is assumed to be negligible and inertial effects due to the ground motion are considered only in the horizontal direction. Seismic action on the frame have been described as equivalent horizontal static forces applied to the joints and the mechanical characteristics of the components are reported in Table 1, where A is the sectional area of the element, I is the moment of inertia, A_s is the shear area, E is the longitudinal elastic modulus and G is the shear elastic modulus. The variation of each stiffness contribution is reported in Figure 2 as a function of the cross sectional area of the brace A_b normalized to the reference area reported in Table 1. The reference area has been chosen in

Figure 2. Stiffness components versus brace sectional area A_b.

order to represent a quite usual situation in steel frame protected by braces, corresponding to a brace stiffness approximatively two times higher than the frame stiffness versus horizontal forces. From the graph, it is evident that the stiffness $k_{s,st}$ overestimates of approximatively 30% $\hat{k}_s$. Moreover, the actual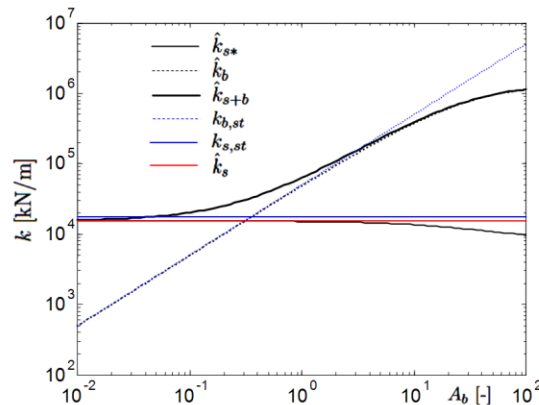 stiffness of the frame $\hat{k}_{s*}$ is affected by the presence of the brace and for $A_b = 1$ the stiffness reduction is approximatively 15% of the stiffness of the frame without brace $\hat{k}_s$. The frame stiffness reduction increases with the sectional area of the brace. For $A_b = 10$ the stiffness reduction of the frame is around 50%. Finally, the stiffness of the brace is also influenced by the interaction with the frame. For $A_b = 1$ the interaction produces a reduction of the brace stiffness $\hat{k}_b$ approximatively equal to 5% of its theoretical "shear-type" stiffness $k_{b,st}$, linearly increasing with A_b. For $A_b = 10$ the interaction produces a brace stiffness reduction of almost 90%.

To express the interaction between brace and frame, an index R was defined as

$$R = \frac{i^T p_{s,t}}{i^T p_t},$$ (3-7)

where i is the dynamic coupling vector composed by unit-components in the earthquake direction and null-components in the other directions, $p_{s,t}$ is the portion of the force vector carried by the frame, as derived from (3-2), and p_t is the force vector acting on the whole system composed by frame and braces. Index R represents the ratio between the shear forces acting on the frame and the shear forces acting on the overall system, under a fixed displacement. It expresses the ratio between the floor stiffness of the frame and the floor stiffness of the whole system. For the case study of Figure 1, the index R is presented in Figure 3 as a function of the braces cross sectional area A_b. The graph shows how the stiffness of the overall braced frame is shared between the frame and the brace. As the area A_b of the brace increase, brace stiffness becomes the contribute more important to the whole stiffness while frame stiffness becomes less significant ($R \rightarrow 0$). Let us note that the R is strongly not linear, versus A_b, due to the interaction between frame and brace. By using the floor stiffness assumption a linear trend for R would instead be assumed. In the middle range of the horizontal axis, say $0.1 \leq A_b \leq 5$, corresponding to usual brace stiffness values varying between 0.1 and 10 times the frame stiffness, the curve trend is approximatively linear, meaning that the forces carried by the frame decrease with the logarithm of the sectional area A_b of the brace and not linearly with the area A_b, as expected according to the floor stiffness assumption.
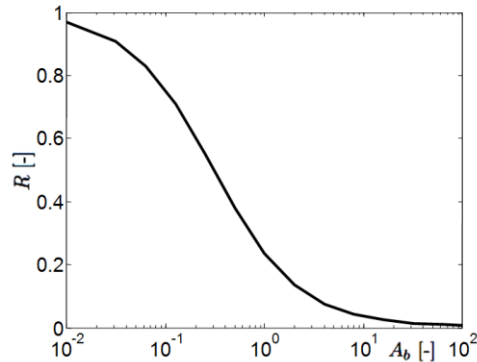
Figure 3. Index R versus brace sectional area A_b.
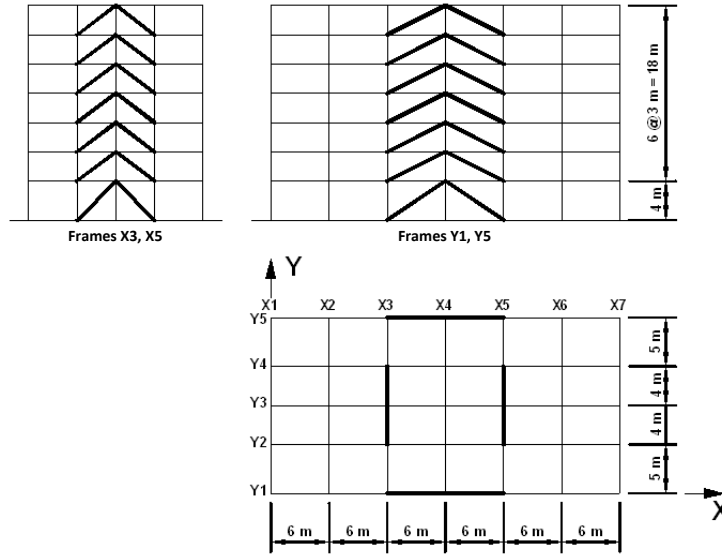
Figure 4. MDOF frame case study.

3B. *Equivalent SDOF system assumption.* Equivalent SDOF systems are used for reducing the complexity of the mechanical problem to be solved. A MDOF system can be reduced to an equivalent SDOF system assuming that its deformed shape is known under dynamic forces applied. In this case, mechanical parameters, describing the mechanical behavior of the system, are reduced to its fundamental vibration period T_s and damping ratio ξ_s. By using this simplification, effects of dissipative braces on the behavior of the SDOF system are easy to be quantified. They generally introduce a reduction of the vibration period, due to the increment of stiffness, from the value T_s to the value T_{s+b}, as well as the increment of the damping ratio, due to added energy dissipation capacity, from the value ξ_s to the value ξ_{s+b}. However the equivalent SDOF system can not describe the actual interaction between the frame structure and the bracing system, as shown as an example in the next case study. The 7-storey frame building, shown in Figure 4, was analyzed. The mechanical characteristics of the frame are listed in Table 2. Inertial forces are considered only in the horizontal directions and each floor is assumed to perform as a rigid diaphragm. Forces acting in the y direction were considered and the following linear path of seismic forces used was

$$p_t = F \frac{m_{s+b}h}{i^T m_{s+b}h} = \phi_p F, \tag{3-8}$$

	EA	EI	GA_s
Lateral and longitudinal beams	4.50×10^6 kN	1.13×10^6 kNm^2	1.44×10^6 kN
Internal transversal beams	4.32×10^6 kN	2.49×10^5 kNm^2	1.38×10^6 kN
Columns	6.30×10^6 kN	3.09×10^6 kNm^2	2.02×10^6 kN
Braces	2.36×10^8 kN		

Table 2. Mechanical characteristics of the MDOF frame case study.

where F is the total seismic force entity, h is a vector containing the heights of each floor, measured from the foundation level, and ϕ_p is the vector expressing the seismic force distribution. As described before, interaction effects are captured by R index. For the forces of (3-8) the following expression of R is obtained from (3-7) and considering (2-6) and (3-2):

$$R = \frac{i^T \hat{k}_{s*,tt} \hat{k}_{s+b,tt}^{-1} \phi_p}{i^T \phi_p}. \tag{3-9}$$

Note that R depends only on the shape of the seismic forces path and not on their amplitude. For the selected case study, index $R = 19.6\%$ indicates that the frame stiffness to the overall structural stiffness is 19.6%. Reduction of the MDOF system to an equivalent SDOF system overestimates this contribution. Since the total mass variation due to braces is neglected, for the equivalent SDOF system, the contribution of the frame stiffness to the whole system stiffness is given by

$$\left(\frac{T_s}{T_{s+b}}\right)^2 = \frac{k_s}{k_{s+b}} = 23.3\%. \tag{3-10}$$

with $T_{s+b} = 0.882\,\mathrm{s}$ the fundamental vibration period of the whole system, $T_s = 1.826\,\mathrm{s}$ the fundamental vibration period of the frame without braces and k_s, k_{s+b} the SDOF equivalent stiffnesses for the frame with no braces and with braces, respectively. For the selected case study, the frame stiffness contribution computed using the SDOF assumption in (3-10) appears about 1.19 times the effective one, computed with (3-9). By using the reduction to a SDOF system, the portion of seismic forces carried by the frame is hence overestimated by 19%.

4. Interaction between brace and damper

Dissipative braces are commonly applied to structure as integral devices that exhibit both functions of stiffnesses and energy dissipators in a single mechanical system as well as combination of different devices with different functional contribution. Both configurations will be referred here as dissipative braces, while the energy dissipation capabilities will be associated to elements generically defined as dampers to be intended as single units as well as components of integral devices. In dissipative bracing system, the interaction between the brace and the additional damping effects has to be considered. To evaluate this interaction, devices characterized by the following behaviors have been considered: viscous linear (VL), viscous nonlinear (VN), viscous elastic (VE), elastoplastic (EP), and friction (FR). The selected behaviors cover the most common typologies of dampers used for protection of frame buildings. It is clear that the installation of generic damper devices reduces the stiffness of the brace. Total strains in each dissipative brace are obtained as the sum of strains in the brace and strains in the damper. Accordingly, the R index evaluated for the structure with only the braces, is always not lower than the one computed for the dissipative bracing system R_d by means of (3-7). The portion of total seismic forces carried by the frame is, in fact, greater if there are dampers installed. This loss of efficiency, in terms of stiffness, for the braces alone can be quantified by the ratio

$$F_R = \frac{R_d}{R} \leq 1. \tag{4-1}$$

The larger the loss of efficiency of the braces due to the deformability of the dampers, the smaller is the parameter F_R.

The second effect of the addition of the dampers is the reduction of seismic forces acting on the whole system due to added energy dissipation capacity. The seismic force vector should be reduced due to higher dissipation capacity of the system. An important issue is the evaluation of the effective dissipation capacity of dissipative braces. It is evident also that the dissipated energy in dampers depends on the stiffness of the supporting braces. For a given damper, the maximum amount of dissipated energy is obtained if the supporting brace has null deformability. In this case, total strains in the dissipative brace affect the dampers performance and produce energy dissipation. The energy dissipation capacity is expressed in terms of equivalent damping ratio, evaluated for stationary oscillations as

$$\xi_{s+b} = \frac{1}{4\pi} \frac{E_d}{E_s} \frac{\omega_{s+b}}{\omega}, \tag{4-2}$$

where E_d is the dissipated energy in the deformation cycle, E_s is the maximum strain energy, ω is the circular frequency of the deformation cycle and ω_{s+b} is the equivalent circular frequency of the system composed by the structure and the braces, defined as

$$\omega_{s+b} = \sqrt{\frac{i^t p_{t,\max}}{i^t m_{s+b} u_{\max}}}, \tag{4-3}$$

where $p_{t,\max}$ is the force vector corresponding to the maximum displacement vector $u_{\max}$.

By using (4-2) and (4-3), the maximum equivalent damping ratio ξ_{s+d} can be computed assuming supporting braces of infinite stiffness. The ratio ξ_{s+d} results always greater than the effective damping ratio of the system ξ_{s+b} evaluated for braces with finite stiffness. Accordingly, the quantity

$$\xi_d = \xi_{s+d} - \xi_s \tag{4-4}$$

represents the maximum damping ratio that the given dampers can add to the original damping ratio ξ_s of the structure, while the actual damping ratio added by the dissipative braces is given by

$$\xi_b = \xi_{s+b} - \xi_s. \tag{4-5}$$

If the phenomenon of interaction between bracing effects and dissipation of energy is considered in terms of damping contribution, it is evident that braces make the dampers less efficient in supporting seismic forces because they reduce their energy dissipation capacity. This loss of efficiency, in terms of damping, can be quantified by the ratio

$$F_\xi = \frac{\xi_b}{\xi_d} \le 1. \tag{4-6}$$

The larger is the loss of efficiency of the dampers due to deformability of the braces, the smaller is the parameter F_ξ.

In Figures 5–9, the variation of R_d, F_R and ξ_{s+b}, F_ξ are represented versus R for different values of ξ_d with the aim of describing the loss of efficiency in terms of stiffness and in terms of damping, respectively. On the abscissa, lower values of R represent stiffer supporting braces, while $R = 1$ represents the frame without braces. The dampers mechanical characteristics have been chosen in order to obtain values of the maximum added damping ratio ξ_d in the range 0.05–0.25. For the damping exponent of the VN
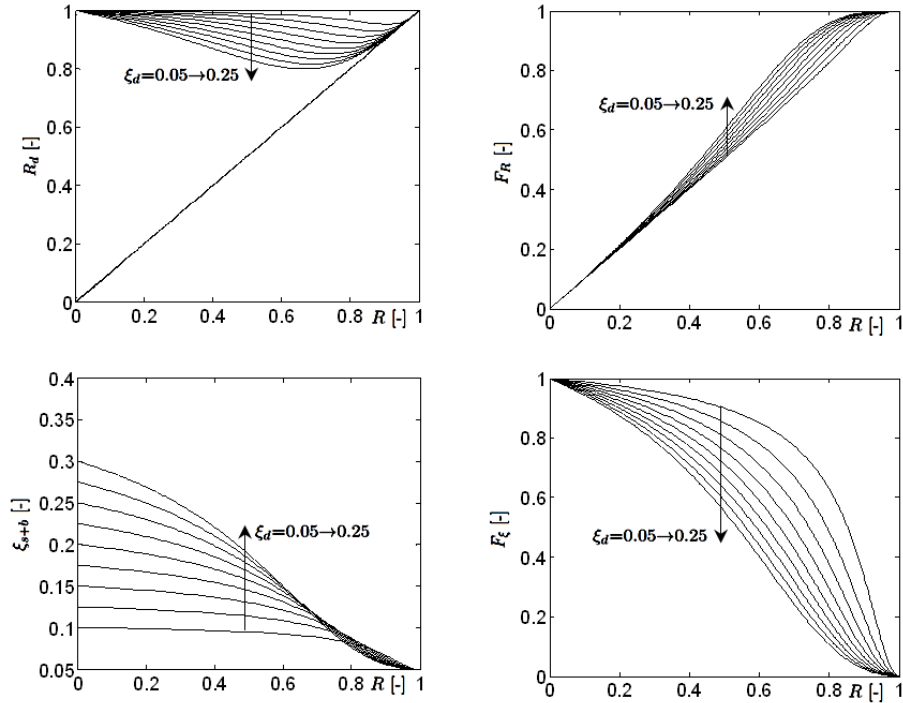
Figure 5. Variation of R_d, F_R. ξ_{s+b}, and F_ξ with R ($\xi_d = 0.05$–0.25) for VL dampers.
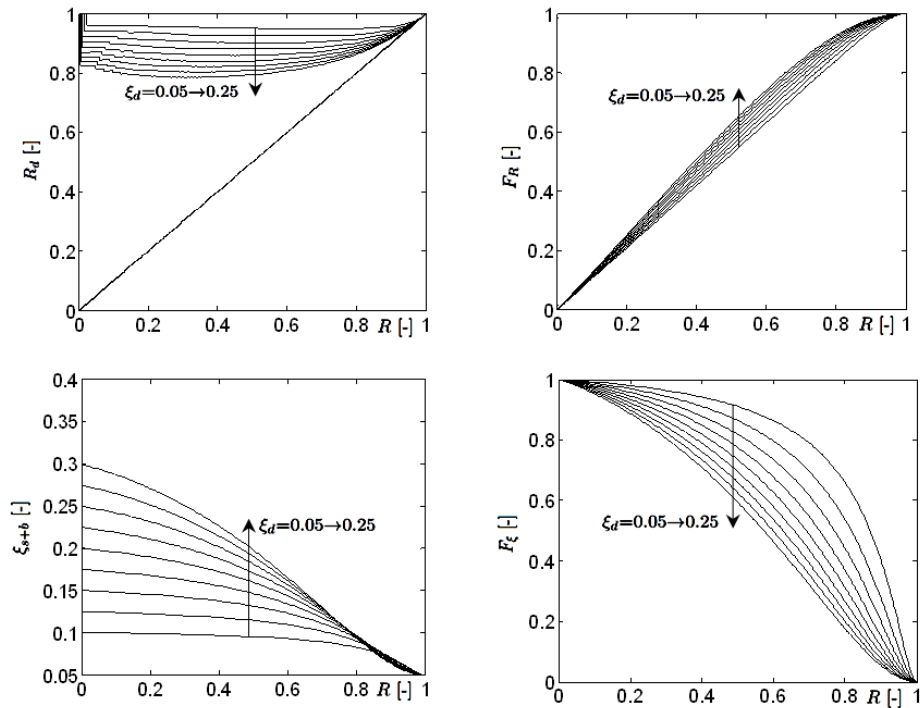
Figure 6. Variation of R_d, F_R. ξ_{s+b}, and F_ξ with R ($\xi_d = 0.05$–0.25) for VN dampers.
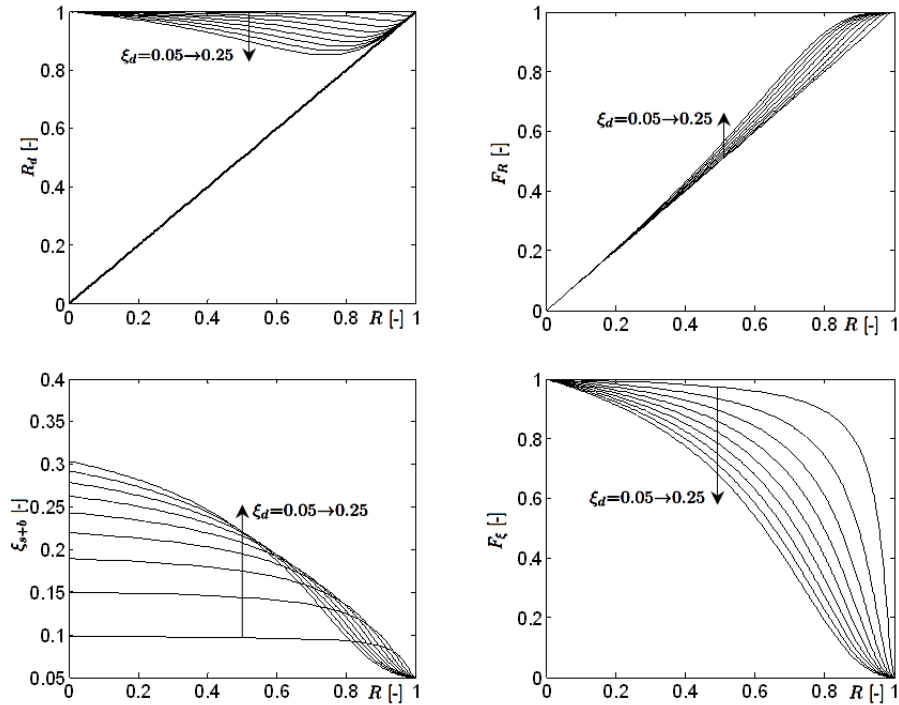
Figure 7. Variation of R_d, F_R. ξ_{s+b}, and F_ξ with R ($\xi_d = 0.05$–0.25) for VE dampers.
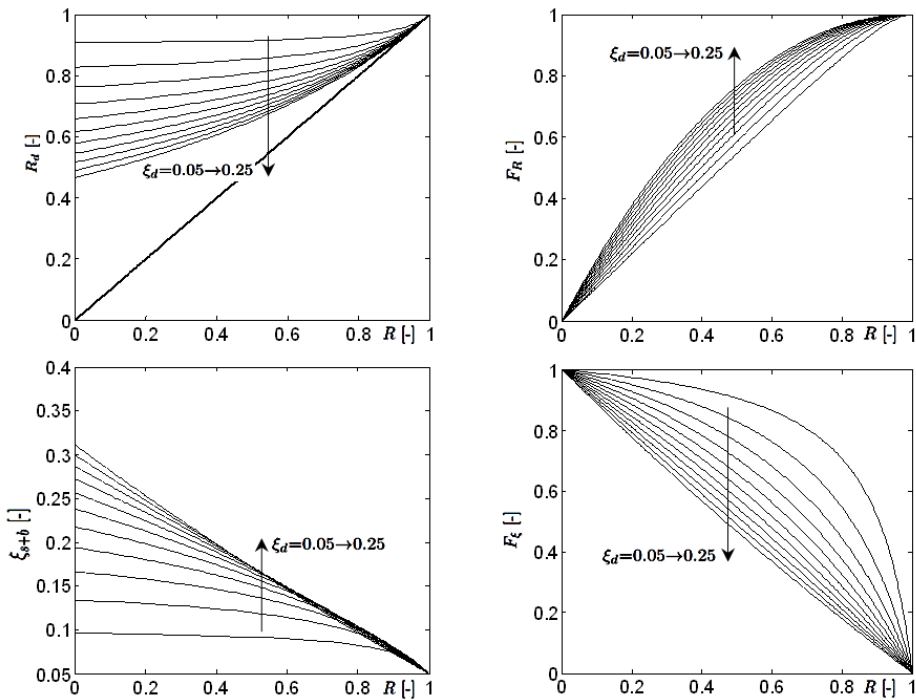
Figure 8. Variation of R_d, F_R. ξ_{s+b}, and F_ξ with R ($\xi_d = 0.05$–0.25) for EP dampers.
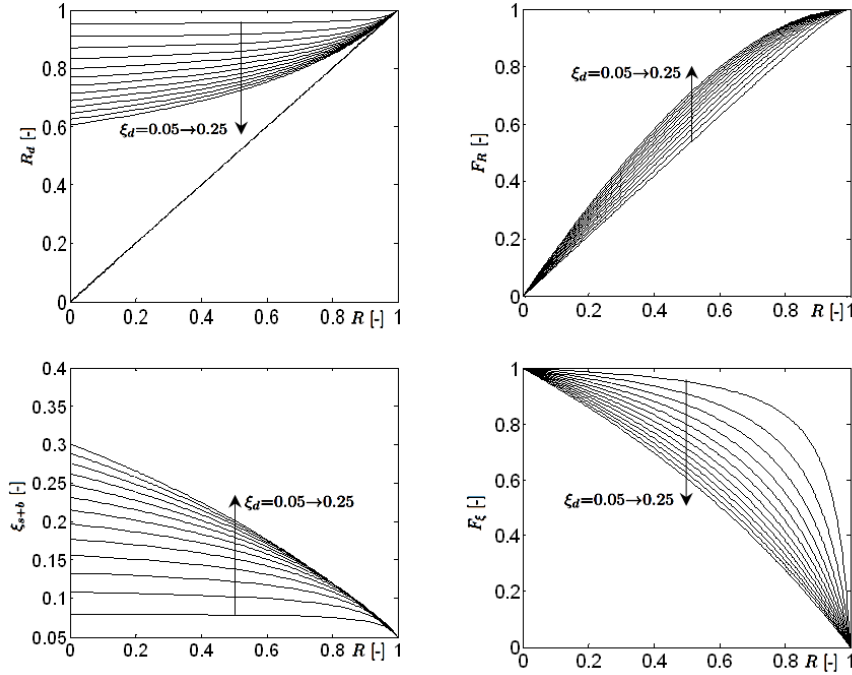
Figure 9. Variation of R_d, F_R, ξ_{s+b}, and F_ξ with R ($\xi_d = 0.05$–0.25) for FR dampers.

dampers the value $\alpha = 0.15$ was considered, for VE dampers a loss factor $\eta_L = 0.80$ was assumed and for the EP dampers the hardening ratio of $\beta = 0.01$ was used.

From these figures, it is evident that the losses of efficiency in terms of stiffness and damping act in a different way. Factor F_R shows that the greater losses of efficiency occurs at low values of R, (stiffer braces), and at low values of ξ_d (for less dissipative dampers). On the other side, factor F_ξ shows that the greater losses of efficiency occur for higher values of R (smaller braces), and for higher values of ξ_d (for more dissipative dampers). For supporting braces with the same stiffness of the frame ($R = 0.5$) and for a damping ratio $\xi_{s+b} = 0.30$, losses of stiffness of 64%, 58%, 78%, 24%, and 40% were experienced due to the insertion of damper types VL, VN, VE, EP, and FR, respectively. EP dampers are then preferable when higher stiffness increments are needed while VE dampers are most indicated for lower increments of stiffness. For supporting braces with $R = 0.5$ and with an additional damping $\xi_d = 0.25$, losses of damping of 33%, 30%, 23%, 40%, and 27% correspond to types VL, VN, VE, EP, and FR, respectively. VE dampers are then less affected by the brace stiffness while EP require very stiff supporting braces in order to ensure their dissipation capacity. The previously defined factors could be combined in a factor describing the global efficiency of the braces:

$$F(R, \xi_d) = F_R(R, \xi_d) \times F_\xi(R, \xi_d).$$ (4-7)

The factor F describes losses of efficiency in terms of both stiffness and damping: dissipative braces with greater values of F are the most efficient both for stiffness and damping. As an example, the left part of Figure 10 shows the F factor versus R index for braces equipped with VL dampers. Values of F factor are always lower than unity. In the presented case, maximum value of F is equal to 0.55 for a R
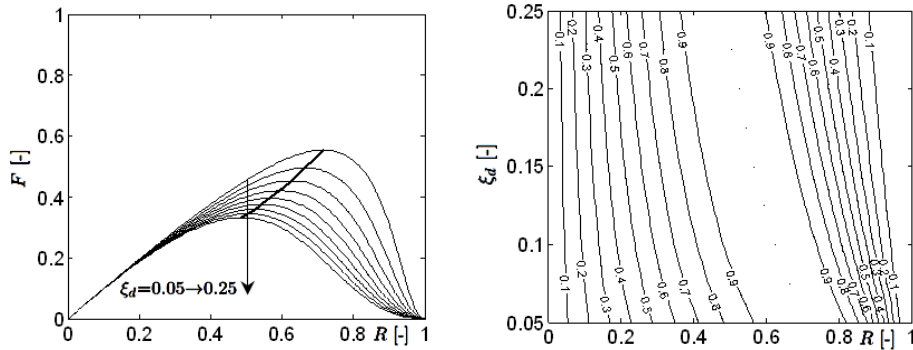
Figure 10. Variation of F with R (left) and contour levels of F^* in the plane R-ξ_d for VL dampers.

value of approximately 0.7. The solid line represents the maximum values of F factor for values of the damping ratio ranging from 0.05 to 0.25.

To assign the value of 1 to the most efficient case (maximum F) a normalization procedure was applied:

$$F^*(R, \xi_d) = \frac{F(R, \xi_d)}{\max\big(F_\xi(R, \xi_d)\big)} \leq 1. \tag{4-8}$$

Figure 10, right, shows the dependence of F^* on R and ξ_d using by contour levels. In the area between the two curves labeled 0.9, the maximum efficiency both in terms of stiffness and damping selection is achieved. Maximum efficiency is observed for the range of damping values 0.05–0.25 centered on different values of R, expressing the stiffness contribution to the total stiffness of the frame alone. It can be observed that, for instance, for a value of ξ_d equal to 0.05 (limited additional damping) the center of the efficiency band corresponds to R approximately equal to 0.7. This scenario indicates that a limited damping addition is particularly beneficial for frames quite stiff originally with limited contribution of the braces to the total stiffness. For larger introduced dissipation capability ($\xi_d = 0.25$) the efficiency is maximized for frames where braces contribute about 50% of the total stiffness. An increase or reduction of additional stiffness reduces the efficiency of the overall system.

Similar charts can be obtained for all the selected damper typologies and could indicate variations of the location of the maximum efficiency range. Figure 11 reports the maximum efficiency range
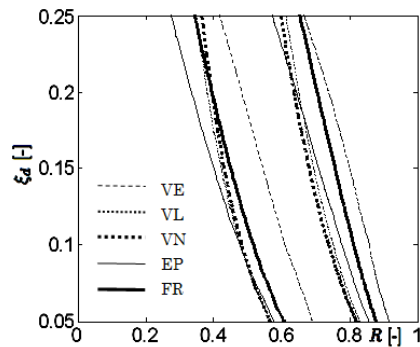
Figure 11. Contour levels corresponding to $F^* = 0.90$ in the plane R-ξ_d.

($F^* = 0.90$) for all the damper types considered. These charts provide useful information for the design and selection of dissipative braces.

5. Design procedure

This section shows how the presented charts can be used for the design of bracing systems. The proposed design procedure essentially follows five steps:

Step 1. Selection of the performance requirements (performance level and reference seismic action).

Step 2. Selection of the target damping level and reduction of the seismic action. The damping level is expressed by the damping ratio ξ_{s+b} for the whole system.

Step 3. Design of elastic braces. For the elastic bracing system, a vector containing R indices computed by (3-7) is evaluated for each level of the frame in order to quantify the interaction between the frame and the bracing system.

Step 4. Choice of characteristics of dissipative braces. The characteristics of dissipative braces depend on the R values selected at Step 3 and on the design charts presented in Figure 12.

Step 5. Validation of the design solution. The behavior of the system composed by the frame and the dissipative braces is studied through non linear analyses in order to verify that the performance requirements are satisfied.

As an example of the procedure application and validity, the 7-storey frame of Figure 4 is considered. The system has four diagonal bracings for each direction. The procedure is applied as described below.

Step A1. Performance requirements are statements of acceptable performance of the structure. The performance target can be specified as limits on any response parameter such as stresses, strains, displacements, accelerations. In the case study, target inter-storey drifts of 0.3% are considered, assuming that the frame should remain elastic under the design seismic action. The elastic spectrum Type 1 given by Eurocode 8 [CEN 2004] for ground type A, with ground acceleration equal to ag=0.35g, is assumed in the design. Seven ground motions were selected by means of specialized software [Gasparini and Vanmarcke 1976] in order to obtain an average acceleration spectrum matching the elastic design spectrum, in accordance with Eurocode 8.

Step A2. The damping ratio $\xi_{s+b} = 0.20$ is chosen as target damping level for the frame equipped with dissipative braces. According to Eurocode 8, the spectrum reduction factor which takes into account damping is $\eta = 0.63$.

Step A3. An elastic bracing system has been designed to ensure compliance with target inter-storey drifts. At each floor level all the braces have the same geometrical characteristics. The vector containing the R indices of the braces, at each floor level, from the bottom to the top of the building, is

$$R = [0.92 \ 0.81 \ 0.86 \ 0.86 \ 0.89 \ 1.00 \ 1.00].$$

Note that for the two upper levels no braces are necessary in order to satisfy the performance requirements ($R = 1.00$).

Step A4. The dissipative braces at each level will have $R_d = R$ and they must provide an additional damping in order to obtain the target damping ratio ξ_{s+b} for the whole system. The supplemental damping
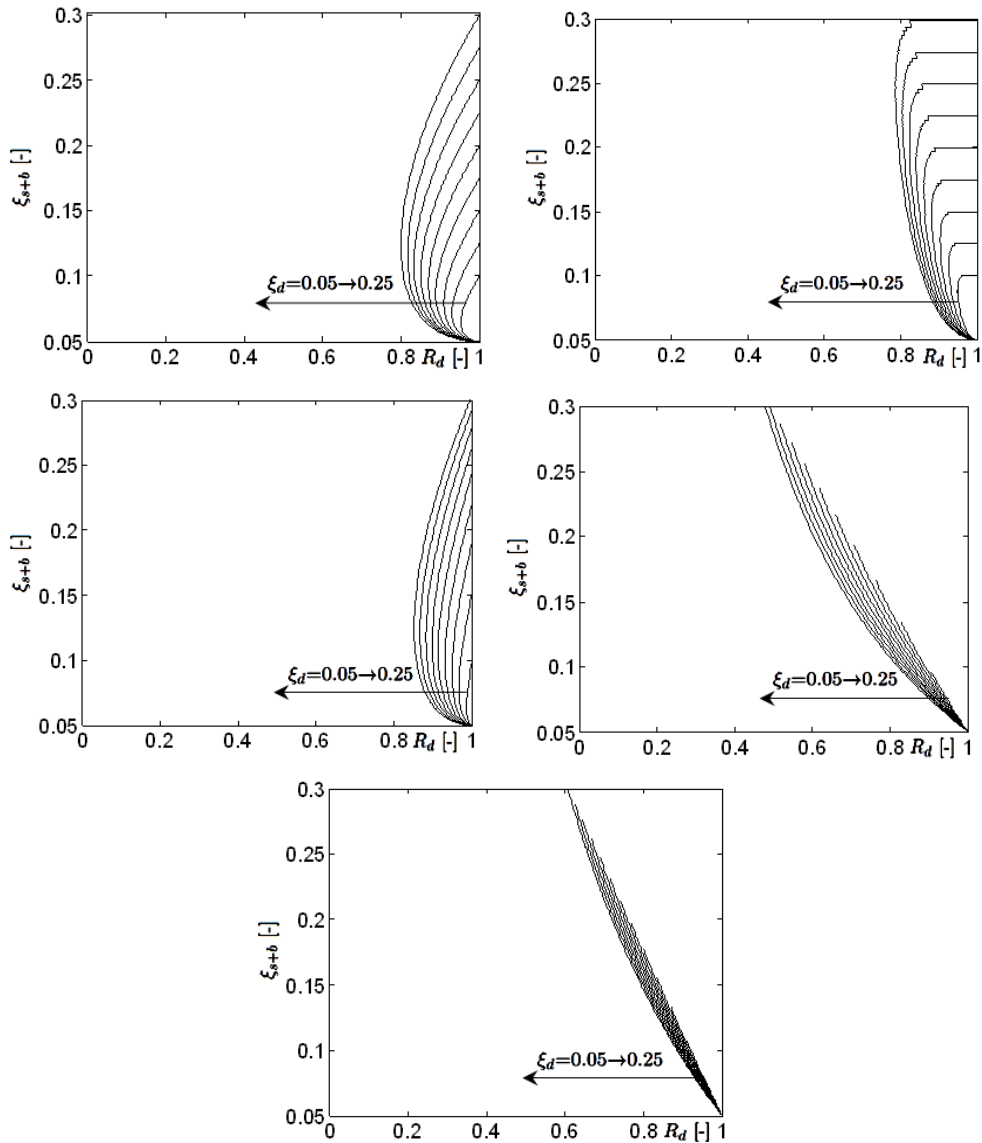
Figure 12. Design charts for different types of dampers: variation of ξ_{s+b} with R_d ($\xi_d = 0.05$–0.25). Clockwise from top left: VL, VN, EP, FR, VE.

value is obtained as the weighted average of the damping value of each storey, proportionally to the storey shear forces. In the analyzed case, the vector containing the damping ratios for each floor level is

$$\xi_{s+b} = [0.29 \ \ 0.27 \ \ 0.23 \ \ 0.18 \ \ 0.12 \ \ 0.05 \ \ 0.05] \, .$$

From R_d and ξ_{s+b} values, the additional damping ratios ξ_d provided by each damper can be estimated from the charts presented in Figure 12. The R values, characterizing the stiffness of the supporting braces, can be calculated from the charts presented in Figures 5–9. Different types of dampers can be chosen
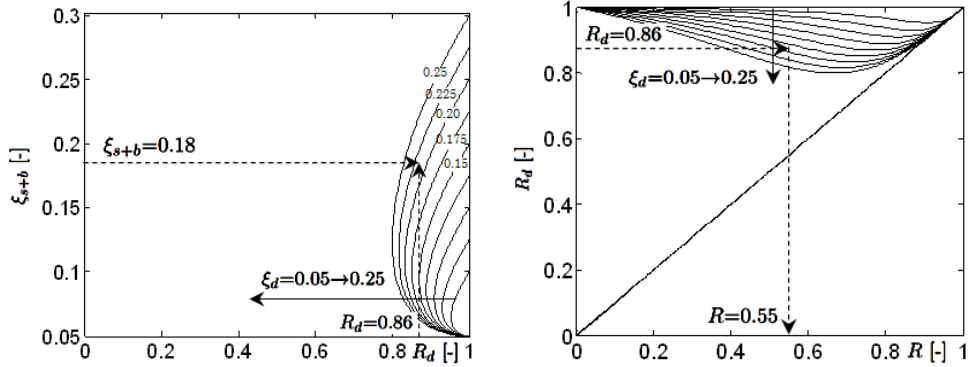
Figure 13. Left: estimation of ξ_d from ξ_{s+b} and R_d. Right: estimation of R from ξ_d and R_d values. In both cases, ξ_d ranges from 0.05 to 0.25.

in order to obtain the desired characteristics. The most efficient ones have been chosen according to the F^* index of (4-8). For example, selection for the fourth storey is presented in Figure 13, left. Given a value of $R_d = 0.86$ and a damping ratio $\xi_{s+b} = 0.18$, the chart indicates an optimum value for ξ_d equal to 0.21. The estimate for the R index is presented in Figure 13, right. Given $R_d = 0.86$ and $\xi_d = 0.21$, the chart indicates an optimum value of 0.55 for R.

The dissipative braces selected for the fourth level are VL dampers characterized by $\xi_d = 0.21$ and supported by elastic braces with $R = 0.55$. It is evident that the interaction between brace and damper implies that the additional damping ratio due to damper $\xi_d = 0.21$ must be higher than the value required at the storey level $\xi_b = \xi_{s+b} - \xi_s = 0.18 - 0.05 = 0.13$, where $\xi_s = 0.05$ is the damping ratio of the elastic structure, because of the loss of efficiency due to the deformability of the brace. At the same time, the elastic braces could support $(1 - R) = (1 - 0.55) = 0.45$ times the whole seismic forces acting at the storey level. They however suffer a reduction of stiffness for the presence of the damper and are able to carry only $(1 - R_d) = (1 - 0.86) = 0.14$ times the whole seismic forces. Results for all the levels of the frame are presented in Table 3.

Note that the required level of damping is obtained by the use of different dampers. VL dampers are most indicated for less stiff braces with lower dissipation capacity, while VN dampers are preferred where more stiffness and damping is required, i.e., at lower levels.

Level	Damper	R	ξ_d
1	Type VN	0.10	0.25
2	Type VN	0.45	0.22
3	Type VN	0.45	0.20
4	Type VL	0.55	0.21
5	Type VL	0.70	0.18
6	—	—	—
7	—	—	—

Table 3. Dissipative braces characteristics (R, ξ_d) derived from the design procedure.
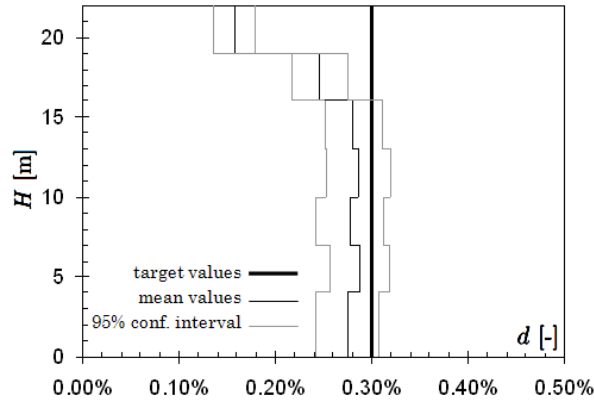
Figure 14. Inter-storey drifts d along the height H of the building.

Step A5. A numerical investigation has been carried out for the structure under consideration in order to evaluate the effects produced by the insertion of the dissipative braces. The braces were modeled as purely elastic springs and purely viscous dampers connected in series. The viscous dampers are characterized by a damping coefficient $c = \xi_d m_d \omega_{s+b}/2$, where m_d is the modal mass supported by the damper and ω_{s+b} is the circular frequency of the fundamental mode of the system. Values of the damping exponent α equal to 1 and 0.15 are assumed for VL and VN dampers, respectively. In addition to the damping provided by the dissipative braces, a global damping ratio of 0.05 for the structure was included using the Caughey damping model [Chopra 1995]. The interstorey drifts are presented as the average values over the seven time histories. The 95% confidence interval is also represented. Results reported in Figure 14 show a good agreement between the target inter-story drift values (bold line) and the average values obtained from the seven time histories. Sectional areas of the supporting braces A_d were estimated on the basis of the R values, assuming that the dissipative portion of the brace is one third of the total length:

$$A_d = [0 \ \ 0 \ \ 0.0076 \ \ 0.0131 \ \ 0.0184 \ \ 0.0146 \ \ 0.0225] \, \text{m}^2.$$

The values A_d can be compared with the sectional areas A_{el} of the elastic bracing system that can ensure the same level of performance requirements without added dissipation:

$$A_{el} = [0 \ \ 0.0159 \ \ 0.0276 \ \ 0.0339 \ \ 0.0399 \ \ 0.0345 \ \ 0.0238] \, \text{m}^2.$$

It is evident that the elastic braces that support the dampers have smaller sectional areas of the elastic bracing system. In the case study, sectional areas of the braces in the dissipative system are on average 0.43 times the sectional areas of the elastic system.

6. Conclusions

Effects associated with two of the most common assumptions adopted in design procedures for dissipative braces are studied. The assumption of constant floor stiffness and the reduction of MDOF systems to SDOF systems are shown to be limited in capturing the interaction between the frame structure and the installed braces. Index R is introduced in order to describe that interaction. Two additional interaction

mechanisms have been studied. The stiffness of the supporting brace has been shown to condition the dissipation capacity of the dampers and vice versa. The ratio F_R quantifies the reduction of brace stiffness due to the damper. For supporting braces with $R = 0.5$ (i.e., with the same stiffness of the frame) and for a system damping ratio $\xi_{s+b} = 0.30$, the maximum reduction value of 78% has been found for VE dampers, while the minimum value of 24% has been found for EP dampers, showing that EP dampers are preferable when higher stiffness increments are needed while VE dampers are most indicated for lower increments of stiffness. Ratio F_ξ quantify the loss of dissipation capacity expressed in term of damping ratio ξ_{s+b} due to the deformability of the brace. For supporting braces with $R = 0.5$ and for an additional damping $\xi_d = 0.25$, the maximum reduction value of 40% has been found for EP dampers, while the minimum value of 23% has been found for VE dampers, showing that VE are less affected by the brace stiffness while EP require very stiff supporting braces in order to ensure their dissipation capacity. A global index of efficiency F^* has also been defined by combining F_R and F_ξ ratios. Contour levels of F^* in the plane R-ξ_{s+b} identify fields of maximum efficiency for the considered type of dampers. A design procedure has been proposed and validated for a seven-storey building, indicating a beneficial effect due to the added dissipation capacity quantified as an average reduction of the sectional areas of the braces of 57% respect to an elastic bracing system.

References

[CEN 2004] European Committee for Standardization (CEN), "Eurocode 8: design of structures for earthquake resistance, part 1: general rules, seismic actions and rules for buildings", standard EN 1998-1, Brussels, 2004.

[Choi et al. 2003] H. Choi, W. B. Kim, and S. J. Lee, "A method of calculating the non-linear seismic response of a building braced with visco-elastic dampers", *Earthquake Engin. Struct. Dyn.* **32** (2003), 1715–1728.

[Chopra 1995] A. K. Chopra, *Dynamics of structures*, Prentice-Hall, Englewood Cliffs, NJ, 1995.

[Ciampi 1993] V. Ciampi, "Development of passive energy dissipation techniques for buildings", pp. 495–510 in *International Post-SMiRT Conference Seminar on Isolation, Energy Dissipation and Control of Vibrations of Structures* (Capri, 1993), 1993.

[FEMA 2000] "NEHRP Guidelines for the seismic rehabilitation of buildings", standard 356, Washington, DC, 2000.

[Filiatrault and Cherry 1990] A. Filiatrault and S. Cherry, "Seismic design spectra for friction-damped structures", *J. Struct. Eng. (ASCE)* **116**:5 (1990), 1334–1355.

[Fu and Cherry 2000] Y. Fu and S. Cherry, "Design of friction damped structures using lateral force procedure", *Earthquake Engin. Struct. Dyn.* **29** (2000), 989–1010.

[Fu and Kasai 1998] Y. Fu and K. Kasai, "Comparative study of frames using visco-elastic and viscous dampers", *J. Struct. Eng. (ASCE)* **124**:5 (1998), 513–522.

[Garcia 2001] D. L. Garcia, "A simple method for the design of optimal damper configurations in MDOF structures", *Earthquake Spectra* **17**:3 (2001), 387–398.

[Gasparini and Vanmarcke 1976] D. Gasparini and E. Vanmarcke, "Simulated earthquake motions compatible with prescribed response spectra", technical report 76-4, Massachusetts Institute of Technology, Department of Civil Engineering, Cambridge, MA, 1976.

[Gluck et al. 1997] N. Gluck, A. M. Reinhorn, J. Gluck, and R. Levy, "Design of supplemental dampers for control of structures", *J. Struct. Eng. (ASCE)* **122**:12 (1997), 1394–1399.

[Goel 2000] R. K. Goel, "Seismic behaviour of asymmetric buildings with supplemental damping", *Earthquake Engin. Struct. Dyn.* **29** (2000), 461–480.

[Goel 2001] R. K. Goel, "Simplified analysis of asymmetric structures with supplemental damping", *Earthquake Engin. Struct. Dyn.* **30** (2001), 1399–1416.

[Lee et al. 2004] S. H. Lee, D. I. Son, J. Kim, and K. W. Min, "Optimal design of visco-elastic dampers using eigenvalue assignment", *Earthquake Engin. Struct. Dyn.* **33** (2004), 521–542.

[Levy et al. 2000] R. Levy, E. Marianchik, A. Rutenberg, and F. Segal, "Seismic design methodology for friction damped braced frames", *Earthquake Engin. Struct. Dyn.* **29** (2000), 1569–1585.

[Lin and Chopra 2002] W. H. Lin and A. K. Chopra, "Earthquake response of elastic SDF systems with non-linear fluid viscous dampers", *Earthquake Engin. Struct. Dyn.* **31** (2002), 1623–1642.

[Moreschi and Singh 2003] L. M. Moreschi and M. P. Singh, "Design of yielding metallic and friction dampers for optimal seismic performance", *Earthquake Engin. Struct. Dyn.* **32** (2003), 1291–1311.

[Park and Min 2004] J. H. Park and J. K. K. W. Min, "Optimal design of added visco-elastic dampers and supporting braces", *Earthquake Engin. Struct. Dyn.* **33** (2004), 465–484.

[Pekcan and Chen 1999] G. Pekcan and J. B. M. S. S. Chen, "Fundamental considerations for the design of non-linear viscous dampers", *Earthquake Engin. Struct. Dyn.* **28** (1999), 1405–1425.

[Phocas and Pocanschi 2003] M. C. Phocas and A. Pocanschi, "Steel frames with bracing mechanism and hysteretic dampers", *Earthquake Engin. Struct. Dyn.* **32** (2003), 811–825.

[Shukla and Datta 1999] A. K. Shukla and T. K. Datta, "Optimal use of visco-elastic dampers in building frames for seismic force", *J. Struct. Eng.* (*ASCE*) **125**:4 (1999), 401–409.

[Singh and Moreschi 2001] M. P. Singh and L. M. Moreschi, "Optimal seismic response control with dampers", *Earthquake Engin. Struct. Dyn.* **30** (2001), 553–572.

[Singh and Moreschi 2002] M. P. Singh and L. M. Moreschi, "Optimal placement of dampers for passive response control", *Earthquake Engin. Struct. Dyn.* **31** (2002), 955–976.

[Takewaki 1999] I. Takewaki, "Displacement-acceleration control via stiffness-damping collaboration", *Earthquake Engin. Struct. Dyn.* **28** (1999), 1567–1585.

[Whittaker et al. 2003a] A. S. Whittaker, M. C. Constantinou, O. M. Ramirez, M. W. Johnson, and C. Z. Chrysostomou, "Equivalent lateral force and modal analysis procedures of the 2000 NEHRP provisions for buildings with damping systems", *Earthquake Spectra* **19**:4 (2003), 959–980.

[Whittaker et al. 2003b] A. S. Whittaker, M. C. Constantinou, O. M. Ramirez, M. W. Johnson, and C. Z. Chrysostomou, "Validation of the 2000 NEHRP Provisions' equivalent lateral force and modal analysis procedures for buildings with damping systems", *Earthquake Spectra* **19**:4 (2003), 981–999.

[Wu and Ou 2003] B. Wu and J. Ou, "The pseudo-viscous frictional energy dissipator: a new device for mitigating seismic effects", *Earthquake Engin. Struct. Dyn.* **32** (2003), 31–48.

[Yamada 2000] K. Yamada, "Non-linear-Maxwell-element-type hysteretic control force", *Earthquake Engin. Struct. Dyn.* **29** (2000), 545–554.

GIUSEPPE LOMIENTO: giuseppe.lomiento@uniroma1.it
Dipartimento di Ingegneria Strutturale e Geotecnica, University of Rome "La Sapienza", Via Eudossiana 18, I-00184 Rome, Italy

NOEMI BONESSIO: noemibonessio@virgilio.it
Dipartimento di Ingegneria Strutturale e Geotecnica, University of Rome "La Sapienza", Via Eudossiana 18, I-00184 Rome, Italy

FRANCO BRAGA: franco.braga@uniroma1.it
Dipartimento di Ingegneria Strutturale e Geotecnica, University of Rome "La Sapienza", Via Eudossiana 18, I-00184 Rome, Italy

SEISMIC ISOLATION AND OTHER ANTISEISMIC SYSTEMS RECENT APPLICATIONS IN ITALY AND WORLDWIDE

ALESSANDRO MARTELLI AND MASSIMO FORNI

Over 10,000 structures have been protected in the world by antiseismic systems and devices, namely by seismic isolation and energy dissipation systems, shape memory alloy devices and shock transmitter units. Such structures are located mostly in Japan, but they are more or less numerous in over 30 other countries as well — for example, in the Peoples' Republic of China, the Russian Federation, the United States, Italy and even countries with very a limited population like Armenia and New Zealand. The number of such systems and devices is increasing everywhere, although the extent of their use is strongly influenced by earthquake experience and the features of the design rules used. Applications have been developed for both new and existing structures of all kinds: bridges and viaducts, civil and industrial buildings, cultural heritage and industrial components and installations, including some high risk plants. The use of such systems in a civil context already includes not only strategic structures (civil defense centers, hospitals, etc.) and public ones (schools, churches, commercial centers, hotels, airports, etc.), but also residential buildings and even many small private houses. This paper provides an overview on the dissemination of such applications worldwide, based on the most recent information available to the authors. Particular attention is paid to Italy, in the context of specific seismic events — for example, the Molise and Puglia event (October 31, 2002) and that of Abruzzo (April 6, 2009) — and the lessons learned from them. Information is also provided on the features of the Abruzzo event, the development of national seismic design rules (which became obligatory only after that event) and some very recent decisions on the part of the Italian government which promote the use of seismic isolation and energy dissipation to enhance the safety level of structures, especially schools. The paper focuses mainly on seismically isolated buildings, but some information is also provided on the use of other antiseismic systems, devices, and applications to structures other than buildings.

1. Introduction

Since the end of the 1980s, great efforts have been devoted by ENEA[1], the Italian GLIS Association[2], the EU/WEC Territorial section of *ASSISi*[3] and EAEE-TG5[4] to the development and application of seismic vibration passive control (SVPC) systems and devices, namely to seismic isolation (SI) and energy dissipation (ED) systems, shape memory alloy devices (SMADS) and shock transmitter units (STUs). This activity was performed in the context of extensive collaborations with the Italian Civil Defense Department (*Dipartimento della Protezione Civile* or DPC) and further national, regional and local institutions [Dolce et al. 2006; Martelli et al. 2008; 2009a; 2009b; 2010a, Sannino et al. 2009; Martelli and Forni 2009a]. Such collaborations also include support to the DPC for emergency and post-emergency management, as well as rebuilding, in the case of earthquakes. In particular, this support was provided after the 2002 Molise and Puglia earthquake and has been ensured in Abruzzo since the event of April 6, 2009.

Recent information on the development and implementation of the SVPC systems and devices was provided in some successful conferences that were organized or coorganized by GLIS, ENEA, *ASSISi*, its EU/WEC Territorial Section and EAEE-TG5. The proceedings of such conferences were published by [Erdik et al. 2007; 2008; Martelli et al. 2008; Santini and Moraci 2008; Sannino et al. 2009; Phocas et al. 2009; Mazzolani 2009; JSSI 2009; Zhou et al. 2009]. Numerous GLIS members and ENEA researchers actively participated in special sessions dealing with the previously cited topics in these conferences and other important recent events that were more generally devoted to seismic engineering and seismology [Martelli 2008a; 2008b; 2009a; 2009b; 2009c; 2009d; 2009e; 2009f; Martelli and Forni 2008a; 2008b; 2009a; 2009b]; part of these sessions were organized by the first author of this paper [Martelli et al. 2008; Santini and Moraci 2008; Katayama et al. 2008; Sannino et al. 2009; Phocas et al. 2009; Mazzolani 2009].

As witnessed by the proceedings of all these conferences, at present there are over 10,000 structures in the world that are protected by SVPC systems and devices. These structures are located mostly in Japan, but they are more or less numerous in about 30 other countries as well (see Figure 1, left), including China, Russia, the United States and Italy, which follow Japan for the number of applications (however, as pointed out in [JSSI 2009], should the number be normalized to that of the residents in each country, Armenia and New Zealand would be those immediately following Japan). Everywhere, the number of such structures is on the rise, although the extent of the use of the SVPC systems and devices is strongly influenced by earthquake experience and the features of the design rules used. Applications address both new and existing structures of all types: bridges and viaducts, civil and industrial buildings, cultural heritage (monumental buildings, museums, ceilings of archaeological excavations, museum display

---

[1] ENEA changed its full name from *Ente per le nuove Tecnologie, l'Energia e l'Ambiente* (Italian Agency for New Technologies, Energy and the Environment) to *Agenzia Nazionale per le Nuove Tecnologie, l'Energia e lo Sviluppo Economico Sostenibile* (Italian National Agency for New Technologies, Energy and Sustainable Economic Development) in September 2009.

[2] The full name of GLIS is *GLIS – Isolamento ed altre Strategie di Progettazione Antisismica* (namely GLIS — Isolation and Other Anti-Seismic Design Strategies).

[3] The EU/WEC Territorial Section of *ASSISi* is the Territorial Section for the European Union and Other Western European Countries of the *Anti-Seismic Systems International Society*. GLIS has been a corporate member of *ASSISi* since the foundation of the latter in 2002.

[4] EAEE-TG5 is Task Group 5 on Seismic Isolation of Structures of the European Association for Earthquake Engineering.
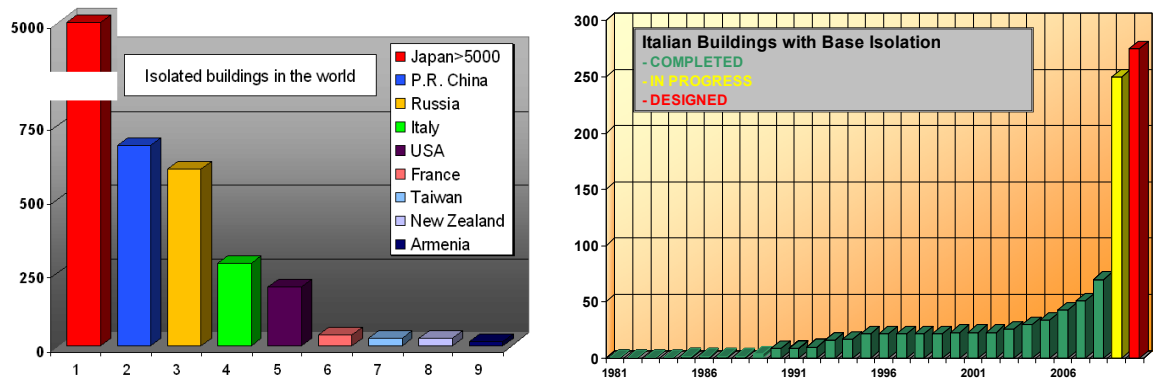
Figure 1. Left: overall number of building applications of SI in the most active countries. Right: overall number of building applications of SI in Italy over the years.

cases and unique masterpieces) and industrial components and installations. The latter include some high risk plants like nuclear reactors, other nuclear facilities and liquefied natural gas (LNG) storage tanks. Applications to civil construction encompass not only strategic ones, such as civil defense centers, hospitals, airports, bridges and viaducts, and public ones such as schools, churches, commercial centers, and hotels, but also many residential buildings and even some private houses.

This paper includes parts of [Martelli and Forni 2009c] and [Martelli 2010a]; more precisely, it summarizes the recent progress in the use of the SVPC systems and devices, mainly based on the information made available at the International Workshop Celebrating the 15 Years Anniversary of JSSI (Tokyo, Japan, September 2009; see [JSSI 2009]) and at the 11th World Conference on Seismic Isolation, Energy Dissipation and Active Vibration Control of Structures (Guangzhou, China, November 2009; see [Zhou et al. 2009]). Particular attention is devoted to applications in Italy (see Figure 1, right), other countries where the use of the SVPC systems is less known and, in general, to isolated buildings, but information is also provided on the use of other SVPC systems in the context of structures other than buildings. With regard to Italy, some remarks are also reported on the seismic risk in this country, on the 6.3 magnitude earthquake that struck the Abruzzo region (in particular, the town of L'Aquila and several surrounding villages) on April 6, 2009, and on the lessons learned from seismic events. Information is also provided on the features of the new national seismic code and some very recent decisions of the Italian government promoting the use of such systems and devices, to increase the seismic safety of schools and other structures. More details on the adoption of the antiseismic systems and devices in Italy and worldwide may be found in [Dolce et al. 2005; 2006; Martelli et al. 2008; Sannino et al. 2009], in a recent DVD [Zhou et al. 2009], as well as (for Italy) in the article [Martelli and Forni 2010].

2. Japan

Japan, thanks to the availability of an adequate specific code since 2000 and the free adoption of SI since 2001, is more and more consolidating its worldwide leadership on the use of the SVPC systems and devices, with over 5,000 buildings or houses protected by SI (Figure 1) and about 3,000 more provided with ED systems [Zhou et al. 2009]. This country, where the first application of base SI dates back to
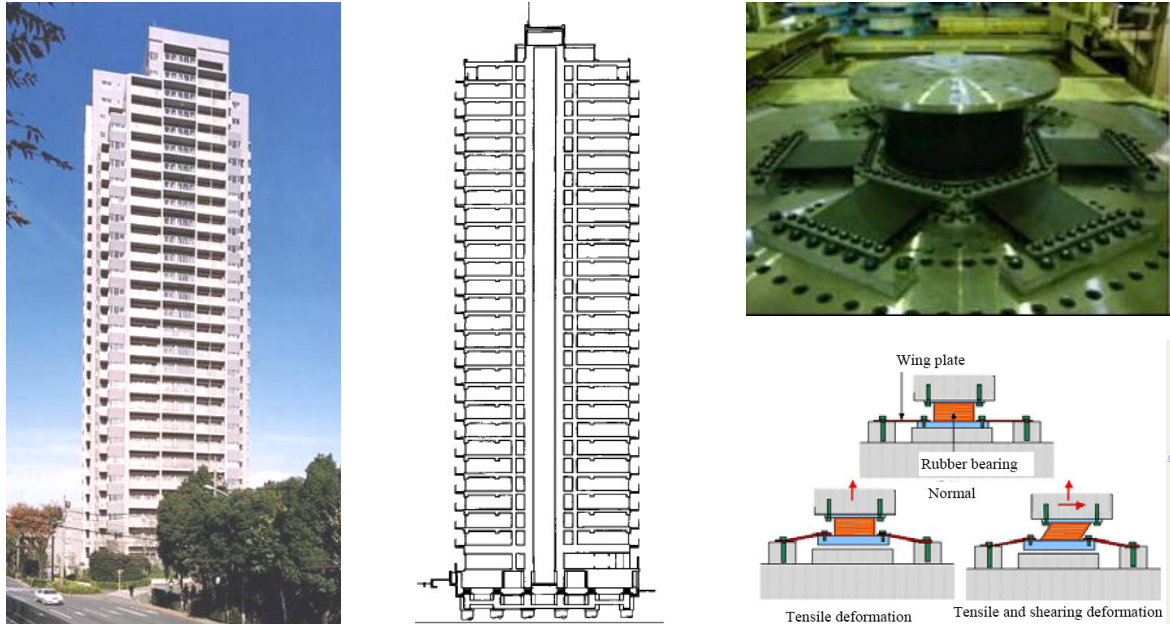
Figure 2. Left and middle: The first Japanese application of SI to high-rises is a 87.4 m high building that was seismically isolated in Tokyo in 2000 by means of 30 low-damping rubber bearings (LDRBs) and 99 elastic-plastic dampers (EPDs), with a period $T = 4$ s. Right: sketch of its LDRBs, provided with an anti-uplift system.

1985, is continuing the extensive adoption of the SVPC systems initiated after the excellent behavior of two isolated buildings near Kobe during the 1995 Hyogo–ken Nanbu earthquake (this behavior was later confirmed for all Japanese buildings protected by SI systems that were struck by subsequent events; see, for instance, [Martelli 2009c].

The Japanese have confirmed the trend, initiated some years ago, of isolating even high-rise buildings (Figure 2) and sets of buildings (Figure 3) supported by a common isolated reinforced concrete (r.c.) structure, called an *artificial ground*, a solution that allows large savings in construction costs (see also Figure 4). Moreover, an ever-increasing number of even very small private houses have been protected by SI (Figures 4 and 5). The isolated high-rise buildings are over 120 and include many condominiums, while the isolated houses are already about 3,000.

About 1,000 Japanese buildings and 2,000 private houses have also been protected by various kinds of dampers: for instance, the applications of the buckling-restrained braces (BRBs) were already over 250 in 2003. The ED systems too behaved very well during various earthquakes. Moreover, approximately 40 Japanese buildings were seismically controlled by tuned mass dampers (TMDs), of active or hybrid types, in June 2007, and so-called *active damping bridges* (ADBs) were installed between pairs of adjacent high-rise buildings to reduce the seismic response of both (Figure 7).

The use of the SVPC systems and devices also recently increased in Japan for the protection of cultural heritage (Figures 8 and 9) and for that of bridges and viaducts. For the latter it began rather later than for buildings; it is being largely based on the use of high damping rubber bearings (HDRBs) and lead rubber

Figure 3. Left: Applause Building in Osaka, with a hybrid control system moving an heliport structure at the top. Right: sketch of the complex of 21 six- to fourteen-storey buildings erected on a unique "artificial ground" isolated at Sagamihara (Tokyo area) with 48 lead rubber bearings (LRBs), 103 sliding devices (SDs) and 83 ball bearings.

Figure 4. Lateral view of the isolated building complex of Figure 3 and the large garage located below the artificial ground plate, with the isolators protected from fire (the SI system lowers the period of the 111,600 t superstructure to $T = 6.7$ s, with a design displacement of 800 mm).

Figure 5. Japanese private houses protected by 2 SDs and 4 HDRBs.

Figure 6. A Japanese private house protected by an SI system formed by steel sphere recirculation isolators, viscous dampers (VDs) and recentering devices.

Figure 7. Left: "green mass damper", used as the TMD of a 45 m tall building of the Keyaki-zaka residential complex, in Tokyo. The garden base is 1 m thick, weights 3,650 t, or 8% of the building mass, and is supported by 46 rubber bearings (RBs) and 22 visco-elastic dampers (VEDs). Right: ADB between Japanese high-rise buildings.

Figure 8. Retrofits with SI in a subfoundation of the National Western Art Museum, designed by Le Corbusier (above), and of the "Gates of Hell" in Tokyo (right column), performed in 1999.

bearings (LRBs) and considerably extended especially after the 1995 Hygo–ken Nanbu earthquake (by becoming obligatory for overpasses in Kobe).

Finally, as to the industrial plants, besides detailed studies for the SI (even with three-dimensional systems) of various kinds of nuclear reactors, the construction of the Nuclear Fuel Related Facility, supported by 32 low damping rubber bearings (LDRBs) and LRBs, was completed (Figure 9). Application
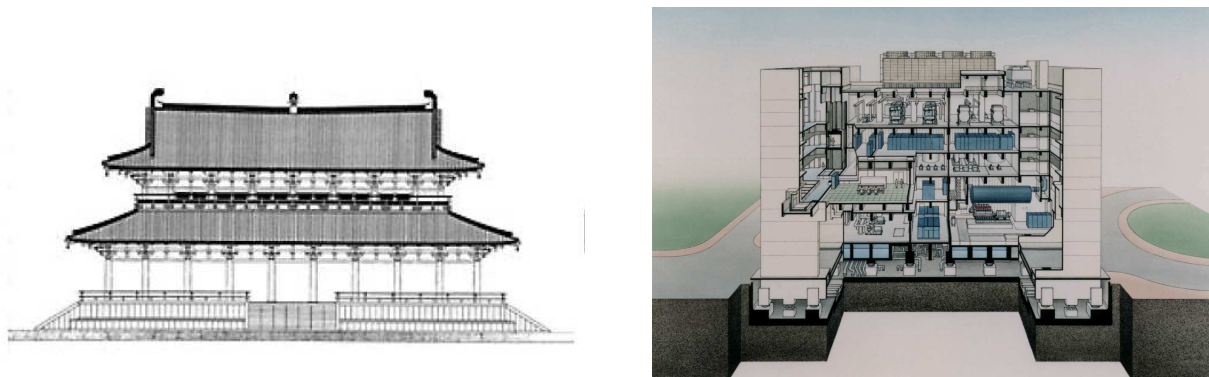
Figure 9. Left: example of retrofit of cultural heritage in Japan, begun for the Daigoku-den at Nara in 2001. Right: the Nuclear Fuel Related Facility, the first nuclear structure to be isolated in Japan.

Figure 10. First seismically isolated Japanese factory for the production of semiconductors (height = 24.23 m, total area $\approx 27{,}000\,\mathrm{m}^2$).

of SI to large industrial factories also began in 2006; the first was a semiconductor plant, built on LRBs and VDs (Figure 10). At least two other similar factories are also already in use.

3. People's Republic of China

In China very ancient monasteries, temples and bridges, protected by means of rough sliding SI systems, are still standing, which withstood numerous earthquakes, including very violent events, up to 8.2 magnitude [Dolce et al. 2005; 2006]; however, the application of modern SI systems began only in 1991. In any case, initially the SI systems, then the ED ones too have rapidly got a footing since that year, so that the isolated buildings were already 490 in June 2005, by leading China to the third place at worldwide level for the number of applications, only slightly after the Russian Federation. Many of these applications were to residential buildings and no less than 270 to the masonry ones [Dolce et al. 2006].

At the end of 2006 the number of the Chinese isolated buildings had increased to more than 550 and included even rather tall constructions (Figure 11); furthermore, SI had already been applied to 5 further

Figure 11. The tallest seismically isolated Chinese building (19 storeys), erected at Taiyuan City, in Northern China (left), and a Chinese high-rise building protected by VDs (center and right).

large span structures and 20 road and railway bridges or viaducts, 30 buildings were already protected by ED devices (Figure 11) and 5 buildings and 6 bridges by hybrid or semiactive seismic vibration control systems. SI had also already been used, for the first time in China, to protect LNG tanks [Erdik et al. 2008].

In 2007 China passed Russia [Erdik et al. 2008]: in fact, Chinese isolated buildings reached 610 in May 2007 (against the approximately 600 in Russia; see Section 4) and those protected by ED systems reached 45. The former included the Isolation House Building on Subway Hub, completed near the center of Beijing in 2006; it consists of 50 seven- to nine-storey buildings, all separately isolated above a single huge two-storey isolated structure containing all services and infrastructures, including railways and subways. The objective of this application had been to optimize the use of a wide and valuable central area, which was previously occupied only by railway junctions and the subway, by also minimizing the consequent vibrations and noise: SI enabled a 25% savings in construction costs, making it possible, within the same budget, to increase the height of the 50 buildings by an average of three storeys.

In the same period, the Chinese started applying three-dimensional SI systems to civil buildings (Figure 12) and isolators or SMADs to cultural heritage (Figure 13). In October 2008, isolated Chinese buildings numbered about 650.

Figure 12. Left: new Chinese buildings protected at Guangzhou by 3D RBs from both horizontal seismic vibrations and vertical traffic vibrations. Center: one of the 3D RBs. Right: its sketch (4 = vertical element). Similar applications exist in Beijing.
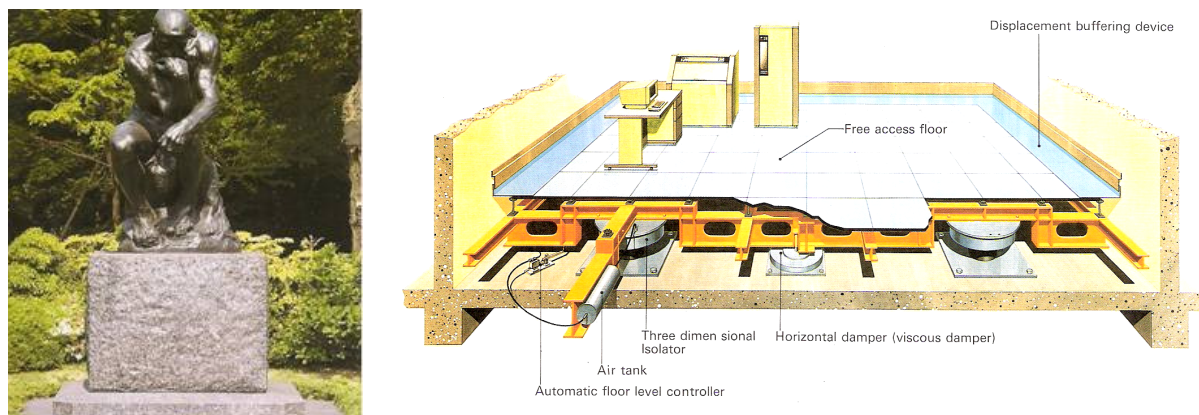
Figure 13. Left: example of an SI-protected of Chinese masterpiece. Right: SI table for the protection of vulnerable equipment or art objects.

In November 2009, a further significant extension of the applications of the SVPC systems in China was reported: the number of isolated buildings erected each year doubled there after the Wenchuan earthquake of May 12, 2008, increasing from 50 to 100 per year [Zhou et al. 2009]. This rapid increase in the number of building applications of SI was due, one the one hand, to the excellent behavior of two r.c. isolated buildings (Figure 14) and a six-storey masonry one during that earthquake — although its violence had been greatly underestimated, by a factor of 10 for the peak ground acceleration! — and, on the other, the fact that the Chinese code (which still requires the submission of the projects the isolated buildings to the approval of a special commission) permits to reduce the seismic loads acting on the superstructure and foundations of such buildings.

Figure 14. Top left: heavy damage was inflicted on this conventionally founded r.c. building by the 2008 Wenchuan earthquake; the building had been designed to withstand events of intensity $I_{\mathrm{MMS}} = 7$. Top right and bottom: this isolated building remained free of structural and nonstructural external and internal damage after the same earthquake.

To date, SI systems have been installed in China in 32 bridges and 690 buildings, while 83 buildings have been protected by ED devices such as EPDs, VDs or VEDs, 16 by TMDs or other type dampers and 5 by semiactive or hybrid systems. The latter have also been installed in 8 bridges. SI is applied not only at the building base or at the top of the lowest floor, but also on more elevated floors (for risings or for erecting highly vertically asymmetric constructions), or at the building top (to sustain, in the case of retrofit, one or more new floors acting as a TMD), or also on structures that join adjacent buildings having different vibrational behaviors.

New applications include sets of buildings on artificial ground (Figure 15), base and roof SI of stadiums (Figure 16) and the protection of valuable objects, such as electronic equipment and artwork, by means of SI tables (Figure 13).
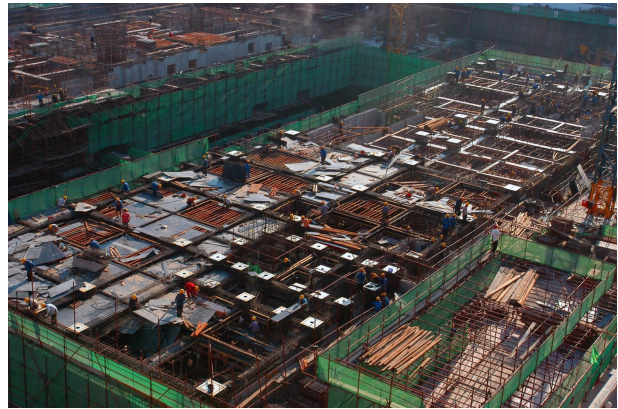
Figure 15. Set of buildings of the Headquarters of China Earthquake Administration during their construction in Beijing on a seismically isolated "artificial ground" slab in 2008 (first Chinese application of this kind).

Figure 16. Left: Chinese stadium (23,000 m^2) protected by RBs and VDs, for which SI reduced the seismic response by a factor of 4.2. Right: and roof SI of the News Centre and Restaurant of Shanghai F1 Autodrome.

4. Russian Federation

The Russian Federation is now third in the number of isolated buildings, with over 600 applications [Zhou et al. 2009]. The use of modern SI systems, formed by rubber bearings (RBs), frequently in conjunction with steel-PTFE Sliding Devices (SDs) and/or dampers (similar to those adopted in the other countries), is going on replacing that of the previous so-called low cost isolators (reversed mushroom-shaped r.c. elements), which had been installed since the 1970s. After the retrofits of some important historical buildings [Dolce et al. 2005; 2006; Sannino et al. 2009], new Russian applications include even high-rise buildings, in particular in Sochi, where the 2014 Olympic games will take place (Figure 17). For some of these, Italian HDRBs have been used.

Figure 17. Top: new Sea Plaza Hotel at Sochi (27 storeys, in addition to 2 underground ones; height ≈ 93 m; total living area $= 40{,}000\,\mathrm{m}^2$), protected by 102 HDRBs. Bottom: new r.c. commercial center, with cinema, underground parking and offices, again at Sochi (21 storeys, in addition to the ground and 2 underground floors; height ≈ 100 m; total living area $= 50{,}000\,\mathrm{m}^2$), protected by 200 LRBs.

5. United States

The United States rank second, after Japan, in the overall number of applications of the SVPC systems and devices [JSSI 2009]. In this country, however, such applications are progressing satisfactorily only for bridges and viaducts and for buildings protected by ED systems. They include both new constructions and retrofits. More precisely, HDRBs, LRBs and, more recently ED devices and STUs have been installed in about 1,000 US bridges and viaducts, in several states (Figure 18), while dampers of various types protect over 1,000 buildings: VDs and friction dampers (FDs) protected approximately 40 and, respectively, 12 buildings in 2001 and BRBs 39 further buildings in 2003 [Dolce et al. 2005; 2006].

By contrast, the number of new applications of SI to buildings remains limited (recently 3 or 4 per year), in spite of the excellent behavior of some important US isolated buildings during the 1994 Northridge earthquake [Dolce et al. 2005; 2006] and the long experience of application of this technique to such structures (since 1985). This is a consequence of very penalizing design codes for isolated buildings. According to recent information, US seismically isolated buildings number between 100 and 200, though they are generally important ones, including monumental buildings (Figures 20–23). About half of them are retrofits.

Figure 18. Left: Carquinez Bridge, California, retrofitted by means of Italian STUs. Right: Marquam Bridge, Oregon, retrofitted by means of Italian RBs and EPDs.
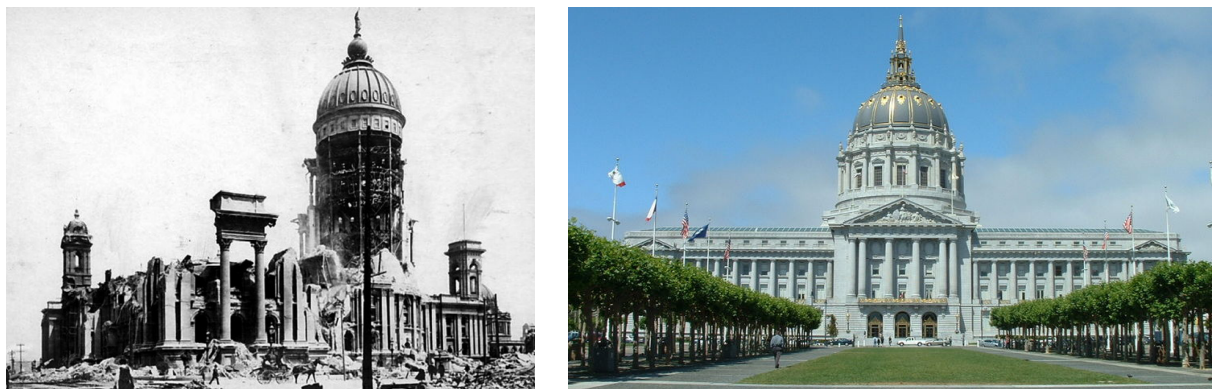
Figure 19. San Francisco City Hall, destroyed by the 1906 earthquake (left), rebuilt in 1912, damaged by the 1989 Loma Prieta earthquake and retrofitted in 2000 using 530 LRBs and 62 SDs (retrofit cost = 105 MUS$, with savings of 11 MUS$ thanks to SI).

Figure 20. Left: construction of the 911 Emergency Communications Center in San Francisco, designed to withstand earthquakes to magnitude $M = 8.3$. Right: view of one of its RBs and the fail-safe system (late 1990s).

Figure 21. Asian Art Museum in San Francisco, during its seismic retrofit (with cut of the foundations and insertion of HDRBs) performed according to the design of the Italian architect Gae Aulenti (late 1990s).

Figure 22. Retrofit with HDRBs of the Berkeley Civic Centre (California).

Figure 23. Further US building retrofits with SI. Left: San Francisco Court of Appeal, retrofitted with FPS. Right: Kerckhoff Hall at the University of California, Los Angeles (total living area = 8,300 m², 6 storeys).

Buildings in the US have been isolated using HDRBs, LRBs (in some cases in conjunction with LDRBs, SDs, VDs and other ED devices) and, more recently, the friction pendulum system (FPS), too. With regard to the design earthquake levels adopted in California, it is noted that they correspond to very large magnitudes M (for example, $M = 8.3$ for the new 911 Emergency Communications Center in San Francisco in the 1990s — see Figure 20 — and $M = 8.0$ for the retrofit of the San Francisco City Hall with 530 LRBs and 62 SDs in 2000 (see Figure 19). This imposes the use of SI as the only possibility for these applications, in spite of its high cost in the US.

6. Italy

Seismic risk in Italy. Despite a significantly lower seismic hazard than, say, Japan, China, or California, Italy is characterized by the highest seismic risk in the European Union and by one of the highest in the industrialized countries; see [Dolce et al. 2005; 2006; Martelli 2009b; 2010a] and Table 1. In fact, the vulnerability of Italian constructions is such that more than half of them (including 75,000 strategic and public buildings) are incapable of bearing the seismic actions to which they may be subjected.

This situation is due to several factors. Italy is home to a good fraction of the world's cultural heritage. There has been, in the last few decades, significant progress in seismology and seismic engineering, and consequently also changes in seismic codes and in the seismic classification of the country's regions.

Event of magnitude M = 7.0			Event of magnitude M = 7.5		
	dead	wounded		dead	wounded
Southern Apennines	5,000–11,000	$\geqslant$ 15,000	Calabria	15,000–32,000	$\geqslant$ 37,000
World (average)	6,500	20,500	World (average)	18,500	75,000
Japan	50	250	Japan	400	2,000

Table 1. Number of victims expected in high seismic hazard areas of Italy, as well as (for an equal population) in Japan and (on average) worldwide [Dolce et al. 2005; 2006].

Italian region or area	Year	Violence
Abruzzo (L'Aquila area)	1639	severe
Abruzzo (L'Aquila area)	1703	severe
Messina and Reggio Calabria	1908	very severe
Abruzzo (Avezzano)	1915	very severe
Friuli (2 main shocks, within 6 months)	1976	severe
Irpinia (Campano–Lucano earthquake)	1980	severe
Marche and Umbria (2 main shocks in the first day)	1997–98	moderate/severe
Molise and Puglia (2 main shocks, in the first and second day)	2002	moderate
Abruzzo (L'Aquila area)	2009	severe

Table 2. Violence of earthquakes in Abruzzo and of the most recent Italian events.

Equally importantly, traditionally there has been a certain lack of awareness, at both the institutional and individual levels, that severe earthquakes occur in Italy too, though less frequently than in other countries. Paradoxically, Italy's problem has been that severe earthquakes are not sufficiently frequent in this country and that, in any case, their return periods are much longer than the duration of its governments (see Table 2). In the past, the consequence was that, when a severe earthquake occurred, the government in office at that time strictly limited its action to emergency management, without investing any resources in prevention, and that seismic risk was soon forgotten even in the struck areas. It has been estimated that the overall cost of this lack of prevention policies has already been almost three times larger than the overall amount of money which would have been necessary to adequately seismically upgrade all the existing Italian constructions (apart from the thousands of avoidable victims).

Lessons learned from the San Giuliano di Puglia tragedy in 2002. With regard to the evolution of knowledge on the seismic hazard in Italy [Dolce et al. 2005; 2006; Erdik et al. 2007; 2008; Martelli et al. 2007; 2008; Sannino et al. 2009], it is noted that 70% of the Italian territory is now defined as seismic, while this percentage was estimated to be only 45% prior to 1998 and 25% prior to 1980 (seismic classification began in Italy after the 1908 Messina and Reggio Calabria earthquake, but, down to the middle of the 1970s, Italian areas were classified as seismic only after having been struck by an earthquake). In addition, although the present seismic hazard map was already known and had already been proposed by the Italian seismologists in 1998, it became official only in 2003, after the collapse of Francesco Jovine Primary School at San Giuliano di Puglia during the 2002 Molise and Puglia earthquake (Figure 24). This collapse killed 27 children, including all the youngest (those born in 1996), and it has been officially recognized that the earthquake itself was not to blame: the deaths were mainly caused by poor construction, worsened by the shoddy addition of another storey.

This seismic reclassification was enforced by an ordinance of the Italian Prime Minister (*Ordinanza del Presidente del Consiglio dei Ministri*), published in May 2003 (OPCM 3274/2003), just because of the inertia shown by the normally responsible national and local institutions (Ministry of Constructions and regional governments). Thanks to this ordinance a new seismic code was also enforced (although not yet obligatorily), which was fully different from the previous (very old and inadequate) one: while the latter was prescriptive, the new one was based on performance, consistently with Eurocodes.

Figure 24. Collapse of the Francesco Jovine primary school in San Giuliano di Puglia (Campobasso) during the 2002 Molise and Puglia earthquake, and search for survivors amid the debris.

In addition, the new Italian seismic code freed and even simplified the use of SI, ED and other modern SVPC systems and devices. In fact, it canceled the previously existing need for submitting the designs of structures protected by such systems and devices to the approval of the High Council of Public Works of the Ministry of Constructions and allowed to partly take into account the decrease of the seismic forces acting on the superstructure caused by SI, when designing the superstructure itself and the foundations. With regard to the need for submitting the aforesaid designs to the approval of the High Council of Public Works, it is worth stressing that, due to the very complicated, time-consuming and uncertain approval process, such a need, instead of correctly being a check of the adequacy of the new technologies, had hindered their development and extensive application, although they aim at saving human life and minimizing damage. Finally, OPCM 3274/2003 prescribed that the seismic safety of all strategic and public structures should have been checked by the responsible national or regional institutions within five years.

The enforcement of OPCM 3274/2003 (which was later improved by two subsequent OPCMs, then by decrees of the Ministry of Constructions in 2005 and 2008 and, finally by the new Technical Norms for Constructions) can be considered as the birth of a real prevention policy in Italy. In particular, thanks to this ordinance, the use of the SVPC systems and devices soon significantly increased in Italy (Figure 1, right), especially for the protection of schools (as a consequence of the San Giuliano di Puglia tragedy): SI of the new Francesco Jovine at San Giuliano di Puglia, which was opened to activity in September 2008, was followed by that of further 16 schools (4 of these were completed in 2009, see below).

Lessons not yet learned prior to the Abruzzo earthquake of April 6, 2009. The change of attitude towards the prevention of seismic risk caused by the San Giuliano di Puglia tragedy was, however, only partial. The consolidated general convincement that earthquakes are not a major problem in Italy was not fully canceled. For instance, only half of the new Italian hospitals designed after OPCM 3274/2003 included SI, although this kind of protection is now indispensable to ensure their full integrity and operability after an earthquake. In addition, since the use of the new code was not obligatory, many (not only designers, but, unfortunately, also some institutions owning public buildings) accelerated the completion

of the designs of even strategic and public buildings and/or of the related approval processes just to make sure that they were allowed to use the old, less stringent, code, which implied lower construction costs.

Moreover, the prescribed verifications of seismic safety of the existing strategic and public constructions went much slower than planned; even now it is far from being completed and no interventions have been undertaken, yet, in several cases, even when the problems detected are not limited to the seismic safety, but also concern the static one. Such unexpected, very worrying, situations were numerous, especially in Southern Italy, even for r.c. buildings (see, for instance, Figure 39). Finally, the obligatory use of the new seismic code was deferred year by year, thus also causing a lot of confusion: even in February 2009 it had been postponed from the end of June 2009 to that of June 2010 and only thanks to the polemics following the Abruzzo earthquake this further extension was canceled during Summer 2009 (also thanks to a resolution of the Commission on Environment, Territory and Public Works of the Italian Chamber of Deputies drafted with the collaboration of the first author of this paper).

Remarks on the Abruzzo earthquake of April 6, 2009. The earthquake which struck the L'Aquila town and 48 further municipalities in Abruzzo on April 6, 2009 (Figure 25), had a magnitude $M_w = 6.3$ and an epicentral depth of 9 km. It occurred at 3:33 local time at about 5 km south east from L'Aquila (seismic zone 1, according to the 2003 seismic reclassification of the Italian territory). It caused 298 dead, 1,600 wounded and 36,000 homeless people. Costs of 8.5 billion Euro have been estimated as necessary for the reconstruction. Here are the values of peak ground acceleration (PGA) predicted in this area for various return periods T_R, according to the Italian seismic classification, which is based on probabilistic seismic hazard assessment (PSHA):

$$
\begin{array}{cccc}
T_R: & 475\,\text{yr} & 975\,\text{yr} & 2475\,\text{yr} \\
\text{PGA}: & 0.261\,g & 0.334\,g & 0.452\,g
\end{array}
$$

Thanks to seismic monitoring systems which had been installed in the area, a large amount of data was made available by this event: in fact, there were 55 recordings of DPC and 114 of the Italian Institute for Geophysics and Volcanology (*Istituto Nazionale di Geofisica e Vulcanologia* or INGV), at epicentral
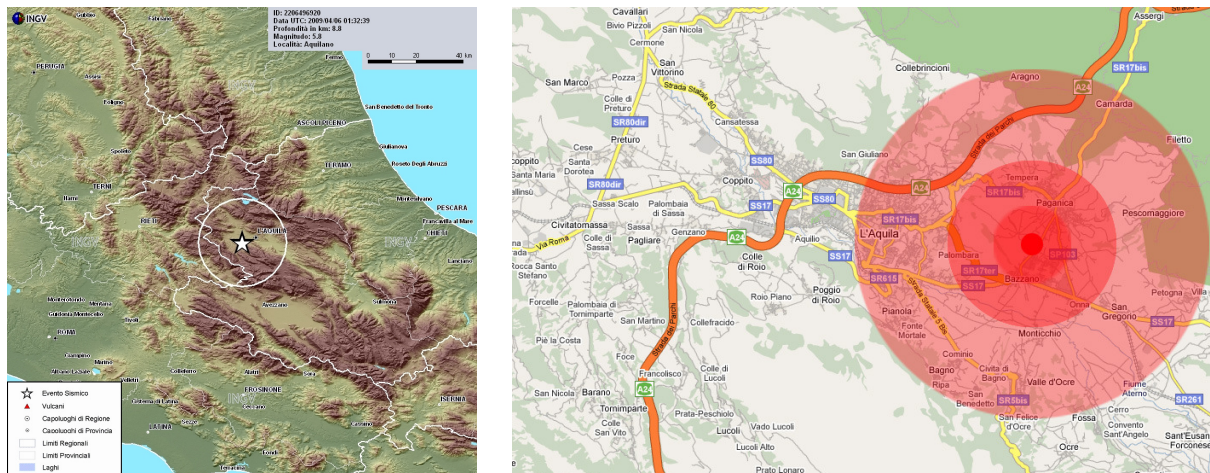
Figure 25. Epicenter of the Abruzzo earthquake of April 6, 2009, and area struck by this earthquake.

distances varying from 4.3 km to 280 km. These recordings form the largest amount of seismological data ever obtained in Italy. The following results of these measurements will be mentioned:

- a PGA value larger than 1 g was measured in one station;
- a residual maximum vertical displacement of 15 cm was detected close to the fault (zero distance);
- amplification of the seismic motion at 0.6 Hz was also detected in the epicentral zone (namely at zero distance from the fault and less than 10 km from the epicenter);
- the attenuation laws which are available in the literature underestimated the PGA values at small epicentral distances and overestimate those at large distances;
- the measurements in the epicentral zone were strongly influenced by source effects;
- the recordings of the main shock showed a clear directivity effect towards south-east;
- most recordings in the epicentral zone showed PGA > 0.3 g and in one spot (del Moro station, close to Pettino) even > 1 g;
- the response spectra ordinates were particularly large especially in the range 2–10 Hz (0.1–0.5 s), which contains the natural frequencies of most buildings of the region;
- the duration of the most energetic part of the acceleration records was only 2–5 s (in one station almost 60% of the energy was released in the first 3 s); this led to a strong impulse at high frequency, even for the vertical earthquake component, which struck buildings with a moderate number of cycles but of large amplitude;
- very large local amplifications were measured, which stresses the presence of rather poor soils.

Thus, most structures that were not ductile nor built according to reasonable engineering requirements, the nonreinforced masonry buildings (including cultural heritage monuments) and a significant part of the other buildings which were characterized by limited ductility and insufficient seismic resistance (due to poor designs or construction problems) were unable to withstand the earthquake (Figures 26–30).

Figure 26. L'Aquila (April 2009): aerial views of some parts of the town where buildings collapsed or were heavily damaged.

Figure 27. L'Aquila (April 2009): collapse of the Prefettura building (provincial headquarters of the national government) and the Santa Maria Paganica Church (right).

Figure 28. The Cathedral of Santa Maria di Collemaggio, a rare example of Abruzzo Romanesque style, prior to the earthquake, and the collapse of the roof of its baroque (not yet retrofitted) part. The façade, which had been protected by some EPDs installed on the roof some years earlier (see Figure 45), survived the earthquake; however, a steel scaffold, previously erected for an already planned retrofit, certainly helped.

Figure 29. L'Aquila (April 2009): pillars in the San Salvatore Hospital, heavily damaged due to very inadequate steel reinforcement and poor concrete quality (no inert materials are visible in the upper part of the pillar).

Figure 30. L'Aquila (April 2009): partly collapsed and heavily damaged private buildings. Note in particular the heavily damaged beam-column joints (top row).

Bridges were also damaged. At the L'Aquila Museum and elsewhere, a number of artistic masterpieces were destroyed or heavily damaged (Figure 31).

As far as cultural heritage is concerned, over 1,000 ancient monumental buildings were heavily damaged or collapsed in part, largely due to earlier incorrect or incomplete retrofits (see Figure 27, right, and

Figure 31. L'Aquila (April 2009): collapse of statues at the Museum.

Figure 32. L'Aquila (April 2009): headquarters of ANAS (the Italian agency for road construction and maintenance), which suffered mainly nonstructural damage (with the exception of two pillars, which, however, are reparable — see right. Retrofit by means of SI was possible and was suggested for this building.

Figure 28). The collapse of numerous r.c. buildings, such as the Student House, or the heavy damage they incurred (including some further public or strategic buildings) was due to very inadequate reinforcement and poor concrete quality (see Figure 27, left, and Figures 29 and 30). The importance of maintenance was evident: similar equally old buildings suffered only limited or even zero damage if they had been adequately maintained, while they were heavily damaged when maintenance had been neglected.

Luckily, several buildings suffered mainly nonstructural damage and/or minor structural one: many of them may be retrofitted by means of SI (see, for instance, Figure 32) or ED systems. To this end, the experience achieved through the retrofit of a three-storey house at Fabriano (Ancona) after the 1997–98 Marche and Umbria earthquake will be very useful: this house (Figure 33) had suffered severe nonstructural damage in the earthquake and was retrofitted by subfoundation and insertion of HDRBs in the new

Figure 33. Three-storey r.c. private house in Fabriano (Ancona), in seismic zone 2, damaged by the 1997–98 Marche and Umbria earthquake. It is the first EU application of SI in a subfoundation, the retrofit of which was completed with 56 HDRBs of three sizes in 2006, with safety certification by A. Martelli.

underground floor. For the reasons mentioned in [Dolce et al. 2005; 2006], the cost of this retrofit allowed for saving 20% of construction costs with respect to a conventional reinforcement. Obviously, SI will also be used to rebuild collapsed buildings or those being so damaged that they must be demolished.

Lessons learned from the Abruzzo earthquake of April 6, 2009. Obviously, the not yet obligatory use of the new seismic code was not to blame for the damage and collapses occurred during the 2009 Abruzzo earthquake. However, the latter were caused by the same reasons for which some builders (thanks to the support of a senator) had tried to postpone the beginning of the obligatory use of the code: again the belief that earthquakes are not a major problem in Italy. In fact, part of the damage to ancient buildings — which could be greatly reduced though not fully avoided — as well as the collapse and damage to many other structures were caused, as mentioned, by bad construction (poor concrete and absent, inadequate or insufficient steel reinforcement, especially for stirrups), not consistent with any code (even the oldest), and by lack of adequate maintenance.

Hopefully, after the Abruzzo earthquake, both Italian institutions and public opinion are now fully convinced that seismic prevention is indispensable and that the related policy will be strengthened and accelerated; in particular, that the presently best available techniques (such as SI and ED) should be extensively used for the reconstruction and retrofits in Abruzzo and that this should be done not only for strategic and public buildings, but also for residential ones. The additional construction costs (if any) are quite limited and safety is much higher. This will strongly reduce casualties and damage during the next shocks, which, by the way (according to history and also to some recent seismological studies), might unfortunately occur in Abruzzo rather soon. In addition, such a prevention policy should be extended to the entire Italian territory, because, if the earthquake of April 6, 2009 had taken place elsewhere in Italy, the consequences would not have been significantly different.

With regard to the seismic protection of existing structures, although the work to be done and money to be spent are enormous (because nearly nothing was done in the past), the efforts should be much increased. Several old buildings should be demolished and rebuilt with safe features, instead of being all considered as cultural heritage, as done to date in Italy after a 50 years life. (Not all constructions are comparable to the Coliseum!) The interventions should be scheduled based on priorities, namely beginning from the most risky structures in the areas characterized by the highest seismic hazard. The latter should be assessed by means of not only the currently used PSHA, but also of the deterministic approach, which should be considered (as it is, in the author's opinion) as complementary and already proved to be quite reliable [Dolce et al. 2005; 2006; Sannino et al. 2009; Martelli 2010b].

Reliable seismic engineering technologies and seismological methodologies exist: thus, there is no more excuse not to widely use them. However, in applying modern technologies like SI, great care must be paid to the selection of the devices, their installation and their protection from external causes of damage and some further construction details, as well as to an adequate maintenance [Martelli 2009f]. In particular, in order to ensure real safety of the isolated structure, correctly qualified, checked and protected devices should be installed and adequate inspection and maintenance should be performed during the entire structure life to ensure that the SI features remain unchanged. Otherwise, these devices, instead of enhancing protection in an earthquake (as SI does, if properly applied), will expose both human life and the entire SI technology to a great risk: in fact, since the Italian seismic code (contrary to the Japanese and US ones) allows for "lightening" both the superstructure and foundations when an SI

system is installed, the inadequate performance of the latter would make an isolated building less safe than a conventionally founded one [Martelli 2009f; 2009g].

Application of SVPC systems and devices in Italy.   As mentioned in [Dolce et al. 2005; 2006; Martelli et al. 2007; Martelli and Forni 2009b], the first applications of SVPC systems in Italy go back to 1975 for bridges and viaducts and to 1981 for buildings — thus predating those in Japan and the US by four years (compare Figure 1, right). These early applications involved the Somplago viaduct of the Udine–Tarviso freeway and a suspended steel-structure fire-command building in Naples. Thanks to its SI system (formed by sliding devices on the piles and rubber springs between the deck and the abutments), the Somplago viaduct survived without any damage the second main shock of the 1976 Friuli earthquake (when one of the decks had already been installed), unlike most other structures similarly located in the epicentral area; for the Naples building, which had been conventionally designed before the 1980 Campano–Lucano earthquake (when the site was not yet seismically classified), the insertion of neoprene bearings (NBs) at the top (to isolate the suspended structure) and, inside, that of floor dampers and STUs, allowed for not fully modifying the original design, in spite of the classification of the Naples area in seismic category 3 only after the earthquake in question.

The excellent behavior of the Somplago viaduct, in the years of construction of the Italian freeway system, caused an immediate rapid extension of the application of SVPC systems to the new Italian bridges and viaducts. Those protected by such systems were already 150 at the beginning of the years 1990s: this ensured the worldwide leadership to Italy for the number and importance of the applications in this field.

As to buildings, the extension of applications was slower in the first years, but the trend had become very promising, in this field too, at the beginning of the 1990s (Figure 1, right), after the erection of the Telecom Italia Centre of Marche Region in Ancona on 297 HDRBs and the impressive on-site tests performed on one of its five buildings. (Their safety was later certified by the first author of this paper, as mentioned, for instance, in [Dolce et al. 2005; 2006].)

On the contrary, the use of the SVPC systems and devices became very limited after such an application (Figure 1, right): in fact, the Italian Ministry of Constructions, by recognizing that no specific rules for structures provided with said systems and devices were included in the Italian seismic code in force at that time, on the one hand decided that all designs of such structures had to be submitted for approval to the already mentioned special commission of the Ministry, but, on the other hand, did not make any specific design guidelines available until the end of 1998. Moreover, such design guidelines, when they were published, resulted to be inadequate and the approval process remained uncertain, very complicated and time consuming.

Thus, in spite of its long tradition, Italy was only fifth, at least for the number of seismically isolated buildings in use, prior to the 2009 Abruzzo earthquake, with over 70 isolated buildings already opened to activity and about 30 further applications of this kind in advanced progress [Sannino et al. 2009]. Some tenths of Italian buildings had also already been protected by ED systems or SMADs (19 at the end of 2007) or STUs (28 at the same date). Moreover, there were already over 250 bridges and viaducts provided with SVPC devices and important applications of such devices, completed or planned, to worldwide known cultural heritage (Upper Basilica of St. Francis at Assisi, damaged by the 1997–98 Marche and Umbria earthquake; the Bronzes of Riace and other structures and masterpieces, such as

those shown in Figures 28 and 45–48). (Italian SVPC devices had been installed in several constructions in other countries too [Dolce et al. 2005; 2006; Martelli 2009b].)

In recent years, however, there has been a large increase of the number of applications completed and, especially, of those in progress or under design (Figure 1, right, and Figures 34–44). This change

Figure 34. Sketch of the new isolated Del Mare Hospital, during its construction in Naples, nowadays in seismic zone 2, and view of some of its 327 HDRBs. Several new Italian hospitals being or to be erected in seismic areas now include the use of SI.

Figure 35. The Emergency and Management Operative Center of the new Civil Defense Center of Central Italy in Foligno (Perugia) was designed by the GLIS board and *ASSISi* member A. Parducci of e-Campus University. Their safety will soon be certified by A. Martelli. The photo on the left shows in the foreground the main building, which is being erected on ten HDRBs of 1 m diameter, two of which are seen on the right, with provisional protective covers. Also seen on the left is the adjacent service building, isolated by HDRBs and SDs. The Foligno Center will include at least seven isolated buildings, three of which have already been completed. Its site was reclassified from seismic category 2 to seismic zone 1 in 2003, but no design changes of the structures and foundations were necessary, thanks to SI. An increase in the diameters of isolators was sufficient, as demonstrated by a study performed by ENEA.

Figure 36. The new Francesco Jovine primary school and Le Tre Torri Professional and University Centre, erected in San Giuliano di Puglia (seismic zone 2 since 2003) on a single seismically isolated slab, and its SI system (61 HDRBs and 12 SDs) during construction. The isolators were donated by the Italian ALGA, FIP Industriale and TIS manufacturing companies. The SI design is by a team of experts coordinated by the GLIS and *ASSISi* member P. Clemente of ENEA, with tests done by the University of Basilicata. Safety was certified by A. Martelli and GLIS member C. Pasquale in September 2008.

Figure 37. The first new school building of Mulazzo (Massa Carrara), protected by LRBs and SDs (right) and the new primary and secondary school of Gallicano (Lucca), protected by HDRBs and completed in September 2009. They are two of the 5 schools rebuilt or being rebuilt with SI in Tuscany, in seismic zones 2. Safety of the Mulazzo school will be certified by A. Martelli, that of the Gallicano was certified by A. Parducci.

was due at first to the new Italian seismic code, enforced in May 2003, which (as mentioned) freed and simplified the adoption of the SVPC systems, then, very recently, to the Abruzzo earthquake [Martelli and Forni 2009a].

Figure 38. The new school in Marzabotto (Bologna), in seismic zone 3, erected on HDRBs and SDs. Its safety was certified by A. Martelli in September 2010.

Figure 39. Romita High School for scientific studies of Campobasso (hosting about 1,300 students), in seismic zone 2, which was at last partly demolished and is now being rebuilt with SI, due to its very poor concrete quality (as demonstrated by an ENEA study performed after the 2002 Molise and Puglia earthquake). Safety of the new seismically isolated buildings will be certified by A. Martelli.

As already mentioned, the enforcement of the new Italian seismic code was largely a consequence of the collapse of the Francesco Jovine school during the 2002 Molise and Puglia earthquake. This school was recently rebuilt: the new Francesco Jovine, opened to activity in September 2008 (Figure 36), is the first Italian isolated school and has been judged as the safest Italian school. It is being followed by 16 further applications of this kind (5 have already been completed). Seismic protection of schools by means of SI, in addition to that of hospitals, other strategic structures and cultural heritage (Figure 31 and Figures 45–48), was a "priority 1" objective in Italy even before the Abruzzo earthquake.

After this event, this kind of protection is being further extended and planned for residential buildings too, in the framework of the retrofit/rebuilding program in Abruzzo, which should make a large use of SI and ED systems.
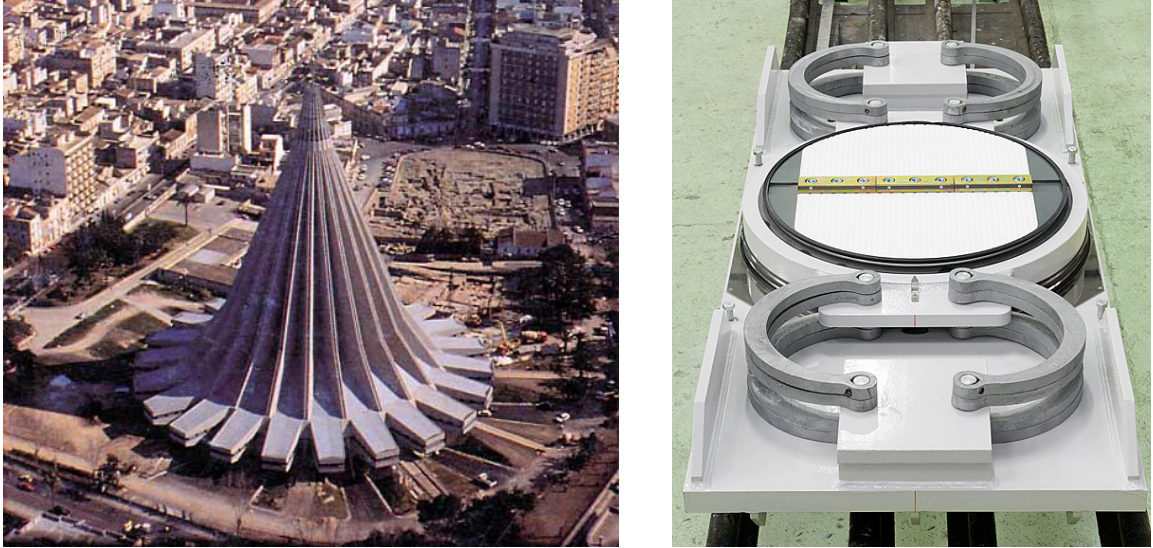
Figure 40. Shrine of the Madonna delle Lacrime in Syracuse (seismic zone 2), designed to fit 11,000: it was retrofitted in 2006 by lifting the dome (22,000 tons) and replacing the previously existing rubber supports by EPDs (right).

Figure 41. Left: Headquarters of the association Fratellanza Popolare – Croce d'Oro in Grassina (Florence), in seismic zone 2, isolated by means of SDs and VDs; it is a L-shaped building to be used for civil defense, designed by the GLIS board and *ASSISi* member S. Sorace of the University of Udine and certified as safe by A. Martelli in 2007. Right: NATO Centre in South Naples, in seismic zone 2 (399 HDRBs and 20 dissipative SDs), during construction in 2007.

In particular, the construction of 184 prefabricated houses of various materials (wood, concrete, steel), each erected on a 21 m × 57 m r.c. platform, 50 cm thick and supported by 40 steel or r.c. columns with curved surface sliding (CSS) devices manufactured in Italy (by ALGA and FIP Industriale) at the top, has been completed: these houses (Figure 44) will host first about 17,000 people who remained homeless after the earthquake and later, in a few years, students.

Figure 42. The four r.c. residential buildings of the new San Samuele Quarter of Cerignola (Foggia), in seismic zone 2, first application of the new Italian seismic code to isolated dwelling buildings, completed with 124 HDRBs (right) in May 2009, with safety certification of A. Martelli.

Figure 43. Left: residential building in San Giuliano di Puglia, isolated by 13 HDRBs and 2 SDs with the collaboration of ENEA, completed in 2007. Right: SI formed by LRBs and SDs of an 8-storey building under construction at Messina, in seismic zone 1; its safety will be certified by A. Martelli.

It is noted, however, that the CSS isolators (besides needing very careful protection from dust and humidity) had never been previously used in Italy. Building applications of similar isolators existed in other countries, like Turkey and Greece, but such devices had been manufactured in Germany (Figures 55 and 59), using a sliding material different from the Italian ones. Thus, a debate was promoted in Italy by the first author of this paper on the need for submitting the Italian CSS isolators to a very detailed experimental verification campaign, including two-directional (2D) simultaneous excitations in the horizontal plane, representing real earthquakes, at the laboratories of the University of California at San Diego, similar to those performed for the German silding isolation pendulum (SIP) devices and,

Figure 44. One of the 184 seismically isolated pre-fabricated houses erected at L'Aquila for homeless residents and CSS devices installed to isolate its supporting slab.

Figure 45. Interior of the Cathedral of Santa Maria di Collemaggio at L'Aquila (see also Figure 28) prior to the 2009 Abruzzo earthquake and view of one of the EPDs which had been installed on the roof at the beginning of the years 2000 to prevent overturning of the façade.

previously, for the American FPS devices, from which the German SIP and Italian CSS isolators derive. This debate is still ongoing (the 2D tests are required neither by the Italian code nor by the European one, although they had been found necessary for both the FPS and the German SIP isolators), but a first positive result has already been achieved: in fact, the CSS isolators of FIP Industriale installed at L'Aquila were submitted to these 2D tests in November 2009, with excellent results.

Legislative measures recently adopted to promote the use of the antiseismic systems. The Italian government, besides making the use of the new seismic code at last obligatory (during Summer 2009, in the framework of the law for the rebuilding in Abruzzo), decided some legislative measures to favor the extension of the adoption of the antiseismic systems and devices (especially of SI). These measures,
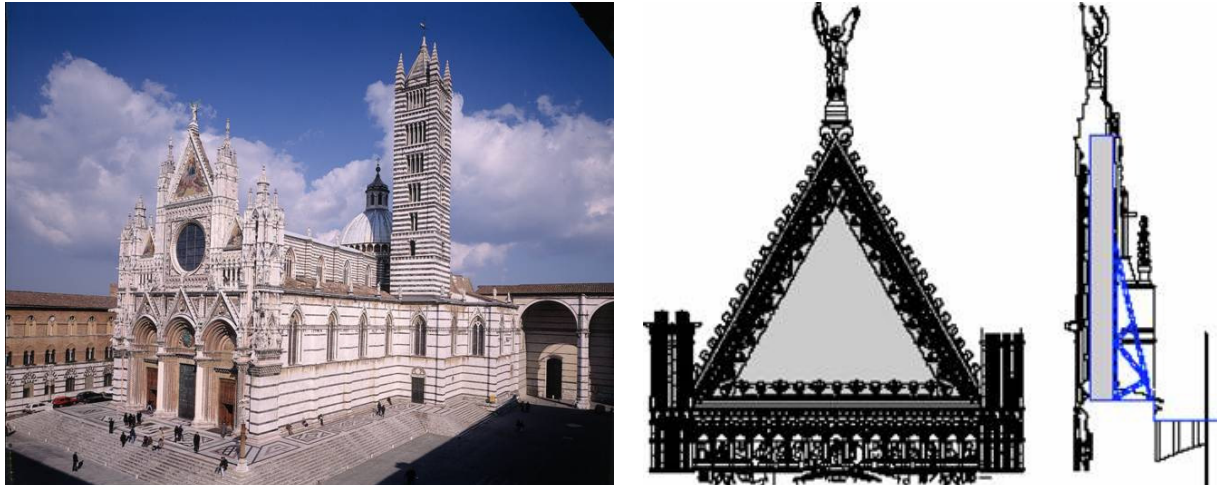
Figure 46. The Orvieto Cathedral. Right: position of the recentering VDs inserted some years ago to prevent overturning of its façade.

Figure 47. The wooden Roman ship excavated at Herculaneum, near Naples, in seismic zone 2, which was recently protected in the local museum by means of 3D isolators formed by three spheres and a re-centering rubber cylinder for the horizontal SI and a spring and a VD for the vertical one.

adopted in December 2009, were largely based on proposals of GLIS and, in particular, of the first author of this paper. For instance, economic incentives have been included in the project of the new so-called "Quality House" national law for those adopting such technologies and even more favorable measures were recently decided by the regional government of Sicily.

With regard to the seismic protection of schools, it is worthwhile reporting a translation of the whole text of an "agenda" (consistent with the declaration [UNESCO-IPRED-ITU 2009], and based on a proposal of Martelli [2010c]), which was submitted by the President of the Commission on Environment, Territory and Public Works of the Chamber of Deputies [Alessandri et al. 2009] in the framework of the

Figure 48. Michelangelo's marble David, displayed at the Galleria dell'Accademia, in Florence: note the worsening of the cracks in its ankles in recent years (right), which make it very vulnerable to both seismic and environmental vibrations. A study to evaluate the feasibility of SI of the masterpiece has been proposed by Prof. Antonio Borri of the University of Perugia and the first author [Dolce et al. 2005; 2006, Martelli 2009a]. Consideration of the losses at the L'Aquila Museum (Figure 31 on page 95) may give pause to the opponents of the development and installation of an adequate seismic protection system for Michelangelo's David.

vote of the 2009 Financial Law on December 16, 2009, and was immediately accepted by the Italian government [Camera dei Deputati 2009, pages VII–VIII]:

"The Chamber of Deputies, considering that:

- paragraph 229 of article 2 of the bill under examination contains measures aimed at guaranteeing the safety of schools and, in this framework, in order to ensure the maximum quickness for the completion of the interventions necessary to put the school buildings in safe condition and to seismically retrofit them, prescribes, in particular, that, within thirty days from the date of enforcement of the financial law itself, the interventions which can be immediately undertaken shall be the first to be identified;

- it shall be stressed in such a framework that, among all construction types, the school buildings, together with hospitals, should be the most protected from earthquakes, which are the events characterized by the highest risk in Italy;

- for such buildings the objective shall be the full safety of the students and the other present persons;

- to this aim, besides preventing the collapse of school buildings in the case of earthquakes (which is the requirement foreseen by the seismic codes, including the new Technical

Norms for Constructions), it is also indispensable to guarantee their full integrity, with no damage even to the nonstructural elements and the objects contained;

- furthermore, the level of the seismic vibrations transmitted by the ground to the buildings shall be minimized, to prevent panic;

- the aforesaid objectives cannot be achieved by the conventional antiseismic design, which is based on the "robustness" of structures, while they can be fully achieved thanks to base seismic isolation and can be achieved to a large extent by inserting energy dissipation systems inside the structures themselves;

- more than half of the school buildings existing in our country result to be inadequate to withstand the earthquakes to which they may be subjected;

- for many of such buildings retrofits able to guarantee a sufficient seismic safety are very difficult or too costly, either because they are monumental buildings (thus also subjected to the conservation requirements), or because they are rather old;

- in the first case it would be desirable to assign the buildings to a different use and move the school functions to other structures, possibly of new construction; in the second the best solution would be demolition and subsequent *ex novo* rebuilding;

- for the new school buildings there are no obstacles of technical nature against their construction with seismic base isolation (in Italy 5 new isolated schools have already been completed and further 12 are under construction); in favor of this technological solution there are, besides the largely higher safety level with respect to a conventionally founded construction, the overall economic balance too (which takes into account not only the construction costs, but also those of demolition and repair, removal and storage of the debris, displacement of the school activities) and the evident environmental and energetic benefits;

- with regard to the sole construction costs, it is worthwhile noting that, in Italy, the school buildings have a limited number of stories and usually do not need for an underground storey; thus, although the new Italian seismic code allows for lightening the superstructure and foundations of seismically isolated buildings, for school buildings with base isolation some additional construction costs due to the use of such a protection (isolators, an additional storey above them, etc.) are sometimes to be foreseen;

- for interventions on existing school buildings, seismic isolation may be used only if the room necessary for the "rigid body" motion which characterizes the building part supported by the isolators exists or can be created around the building; the related costs may be even significantly lower than those characterizing a conventional retrofit, because it is possible to avoid stripping the structure, strengthening pillars and beam-pillar nodes and inserting shear walls;

- when seismic isolation is not applicable, it is usually possible to seismically improve the buildings by inserting dampers inside them; in this case the cost of dampers is usually largely balanced by the possibility of avoiding stiffening of the structure;

- in Italy the most famous seismically isolated building is the new Francesco Jovine or "Angels of San Giuliano", school; such a school was the first, among those protected by seismic isolation, to be completed in Italy, in September 2008; the isolation system was designed by a team of experts coordinated by ENEA and the structure was subjected to inspections during construction and safety certification of an expert of the Agency; ENEA also contributed to the design of the seismic isolation system and/or certified or will certify the safety of further new schools, in Marzabotto (Bologna), Campobasso, Vado (Bologna) e Mulazzo (Massa); to be cited are also the design and safety certification of 4 further new seismically isolated schools in Tuscany, performed in the framework of the Collaboration Agreement on "Applications of seismic isolation and other modern antiseismic technologies to constructions and buildings, in particular for educational use" signed by Tuscany region, ENEA and GLIS in 2004;

- previously other existing schools had been seismically improved by means of energy dissipation systems, first of all at Potenza and its province, then in the Marche region too: among the latter it is worth citing the Gentile Fermi school in Fabriano, of rationalist architecture, which, due to the damages suffered during the 1997–98 Marche and Umbria earthquake, was seismically improved by means of visco-elastic dampers developed in the framework of the EU-funded project REEDS promoted by ENEA;

- ENEA, in the framework of school building, may profitably contribute in its specific competence fields, among which:

  - the development of new antiseismic devices and, by means of its experimental equipment, tests on such devices and mock-ups of structures protected by them;
  - the definition of seismic input, also by means of on-site seismic tests, and analysis of local seismic response and seismic microzoning, with definition of site-specific spectra and/or acceleration time-histories;
  - the evaluation of the seismic vulnerability of existing buildings, also by means of experimental tests on the materials and structures, with the identification of the most suitable techniques for the seismic retrofit of the structures;
  - specialist consultancy in support to the structural design, with particular reference to the sizing and verification of the modern seismic protection systems, for both new buildings and retrofits of existing buildings;
  - specialist consultancy in support to the installation of the antiseismic devices;
  - inspections during construction and final safety certification of the buildings;
  - seismic monitoring of the structures,

commits the government, in the framework of the realization of the provisions of paragraph 229 of article 2 of the bill under examination, to evaluate the opportunity of involving ENEA and, in the affirmative, to draw up specific agreements, as to define interventions for the seismic safety of schools which are not only highly effective, but are also both the most advanced with regard to the construction technologies to be adopted and as advantageous as possible as far as costs, safety and functionality are concerned."
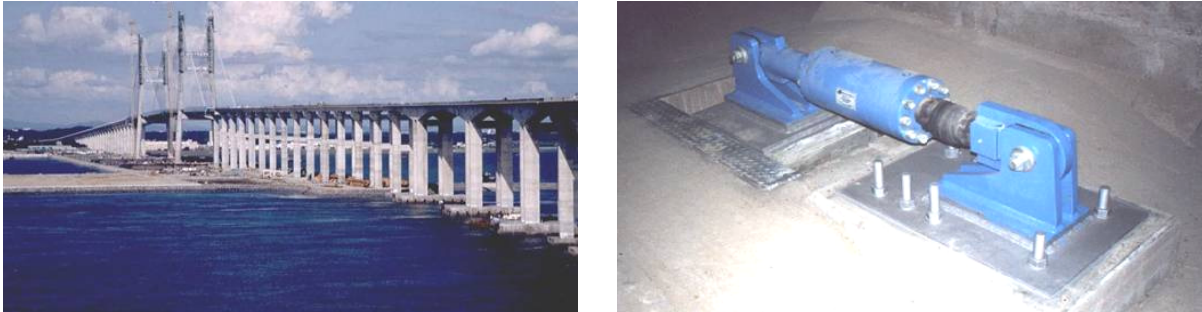
Figure 49. Approaches of the Seo-Hae Granel Bridge in South Korea (overall length 5820 m, height of piles 12–60 m), which were retrofitted by means of 54 Italian VDs ($K = 100$ kN/mm) in 2000–2001.

7. South Korea

In South Korea SI has already been applied for several years [Zhou et al. 2009]. Nowadays, it includes about 400 bridges and viaducts, partly with devices manufactured in Italy (Figure 49), as well as 13 large LNG tanks at Inchon and Pyeong–Taek. In October 2008, however, only one building was seismically isolated (in 1999) and only one (a 30-storey residential building) was protected by dampers (VEDs). Anyway, the use of the SVPC systems is now rapidly increasing, especially for ED, which is being more and more used for protecting high-rise buildings and long span bridges. This is a consequence of the magnitude 7.0 Busan–Fukuoka earthquake of 2005 (with epicenter between Korea and Japan) and of the more recent event of January 2007, with a much lower magnitude ($M = 4.8$), but with epicenter in the Korean territory.

8. Taiwan

After the 1999 Chi Chi earthquake and the consequent modifications of the national seismic code (performed in 2002 and 2006), which now permits and even promotes the use of SI and other SVPC systems in Taiwan, the adoption of such systems is increasing more and more in this country and includes both new constructions and retrofits [Zhou et al. 2009]. Frequently, SVPC devices manufactured in Italy have been used. As to the isolated buildings, those completed or under construction (initially mainly hospitals, but, more recently, residential buildings too) were already 29 in May 2007, against the 25 of June 2005; at the same date, the isolated bridges and viaducts were over 20. In addition, there is an even larger number of buildings that are protected by ED systems in Taiwan: these were already 85 in 2005. The isolators used for buildings are HDRBs and LRBs and have been installed either at the base or the top of the first floor. Dampers are of various types, namely BRBs, EPDs, VDs, VEDs, etc.

9. Continental France and Martinique Island

France was one of the first countries that developed and applied the modern SI systems [Erdik et al. 2008]. Its first applications date back to the 1970s, when they amounted to a few nuclear plants and structures and some civil buildings and industrial components. The isolators used were multilayer NBs and, in

Figure 50. An isolated school in the French Martinique island (France), with a view of some NBs and VDs that protect it.

particular, the so-called "GAPEC System". From 1977 to 1989 this system was adopted both to protect new constructions in the continental France and to erect or retrofit some plants and electrical or electronic components in the US and Chile. The applications in France in this period included 11 new residential buildings and (in 1978) the new high school of Lambesc (a town that had been partially destroyed by the 1909 Provence earthquake), besides 4 industrial (partly high risk) components or structures and 3 LNG tanks (in Rognac in 1993). Later, VDs were also developed in France and were applied to bridges, viaducts and some buildings and chemical plants too, both in this country and abroad (e.g., together with Italian SDs, to the building of Figure 41).

As to the French applications of SI performed in the nuclear field in the 1970s, it is worthwhile reminding those to the Pressurized Water Reactors (PWRs) of Cruas and spent nuclear fuel storage pools of La Hague, carried out to allow for the use of standardized plant designs in these sites too, which are characterized by seismic intensities larger than those considered in such designs (for the same reason SI was also used to protect the Koeberg PWR, in South Africa, which was built by the French industry). Based on this experience and the subsequent remarkable developments of SI techniques, the French already decided to isolate both the Jules Horowitz Reactor (for which construction is in progress) and the ITER plant for the controlled fusion, both located at the Cadarache Research Center (PGA = 0.33 g).

With regard to civil buildings, on the contrary, the most important French building applications of SI are now in progress in its Martinique island. This has a relatively small area, thus, the whole territory will shake in an earthquake. Buildings and houses are very vulnerable there (similar to the neighboring Guadeloupe). There is no hope for the inhabitants to benefit from safe zones. Moreover, the insular situation complicates the arrival of helps, taking into account that two thirds of the airport landing strip are liquefiable. The most recently isolated buildings that were built in the island make use of French devices, namely NBs (the "GAPEC System" until 2001) in parallel (at least for the protection of important structures) to VDs (Figures 50 and 51). We note that, some years ago, the Martinique Regional Council decided that all secondary schools, all Council buildings and all other public buildings it funds, even in part, must be seismically isolated, and financial support must be provided to private individuals using SI [Erdik et al. 2008]. By March 2007, SI had already been used to protect four primary or secondary schools (each consisting of several buildings — see Figure 50), two residential buildings and the Earth

Figure 51. Left: a small seismically isolated building in the French Martinique. Right: the New Zealand Parliament at Wellington, a historic building erected in 1921 and retrofitted using LDRs in 1992–93.

Science Centre at Saint-Pierre (which was designed to withstand a PGA of 0.45 g). New applications that were in the design phase included two more secondary schools, one college, four residential buildings, two important public buildings, a museum and a private clinic.

In continental France, by contrast, further application of SI to civil buildings has been hampered by an unfavorable seismic code that has been in force for several years, the moderate seismic hazard of most of its territory and the consequent limited interest of the French public opinion and institutions in seismic risk mitigation.

10. New Zealand

New Zealand, which is characterized by a high seismicity, is one of the countries where the SVPC systems took origin [Zhou et al. 2009]. These are, in particular, the LRBs (which have been applied since 1974 based on researches begun in 1967) and other devices based on the lead technology (e.g. lead dampers). Nowadays, SI is a fully accepted construction technique in this country, to protect both buildings (even the historic ones) and bridges and viaducts. In addition, the New Zealand manufacturing industry is very active in other countries, as well (e.g., in Turkey).

In spite of the country's limited population, 19 buildings, besides several bridges and viaducts, had already been protected by means of SI in June 2005 (Figure 51, right, and Figure 52). In May 2007, the

Figure 52. Wellington, New Zealand: the isolated Te Papa Museum (left) and the Maritime Museum (right), retrofitted with SI in 1993.

construction of the Wellington Regional Hospital (supported by 135 LRBs and 135 SDs) was in progress, and 2 new buildings of the Wanganui District Hospital were being designed. The latter are isolated by 90 RoGliders, a new SI system conceived in New Zealand, combining a SD with a rubber membrane: this system is very suitable for light structures, like the aforesaid buildings [Erdik et al. 2008]. Further new applications that were already planned in 2007 included the Christchurch Hospital (which behaved very well during the quake of September 3, 2010), the New Zealand Supreme Court Building, the retrofit of a Rankine commercial building (performed without any interruption of the activities) and rising of an existing eight-storey building at Wellington, with further 8 stories. At the time being the seismically isolated buildings in New Zealand are over 30, which makes this country third at worldwide level (after Japan and Armenia) for the number of such a kind of applications per residents.

11. Armenia

With regard to Armenia, it is worthwhile stressing again that, after Japan, this country has the largest number of building applications of SI per capita, despite being a small developing country that did not start using SI until several years after most of the countries mentioned earlier [Zhou et al. 2009]. Such applications already number 32, to both r.c. and masonry buildings, including some important retrofits. Retrofits consist of both base SI and the erection of a so-called additional isolated upper floor (AIUF). The related developed and applied techniques allow for not interrupting activities or occupation of the buildings. Moreover, since 2003–2004 even rather tall isolated buildings have been erected at Yerevan, which hosts a large part of the Armenian population (Figure 53 and Figure 54, left).

After the first applications, which made use of LDRBs and HDRBs, the SI devices used at present in Armenia are medium damping rubber bearings (MDRBs), which are steel-laminated neoprene isolators characterized by 8%–10% damping ratios. The MDRBs are manufactured in Armenia and have been also exported (e.g., for applications to bridges and viaducts in Syria). In the aforesaid tall buildings they are arranged in groups of relatively small diameter isolators in each SI position, also in order to minimize torsion effects. Experts of the American University of Armenia have provided important contributions as

Figure 53. Left: the Our Yard multi-functional complex in Yerevan, with 10 to 16 storeys, was isolated in 2006 by means of MDRBs. Right: a group of such bearings.

Figure 54. Left: the 15-storey Cascade multifunctional complex, isolated in Yerevan by MDRBs in 2006. Construction of even taller buildings is in progress. Right: the roof of the new Ataturk Airport in Istanbul, isolated by means of 100 FPS devices in 1999.

collaborators with projects in the Russian Federation (including the first of the previously cited retrofits performed in that country), Romania and Nagorno-Karabakh.

12. Turkey

The Turkish applications of the SVPC systems started after the 1999 Kocaeli and Duzce earthquakes, which damaged the now seismically isolated new Ataturk airport in Istanbul (it was being conventionally constructed at that time) — see Figure 54 — while the Bolu viaduct of the Istanbul–Ankara freeway was saved from collapse by EPDs manufactured in Italy [Dolce et al. 2005; 2006]. Thus, the airport was retrofitted by inserting FPS devices below the roof. Further applications of SI were later performed, to both new and existing structures, including, by May 2007, the retrofit of the Antalya international airport terminal, two new hospitals, one hotel, freeway viaducts (including the Bolu viaduct) and two large LNG tanks at Aliaga; see Figure 55 and [Dolce et al. 2005; 2006].

Figure 55. Isolated buildings in Turkey. Left: the T.E.B. Headquarters, a building which was under construction on 87 LRBs and LDRBs in Istanbul in 2006. Right: Söğütözü Congress and Commercial Centre in Ankara, isolated using 105 SIP devices manufactured in Germany in 2007.

Further applications completed in the last two years or in progress include important bridges and viaducts, two further airport structures (one terminal and one hangar), a high school and a mosque. The SI retrofitting of numerous schools and hospitals in Istanbul is foreseen in the framework of an important project [Zhou et al. 2009]. The SI systems initially used in Turkey consisted of FPS devices, while now RBs (partly manufactured in Italy) and SIP devices manufactured in Germany are also being used.

13. Mexico

In May 2007 the Mexican applications of SI were only seven (besides four new projects under development, including the construction of the new Basilica of Guadalajara), while those of ED systems were already 25 [Erdik et al. 2008]. The first, begun in 1974, encompasses two bridges, three civil buildings,

Figure 56. The Legaria Secondary school at Mexico City (first Mexican application of SI, performed in 1974) and one of its rolling SI devices, developed in Mexico.

Figure 57. SI of the printing press of the Mexican Reforma Newspaper (1994) and of the Mural Newspaper building (1998).

one factory for the production of microchips at Mexicali and the printing press of the Reforma Newspaper (Figures 56 and 57). Most of these applications (5) make use of an SI rolling system developed in the country. Those of ED, on the contrary, initiated in 1989 and all to buildings (16 at Mexico City and 9 at Acapulco), were performed with devices manufactured in the USA: the most common (in 16 cases) were the so-called added damping and stiffness (ADAS) EPDs, but VDs too are getting a footing. Fourteen of the aforesaid applications were retrofits of existing buildings.

14. Greece

In Greece, the SVPC systems have already been applied to a limited number of civil structures (only four buildings and some bridges and viaducts had been completed with such systems in 2007), but also to two large LNG tanks, which were isolated at Revithoussa with FPS devices in the 1990s, and a ceiling of archaeological excavations [Erdik et al. 2008]. It is noted that some important Greek civil structures have been protected by isolators or dampers manufactured in Italy [Dolce et al. 2005; 2006] Remarkable examples of application of Italian devices are the ceiling of the new international airport Eleftherios Venizelos, isolated by means of 8 HDRBs and 128 multidirectional RBs with superposed friction plates in 1998, and more recent applications such as those shown by Figure 58. In October 2008 only two Greek buildings were isolated by devices manufactured in countries other than Italy, in this case German SIP devices: both were located in the Onassis Centre in Athens (Figure 59).

Figure 58. Left: the Rion–Antirion bridge in Greece, 12 km in length and protected, together with its approaches, by Italian SVPC devices, including 188 VDs. Right: the International Broadcasting Centre in Athens, isolated in 2003 by means of 292 Italian HDRBs.

15. Cyprus

Cyprus lies on the southern part of the diffuse boundary between the African and Eurasian plate in a relatively active seismic zone; there, the majority of buildings is relatively stiff, with fundamental vibration frequencies that fall within the usually high seismic energy field, rendering them ideal candidates for the application of SI. Nevertheless, in May 2009 its use and, in general, that of SVPC techniques were still

Figure 59. Left: the Onassis Centre in Athens, with the Acropolis Museum, isolated in 2007 by 94 German SIP devices in 2006 (left). Right: the Onassis House of Letters and Fine Arts, during its construction, again with German SIP devices.

limited to a handful of practical applications: a multistorey r.c. building of the Cyprus Sports Organization, which had been protected by steel braces with VDs prior to May 2007; three commercial/industrial buildings with steel rigid frames and frames with eccentric bracing, where HDRBs (Figure 60) or FPS devices were placed on top of the basement columns; a retrofit planned for a multistorey building for the Telecommunications Authority of Cyprus, to be partly supported FPS devices; and three highway bridges, supported either by LRBs or FPS devices [Phocas et al. 2009].

Figure 60. The Shakolas Park Commercial Centre at Nicosia (Cyprus), designed by the Italian GLIS board and *ASSISi* member G. C. Giuliani and his son of Redesco (Milan), formed by two buildings with mixed r.c. and steel structure, with 164 Italian HDRBs installed at top of the basement columns, during construction in 2007.

16. Portugal

In Portugal, the use of the SVPC systems has been so far almost exclusively limited to bridges and viaducts, to which there is already a significant number of applications. In October 2008 [Sannino et al. 2009], the only isolated buildings were the La Luz new hospital and the adjacent residence for old people; they were isolated with 315 HDRBs (Figure 61). The isolators installed in these buildings and the SVPC devices used in a large part of the Portuguese bridges and viaducts were manufactured in Italy.

Figure 61. The new La Luz new hospital in Lisbon, which was base-isolated in 2006, together with a residence for old people, by means of 315 Italian HDRBs.

17. Iran

In Iran the use of SVPC systems recently began in an extensive way, mainly with the application of RBs manufactured in Malaysia to a huge number of residential buildings (several hundreds) at Parand, a new town being constructed near Tehran; however, some problems occurred during construction and only 5 buildings were completed to date [JSSI 2009]. Installation of SVPC devices manufactured in Italy also began (a hotel was retrofitted by means of Italian dampers). In addition, there are some very interesting designs, for instance one for the retrofit of the Iran Bastan Museum at Teheran with SI, developed in the framework of a collaboration between Italy an Iran, which (among others) involves the International Institute of Earthquake Engineering and Seismology of Tehran, *ASSISi* and GLIS members representing the Mediterranean University of Reggio Calabria, ENEA and the Abdus Salam International Centre of Theoretical Physics of Trieste [Erdik et al. 2008].

18. Canada

In Canada the use of ED systems (frequently BRBs) is rather popular [Zhou et al. 2009], but that of SI devices began only recently (Figure 62): the beginning of construction of the first Canadian isolated building was recently reported.
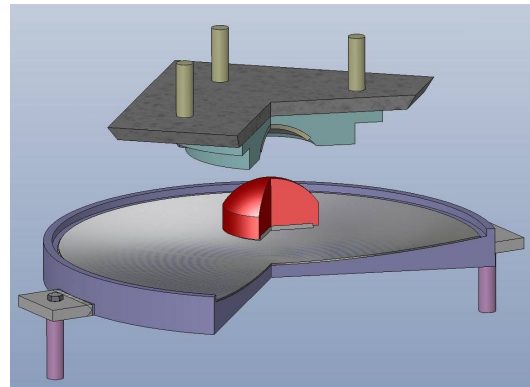

Figure 62. Golden Ear Bridge (Canada), isolated in 2007 by means of Italian CSS devices.

Figure 63. The new building of the Hospital Militar de Santiago (80,000 m^2), in the community of La Reina, under construction in 2006. It is equipped with 114 HDRBs and 50 LRBs.

19. Chile

Chile, where the first isolated building (the Communidad Andalucia residential building) dates back to 1992 [Dolce et al. 2005; 2006], is particularly active in the development of new antiseismic systems, but new application of SI to buildings is hampered by very penalizing design rules, consistent with US ones [Erdik et al. 2008]: the only new isolated building under construction in 2006 was a large hospital in Santiago (Figure 63), completed in 2009. Notably, the buildings just mentioned behaved very well during the quake of February 27, 2010.

20. Venezuela

In Venezuela a considerable number of railway bridges and viaducts have been protected by dampers manufactured in Italy; see Figure 64 and [Sannino et al. 2009].

Figure 64. The The Caracas – Tuy Medio railway in Venezuela (26 isostatic span viaducts, overall length = 7,775 m, 217 spans), protected by over 1,500 isolators manufactured in Italy in 1999–2003.

21. Indonesia

In Indonesia there are already at least two isolated constructions: a demonstration residential building erected on HDRBs in 1994, in the framework of an UNIDO-funded project [Dolce et al. 2005; 2006], and the Medan City Hall, later protected by Italian isolators [Sannino et al. 2009].

22. Macedonia

In Macedonia Italian HDRBs were used to isolate the new Test Laboratory Building of the Skopje University some years ago. Furthermore (see [Erdik et al. 2008] and Figure 65, left), the poorly steel-laminated and very degraded LDRBs of Johan Heinrich Pestalozzi Primary School at Skopje (which was the first modern application of SI) were replaced by locally manufactured HDRBs in 2007: the previous bearings had been installed to protect the aforesaid school when it was erected in the 1960s, after the violent Skopje earthquake of 1963.

Figure 65. Left: the isolated Pestalozzi school at Skopje (Macedonia), built in the 1960s. Top right: a very degraded original low damping rubber bearing (LDRB). Bottom right: a new HDRB, next to original LDRBs yet to be replaced.

23. Romania

In Romania the use of SI began only recently (Figure 66, left), with Italian and Armenian projects (see end of Section 11). Romania is expected to invest heavily in SI, due to the large energy content at low frequencies which characterizes earthquakes in a considerable part of its territory [Sannino et al. 2009].

24. Other countries

The authors are aware of at least one isolated building each in Algeria, Argentina, Israel, India and Switzerland, and a certain number of isolated bridges and viaducts in further countries such as Bangladesh.

Figure 66. Left: retrofit design with SI of the Victor Slavescu monumental building in Bucharest, Romania, erected in 1905 (55.2 m × 20.87 m; height = 22.5 m). Right: residential building for university students at Mendoza, Argentina, isolated by means of four 3D German GERB isolators.

The building in Argentina, erected at Mendoza close to an active fault, has been protected by German 3D isolators (Figure 66, right).

25. Conclusions

SI and the other SVPC technologies have been already widely used in over 30 countries and their application is increasing more and more, for both new constructions and retrofits, for all kinds of structures. The features of the design rules used, as well as earthquake experience, have plaid a key role on the success of the aforesaid technologies. Japan is largely the leading country for the number of applications of both SI and ED systems. It is now followed by China, Russia, the US and Italy. Iran might soon get the second place for the number of isolated buildings, if the huge project consisting in the SI of hundreds of new residential buildings at Parand (a new town under construction near Tehran) will be completed as planned.

Italy (where the contributions provided by ENEA have been of fundamental importance) is the leading country at European level, with regard to both SI and ED of buildings, bridges and viaducts. In addition, it is the worldwide leading country for the use of SVPC systems (in particular SMADs and STUs) to cultural heritage. Its applications are being significantly extended after the 2009 Abruzzo earthquake. Italian SVPC devices have been installed in several other countries too.

SI is now worldwide recognized as particularly beneficial for the protection of strategic constructions like civil defense centers and hospitals (by ensuring their full integrity and operability after the earthquake) and for schools and other highly populated public buildings (also because the large values of the superstructure vibration periods minimize panic). Some codes (e.g., those adopted in Italy, China, Armenia, etc.) allow for taking advantage of the reduction of seismic forces operated by SI: their use makes SI attractive for the residential buildings too, because the additional construction costs due to the use of this technique (if any) are very limited.

In order to really strongly enhance the seismic protection of our communities, an extensive application of the antiseismic systems is necessary [JSSI 2009]: to achieve this objective, legislative measures and economic incentives, such as the first ones that were recently decided in Italy, may considerably contribute, especially in the countries where the perception of seismic risk is not yet sufficient.

Hopefully, the use of SVPC systems (in particular SI) will strongly increase for the protection of cultural heritage and high risk plants, as well. For the first, the problem is the compatibility with the conservation requirements. With regard to the latter, SI has a great potential not only for nuclear structures, but also for chemical components like LNG tanks, for which, to date, only very few applications exist (in South Korea, China, Turkey, France, Greece and, soon, Mexico: in fact, detailed studies have shown that SI is indispensable for such components in highly seismic areas [Dolce et al. 2005; 2006; Martelli 2009a].

However, it should be kept in mind that the use of SI in countries like Italy, where designers are allowed by code to decrease the seismic forces when adopting this technology, requires very careful selection, design, installation, protection and maintenance *during the entire life* of the isolated structure: otherwise, safety could be lower than for if conventional techniques were used.

References

[Alessandri et al. 2009] A. Alessandri, F. Rainieri, and M. Lanzarin, "Ordine del giorno n. 9/2936-A/50 (Agenda nr. 9/2936-A/50)", pp. 51–53 in Atti parlamentari, XVI Legislatura – allegato A ai resoconti – seduta del 16 dicembre 2009 – N. 259, Rome, 2009.

[Camera dei Deputati 2009] Camera dei Deputati, Roma, Atti parlamentari, XVI Legislatura – allegato A ai resoconti – seduta del 16 dicembre 2009 – N. 259, 2009.

[Dolce et al. 2005] M. Dolce, A. Martelli, and G. Panza, *Proteggersi dal terremoto: le moderne tecnologie e metodologie e la nuova normativa sismica*, 2nd ed., 21mo Secolo, Milan, 2005.

[Dolce et al. 2006] M. Dolce, A. Martelli, and G. Panza, *Moderni metodi di protezione dagli effetti dei terremoti*, 21mo Secolo, Milan, 2006.

[Erdik et al. 2007] M. Erdik et al. (editors), Abstract book for the *ASSISi* Tenth World Conference on Isolation, Energy Dissipation and Active Vibrations Control of Structures (Istanbul, 2007), TASI, 2007.

[Erdik et al. 2008] M. Erdik et al., *Isolation, energy dissipation and active vibrations control of structures – proceedings of the ASSISi 10th World Conference* (Istanbul, 2007), 2008.

[JSSI 2009] *Proceedings of the International Workshop Celebrating the 15 Year Anniversary of JSSI*, in DVD, Tokyo, 2009.

[Katayama et al. 2008] T. Katayama, J. Chen, et al., Proceedings of the Fourteenth World Conference on Earthquake Engineering (14WCEE) (Beijing, 2008), CAEE and IAEE, Beijing, 2008.

[Martelli 2008a] A. Martelli, "Recent progress of application of modern anti-seismic systems in Europe, 1: Seismic isolation", in Proceedings of the 14th World Conference on Earthquake Engineering (14WCEE) (Beijing, 2008), edited by T. Katayama et al., CAEE and IAEE, Beijing, 2008.

[Martelli 2008b] A. Martelli, "Recent progress of application of modern anti-seismic systems in Europe, 2: Energy dissipation systems, shape memory alloy devices and shock transmitter units", in Proceedings of the 14th World Conference on Earthquake Engineering (14WCEE) (Beijing, 2008), edited by T. Katayama et al., CAEE and IAEE, Beijing, 2008.

[Martelli 2009a] A. Martelli, "Application of passive anti-seismic systems", pp. 281–293 in *Earthquake resistant engineering structures, VII* (Proceedings of ERES 2009), edited by M. Phocas et al., Wit Press, Southampton, 2009.

[Martelli 2009b] A. Martelli, "Lessons learned from recent earthquakes in Italy: from the San Giuliano di Puglia tragedy in 2002 to the collapses in Abruzzo in 2009", in Extended Abstract Volume, UNESCO-IPRED-ITU International Workshop on "Make the Citizens a Part of the Solution" (Istanbul, 2009), 2009.

[Martelli 2009c] A. Martelli, "Anti-seismic systems: state of the art of development and application", pp. 41–70 in *Modern systems for mitigation of seismic action* (Bucharest, 2008), edited by U. Sannino et al., AGIR, Bucharest, 2009.

[Martelli 2009d] A. Martelli, "Development and application of innovative anti-seismic systems for the protection of cultural heritage", pp. 43–52 in *Proceedings of the First International Conference on Protection of Cultural Heritage* (PROHITECH 2009), CRC Press / Taylor and Francis, Leiden, 2009.

[Martelli 2009e] A. Martelli, "Application of seismic isolation in Italy and other countries", pp. 4 and 13–20 in *Proceedings of the International Workshop Celebrating the 15 Year Anniversary of JSSI*, Tokyo, 2009.

[Martelli 2009f] A. Martelli, "Edifici isolati, effetto traino dell'Abruzzo: Le recenti applicazioni dei sistemi antisismici e le raccomandazioni della comunità scientifica internazionale per il loro corretto utilizzo", *Rivista degli Ingegneri del Veneto* (*FOIV*) **27** (2009), 38–44.

[Martelli 2009g] A. Martelli, "Speciale moderne tecnologie antisismiche: Dal 17 al 21 novembre 2009 si è tenuta a Canton l'"11th World Conference on Seismic Isolation, Energy Dissipation and Active Vibrations Control of Structures", manifestazione biennale dell'*ASSISi* – Edifici isolati, crescono le applicazioni in Cina, in Italia ed in altri paesi – Un effetto dei terremoti di Wenchuan e dell'Abruzzo", **20**:4 (2009), 49–57.

[Martelli 2010a] A. Martelli, "Lessons learned from recent earthquakes in Italy: from the San Giuliano di Puglia tragedy in 2002 to the collapses in Abruzzo in 2009", in Proceedings of the UNESCO-IPRED-ITU International Workshop on "Make the Citizens a Part of the Solution" (Istanbul, 2009), 2010.

[Martelli 2010b] A. Martelli, "On the need for a reliable seismic input assessment for optimized design and retrofit of seismically isolated civil and industrial structures, equipment and cultural heritage", *Pure Appl. Geoph.* (2010). Pageoph Topical Volume on Advanced Seismic Hazard Assessments, DOI 10.1007/s00024-010-0120-2.

[Martelli 2010c] A. Martelli, "Sicurezza sismica delle scuole: possibili contributi dell'ENEA", in *Il portale dell'ingegneria sismica*, 2010. Available at http://tinyurl.com/MartelliSicurezza.

[Martelli and Forni 2008a] A. Martelli and M. Forni, "State of the art of development and application of antiseismic systems in Europe and other countries", pp. 1272–1293 in *Proceedings of the 2008 Seismic Engineering International Conference Commemorating the 1908 Messina and Reggio Calabria Earthquake* (MERCEA'08), edited by A. Santini and N. Moraci, American Institute of Physics, Danvers, MA, 2008.

[Martelli and Forni 2008b] A. Martelli and M. Forni, "Prevention and mitigation of seismic risk of strategic, public and residential constructions, cultural heritage and industrial plants and components by means of seismic isolation and energy dissipation in Italy and worldwide", in short and extended abstracts DVD of Global Risk Forum (Davos, Switzerland), 2008.

[Martelli and Forni 2009a] A. Martelli and M. Forni, "State of the art on application, R&D and design rules for seismic isolation, energy dissipation and vibration control for civil structures, industrial plants and cultural heritage in Italy and other countries", in Proceedings (on DVD) of the 11th World Conference on Seismic Isolation, Energy Dissipation and Active Vibration Control of Structures (Guangzhou, 2009), University of Guangzhou, 2009.

[Martelli and Forni 2009b] A. Martelli and M. Forni, "Recenti applicazioni dei sistemi di controllo passivo delle vibrazioni sismiche", pp. 250–252 in Proceedings (on DVD) of the 13th National Congress "L'Ingegneria Sismica in Italia", Italian National Association for Earthquake Engineering (ANIDIS), Bologna, 2009.

[Martelli and Forni 2009c] A. Martelli and M. Forni, "Progress of worldwide application of seismic isolation and energy dissipation", pp. 102–111 in *Lightweight structures in civil engineering: 15th International seminar of IASS Polish Chapter* (Warsaw, 2009), Jan B. Obrębski Wydawnictwo Naukowe, 2009.

[Martelli and Forni 2010] A. Martelli and M. Forni, "Recenti applicazioni dei sistemi di isolamento sismico in Italia", *Ingegneria Sismica* **1** (2010), 63–74.

[Martelli et al. 2007] A. Martelli, S. Rizzo, V. Davidovici, M. Forni, K. N. G. Fuller, F. Hubert, M. Indirli, P. Komodromos, M. Phocas, V. Renda, A. Santini, and P. Sollogoub, "Current status of application of seismic isolation and other passive antiseismic systems to buildings, cultural heritage and industrial plants in Italy and worldwide", in Proceedings (on CD-ROM) of the 10th World Conference on Seismic Isolation, Energy Dissipation and Active Vibration Control of Structures (Istanbul, 2007), 2007, 2.

[Martelli et al. 2008] A. Martelli, U. Sannino, A. Parducci, and F. Braga, *Moderni sistemi e tecnologie antisismici: una guida per il progettista*, 21mo Secolo, Milan, 2008.

[Mazzolani 2009] F. Mazzolani (editor), *Proceedings of the First International Conference on Protection of Cultural Heritage* (PROHITECH 2009), CRC Press / Taylor and Francis, Leiden, 2009.

[Phocas et al. 2009] M. Phocas, C. A. Brebbia, and P. Komodromos (editors), *Earthquake resistant engineering structures VII.* (Proceedings of ERES 2009), Wit Press, Southampton, 2009.

[Sannino et al. 2009] U. Sannino, H. Sandi, A. Martelli, and I. Vlad (editors), *Modern systems for mitigation of seismic action* (Bucharest, 2008), AGIR, Bucharest, 2009.

[Santini and Moraci 2008] A. Santini and N. Moraci (editors), *Proceedings of the 2008 Seismic Engineering International Conference Commemorating the 1908 Messina and Reggio Calabria Earthquake* (MERCEA'08), American Institute of Physics, Danvers, MA, 2008.

[UNESCO-IPRED-ITU 2009] Declaration of participants in the UNESCO-IPRED-ITU International Workshop on "Make the Citizens a Part of the Solution" (Istanbul, 2009), 2009.

[Zhou et al. 2009] F. L. Zhou et al. (editors), Proceedings (on DVD) of the 11th World Conference on Seismic Isolation, Energy Dissipation and Active Vibration Control of Structures (Guangzhou, 2009), University of Guangzhou, 2009.

ALESSANDRO MARTELLI: alessandro.martelli@enea.it
ENEA, I-40129 Bologna, Italy

MASSIMO FORNI: massimo.forni@enea.it
ENEA-UTSISM, I-4129 Bologna, Italy

SEISMIC ISOLATION OF LIQUEFIED NATURAL GAS TANKS: A COMPARATIVE ASSESSMENT

JOAQUÍN MARTÍ, MARÍA CRESPO AND FRANCISCO MARTÍNEZ

In severe seismic environments, tanks for storage of liquefied natural gas may benefit from seismic isolation. As the design accelerations increase, the inner tank undergoes progressively greater demands and may suffer from corner uplift, elephant's foot buckling, gross sliding, shell thickness requirements beyond what can be reliably welded and, eventually, global uplift. Some of these problems cause extra costs while others make the construction impossible. The seismic environments at which the previous problems arise are quantified for modern 160,000 m³ tanks, whether supported on shallow or pile foundations, for both a conventional design and one employing seismic isolation. Additionally, by introducing some cost assumptions, comparisons can be made as to the cost of dealing with the seismic threat for each seismic environment and tank design option. It then becomes possible to establish the seismic environments that require seismic isolation, as well as to offer guidance for decisions in intermediate cases.

1. Introduction

Earthquakes contribute significant demands to the design of structures in many parts of the world. These demands can be dealt with in a conventional fashion or, alternatively, seismic isolation may also be provided to lessen their impact. The object of seismic isolation is to decrease the stresses and other demands that the earthquakes cause on the structure, even if this might entail other less desirable side effects such as increased relative displacements. The present paper attempts to clarify the advantages and disadvantages of the seismic isolation strategy in relation with storage tanks for liquefied natural gas (LNG).

Natural gas is primarily made of methane, which in gas form has a very small density. For moderate distances overland, gas-lines can be used to transport the gas efficiently. However for transport over very large distances or across oceans, the only alternative is to ship it in gas tankers in liquid form, which increases its density by a factor of about 600. At atmospheric pressures this implies operating at temperatures on the region of $-166°C$. To allow reasonably fast and predictable loading and unloading of the gas tankers, storage tanks must be provided; at export terminals they store the LNG produced in the liquefaction plant pending its transfer to the tanker, while at import terminals they receive and store the cargo that the vaporization plant will then process gradually.

Currently the more extended type of storage tank is the above-ground, full containment tank; the latter means that it provides containment for both liquid and vapor at operating temperatures. Underground tanks also exist but they are more expensive and cumbersome to build and, with the exception of Japan where the regulations often require them, they are considerably less common. Modern above-ground

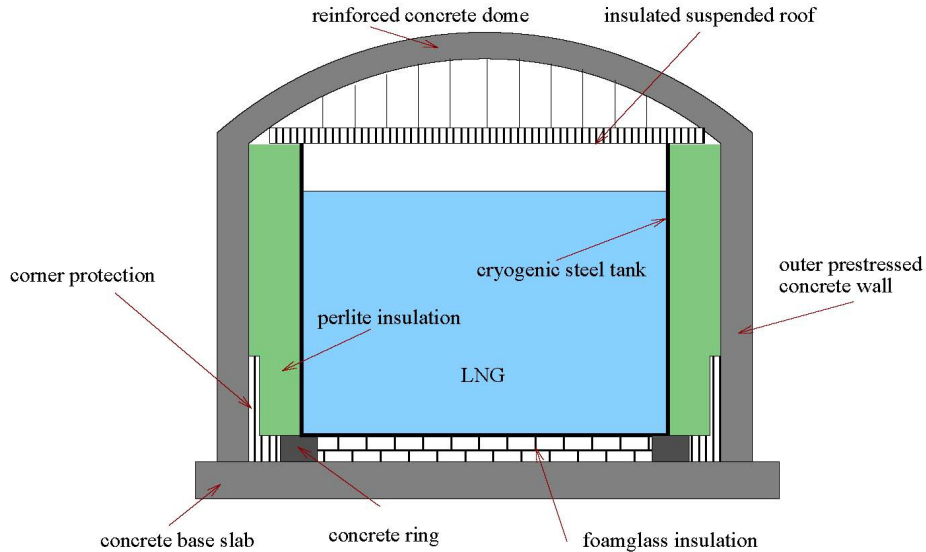*Keywords:* seismic isolation, LNG tank.

Figure 1. Schematic view of a modern LNG tank.

tanks typically have a storage capacity of around 150,000 m³, which is also consistent with the capabilities of the modern fleet.

A full containment tank is composed of an inner, self-standing, steel tank and an outer concrete tank. The inner tank is cylindrical and open at the top; it is made of cryogenic steel (9% Ni) in order to ensure adequate ductility at the operating temperatures and rests on thermal insulation placed on the base slab of the outer tank. The outer tank is made of concrete. The cylindrical wall is post-tensioned, both in the vertical and hoop directions. The base slab and the spherical dome consist of simply reinforced concrete. Adequate thermal insulation is provided between the two tanks. In the more common case in which the base slab is in direct contact with the ground, electrical heating is provided inside the slab in order to keep the ground from freezing, which would lead to unacceptable volume changes in the foundation.

With relatively minor variations, the global dimensions of modern LNG tanks tend to be 80 m for the diameter and 40 m for the wall height, with a peripheral space of 1 m between the two tanks. The dome radius is normally equal to the tank diameter, which means that the dome slopes 30° at the periphery. The wall thickness is usually 80 cm and the minimum dome thickness is 40 cm. Figure 1 shows a schematic view of the overall arrangement.

2. Seismic concerns in the design

LNG tanks are considered to be high responsibility structures due to the chemical energy that they store. As a consequence, their design requirements [API 2004; BSI 1993; CEN 2006; CEN 2007; NFPA 2006] are fairly stringent. From the viewpoint of seismic demands, they take into account an Operating Basis Earthquake (OBE) with a return period of 475 years and a Safe Shutdown Earthquake (SSE) with a return period on the region of 2500 to 5000 years, depending on the specific standard being used. They also include many other requirements and postulated accidents.

The design must finally satisfy all of the requirements imposed. However, seismic considerations govern only certain specific aspects of the design, their implications obviously growing as the design motions increase. But for many of the tanks' characteristics, the design is largely unaffected by the seismic specifications.

The design of the outer tank is seldom governed by earthquake considerations. This is because, being the outer protective skin, it must be sufficiently robust to withstand all other threats from outside the tank and even some from inside. The design events include low probability winds, impacts from flying missiles, overpressures from a hydrocarbon cloud deflagration, etc. But the two more demanding ones are the major leak and the external fire. In the former the liquid gas is postulated to escape from the inner tank, fill the annular space and apply its hydrostatic pressures and low temperatures directly to the concrete; in the latter the tank is subjected to high thermal fluxes for certain periods of time. As a consequence, except for perhaps having to add a small amount of reinforcement in the dome, the design of the outer tank is barely affected by the specified seismic motions.

The inner tank though, protected as it is from most external events by the outer tank, is only designed to contain the liquid gas. It is therefore much more sensitive to seismic effects, which are practically the only demands beyond operating conditions for which the outer tank provides little protection.

An increase in the input motions leads to larger seismically generated stresses, liquid pressures, forces and displacements. In principle, this type of consequences can be handled simply by increasing material quantities; in this case the seismic effects on quantities and costs are gradual, growing with the size of the design motions. However, there are some thresholds beyond which the strengthening process cannot be pursued continuously; at those points, either a new feature must be incorporated to the design or, in some cases, the construction of the tank becomes impossible.

One of the consequences of the earthquake is sloshing, the generation of standing waves in the free surface of the liquid. The predicted wave height must be incorporated as additional freeboard of the inner tank in order to prevent spills. This increases the height requirements of both inner and outer tanks, with considerable financial consequences. However, the typical sloshing periods are very long (about 10 s); and although the periods of nonisolated and isolated tanks differ substantially (about 0.5 s and perhaps 2–3 s, respectively), they are so far removed from the sloshing period that the wave height is generally not affected by seismic isolation. In short, sloshing implies an increase in costs but, the increase being similar for isolated and nonisolated tanks, it does not lead to a differential advantage.

Apart from sloshing, which involves the so-called convective liquid mass, the movements of the rest of the liquid mass, the impulsive mass, entail important pressure variations in the liquid. The same occurs with the vertical ground movements, which also excite the liquid mass. All of them imply departures from the preexisting hydrostatic pressures, which the inner tank must be able to deal with.

Additionally rocking excitations may lead to excessive compression of the tank wall (producing the elephant's foot buckling) and/or lift-off at the opposite corner of the tank; anchor straps may provide some help in respect of the latter problems, although that strategy is not totally free of uncertainties and disadvantages: undesirable thermal bridges across the insulation, stress concentrations in the shell, a protracted construction schedule and even some uncertainties in the seismic response; these aspects will be discussed later in more detail. The problems linked to rocking are of course alleviated by a flatter aspect ratio of the tank, though this strategy has adverse implications on space occupancy.

Another undesirable response of the inner tank would be gross sliding. The inner tank rests on a thin leveling layer of sand, placed above the thermal insulation. The horizontal demands, coupled with a dynamically decreased vertical weight, may lead to gross sliding of the inner tank. There is little that the designer can do to avoid this problem if it does tend to occur, even a flatter aspect ratio would not improve the situation.

Finally, if the vertical accelerations were sufficiently high, the upward vertical forces might exceed the static weight, whereupon the inner tank and the liquid would lift off globally. Again, no practical solution exists for this problem.

In summary, for the present evaluation of the possible contribution of seismic isolation, the following problems, as developed by a gradually increasing seismic input, will be taken into account together with their solutions when they are feasible:

– Larger liquid pressures and increased compression of the wall. The traditional solution is to use a thicker shell and/or provide additional stiffening.

– Corner uplift. When expected, a common solution strategy is to anchor the inner tank in spite of the possible disadvantages already mentioned.

– Gross sliding of the tank. This problem has no known solution, even changing the aspect ratio of the tank will not resolve it.

– Required thickness of inner tank exceeds about 50 mm. The thickness of cryogenic steel that can be reliably welded is limited; the specific limit may be arguable to some extent, here it will be assumed to be 50 mm.

– Global uplift of the tank. Again, when this is expected, no practical solution is known.

The first two items above are not fatal, in the sense that they simply require additional expenditure. The last three, however, have no known solution in current practice; hence, when those thresholds are reached, the tank can no longer be built according to the current standards.

Analyses will be conducted here to compare how the additional costs evolve with increasing seismic demands, depending on whether seismic isolation is used or not; both shallow and pile foundations will be considered, as this aspect has important implications on the results. The calculations will also allow determining when the construction of the tank ceases to be feasible with each design strategy.

3. Seismic isolation

Seismic isolation is a wide field. The reader is referred to [Skinner et al. 1993; Naeim and Kelly 1999] for a general review of the subject. The seismic isolation of liquid storage tanks has received some attention in recent years. Some examples are provided in [Tajirian 1998; Wang et al. 2001; Shrimali and Jangid 2002; 2004; Cho et al. 2004]. Numerical techniques have also been developed in order to treat the complexity of the seismic response of isolated tanks, as in [Wang et al. 2001; Kim et al. 2002; Cho et al. 2004]. However, LNG tanks pose their own specific requirements, which arise mainly from the cryogenic temperatures at which they operate and from the potentially serious consequences of any accidental releases.

The fast growth of the gas market worldwide over the last couple of decades, in both stable and earthquake prone regions, has led to research and applications of seismic isolation for LNG storage

tanks. Malhotra [1997; 1998] has proposed some novel isolation ideas which, at least for LNG tanks, would be rather difficult to implement in practice. The majority of the studies carried out concentrate their attention either in high damping rubber bearings (HDRBs), with or without a lead core, and in friction pendulum systems (FPSs). Some recent accounts have been provided by [Tajirian 1998; Böhler and Baumann 1999; Kim et al. 2002; Rötzer et al. 2005; Gregoriou et al. 2006; Manabe and Sakurai 2007; Christovasilis and Whittaker 2008]. Also relatively recently, Project INDEPTH, financed by the European Union over the period 2003-6, contributed considerable research on this topic [Crespo et al. 2006; Bergamo et al. 2007]; indeed the present paper uses some results from that project.

From the viewpoint of practical implementations, the authors are aware that seismic isolation has been provided at LNG tanks in the following sites: Revithoussa in Greece (2 tanks), Inchon in South Korea (3 tanks), Pyeong-Taek again in South Korea (10 tanks), Aliaga in Turkey (2 tanks) and Guangdong in China (2 tanks); the Manzanillo tanks in Mexico, currently under construction, are also expected to rest on seismic isolators. The Greek tanks are exceptional in that they are rather small (their capacity is only 65,000 m^3 per tank), located below ground, and use a friction pendulum system for isolation. The rest of the tanks are larger (100,000 m^3 to 150,000 m^3 per tank), located above the ground surface and relying on elastomeric bearings, with or without a lead core for providing the required damping.

It is clear that the use of seismic isolation can decrease the seismic demands developed in the tank structure. Its beneficial action can be exerted in two ways. The first horizontal frequencies of the tank are about 2 Hz for the inner tank full of LNG and about 5–7 Hz for the outer tank; this frequency range corresponds to the plateau region in practically all design spectra, as can be seen in the spectra shown in the next section. Consequently a first line of action is that if the isolation were to lower those frequencies, this would immediately entail a decrease of the seismic demands. In essence, reducing the stiffness that opposes the horizontal displacements of the base of the structure introduces a first mode in which the overall tank moves, with the distortions mainly developing in the isolation system, thereby minimizing the internal distortions of the tank. Of course a second way in which the isolation can be beneficial is by dissipating energy in the case of systems that have this capability.

The reduction of the spectral accelerations caused by a shift in the resonant frequency does have some deleterious effects though, namely an increase in the relative displacements between the ground and the tank. It should be remembered that about 20 lines go from the ground to the tank; they escalate the wall and enter the tank through penetrations located in the dome. The lines include large diameter pipes for loading and unloading the LNG, but also nitrogen, water and many other service pipes, as well as power cables, instrumentation, etc. All of them must be provided with flexible connections, able to accommodate the dynamic evolution of the relative displacements during the earthquake, which will be particularly large in the two horizontal directions. The cost of the necessary flexible connections, that must prevent leakage from large diameter pipes operating at high pressures and cryogenic temperatures, may be considerable.

It is worth highlighting that a seismic isolation system for an LNG tank essentially must limit its scope to acting in the horizontal direction. The vertical stiffness has to remain high in all cases and the supporting surface of the inner tank cannot depart much from a horizontal plane. Indeed, norms such as BS 7777 or the newer EN 14620 limit the differential settlements, even under the hydraulic test in which the tank is filled with water to reach 1.25 times the operating weight of LNG. The limitation stems from the sensitivity of the inner tank to the distortions caused by differential settlements, a sensitivity that is

easily understood when considering that the upper part of the inner tank wall has a shell thickness of only 10–12 mm and a diameter of some 80 m.

Hence, although seismic isolation provides help in the horizontal direction, practically nothing can be done in the vertical one. Thus the traditionally smaller role of the vertical demands becomes proportionally much more important in seismically isolated tanks and may even govern parts of the design.

When considering vertical effects, there is one aspect that is often disregarded. For horizontal motions, the decomposition of the liquid mass into its impulsive and convective components is perfectly standard [ASCE 1984; Veletsos and Tang 1990], but for vertical motions the liquid is normally considered to act as a rigid mass that moves with the base slab. In many situations this assumption becomes insufficient and a decomposition of the liquid mass must also be incorporated for the vertical motions [Veletsos and Tang 1986]. When this is done, only part of the liquid mass moves rigidly with the slab; the rest oscillates with the frequency of the first breathing mode of the inner tank, which is typically around 2 Hz.

No attempt will be made here to compare different seismic isolation strategies. As mentioned earlier, all implementations of seismic isolation in LNG tanks to date, with the exception of the smaller Revithoussa tanks, have used elastomeric bearings. This will be the system adopted here; it will also be assumed that the design of the seismic isolators is carried out to comply with the AASHTO Guidelines [AASHTO 2000]. The vertical stiffness of the tank support is assumed to remain unaffected by the isolation; in the horizontal direction the characteristics of the isolation are such that the first horizontal frequency of the tank is 0.4 Hz with 15% damping. The displacement requirements imposed on the isolators will of course be a function of the level of the design motions.

4. Implications of the seismic loads

The seismic input has been defined here by means of two features: a spectral shape and a reference acceleration used for scaling the previous spectral shape. For the spectral shape, three different ones have been considered, one corresponding to a medium type spectrum and two which are enriched either in the low or in the high frequency range of the spectrum. More specifically, the three spectral shapes adopted are those that Eurocode 8 [CEN 2004] recommends for soil types B, C and D and type 1 earthquakes (magnitude $M_s > 5.5$). The normalized spectra are shown in Figure 2; these spectra should be multiplied
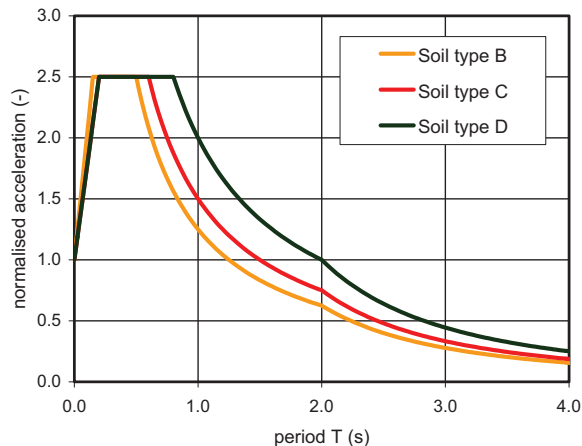

Figure 2. Spectral shapes used in the calculations.

by the Zero Period Acceleration (ZPA), $a_g S$ using EC8 terminology, which includes the influence of the soil through the soil factor S. For vertical motions, the spectral shapes have been obtained by multiplying the previous ones by 0.7.

The reference acceleration a_g will be taken as a continuously varying parameter, descriptive of the hazard level at the site. For a given spectral shape, this will allow studying the acceleration levels that trigger the various events. Incidentally, simply looking at the figure, the advantages of using seismic isolation for moving the first frequencies from their normal values (around 2 Hz for the inner tank and some 5–7 Hz for the outer tank) to somewhere in the 0.3–0.5 Hz range are immediately obvious.

The nonisolated tank with a shallow foundation is assumed to rest directly on reasonably competent ground; otherwise it would not have been able to fulfill the requirements that [BSI 1993] imposes on differential settlements. Specifically, a soil with an effective shear modulus of 180 MPa and a density of 2000 kg/m^3 is assumed, resulting the shear wave velocity of 300 m/s. Classical formulae for the calculation of the horizontal, vertical and rocking stiffnesses have been used [ASCE 2000]. In the case of a tank supported on piles, the foundation has been assumed to consist of 300 concrete piles, each 1.5 m in diameter and 40 m long. The global horizontal and vertical stiffnesses calculated for this foundation are nearly 4 times those of the shallow foundation, while for the rocking stiffness the factor is approximately 1.5.

From the viewpoint of the material properties of the structure, only the properties of the inner tank have an influence on the results. For the 9% Ni steel, it is assumed that the Young's modulus is 200 GPa, the Poisson's ratio is 0.3 and the density is 7850 kg/m^3.

Since a cost comparison is being sought, this requires information on unit costs which contractors are loath to disseminate. The assumptions given below should only be considered reasonable approximations, with a certain range of uncertainty. Nevertheless, the final conclusions are thought to be fairly robust and, apart from perhaps some minor variations, they should stand in spite of the shortcomings of the unit costs employed. The specific assumptions follow.

As mentioned earlier the AASHTO Guidelines were used to design the elastomeric seismic isolation. It should be noticed that costs may be strongly affected by the code used: for example a design following the Italian seismic code will result in higher costs, while the Japanese code will probably lead to lower ones. The cost of the isolation system is a strong function of the design relative displacements, increasing from 1.2 M€ for 20 cm to about 4.5 M€ for 60 cm displacement.

The relative movement between the various structures and the ground allowed by the seismic isolation requires providing the piping with connections that maintain their function in spite of those relative movements. For a typical LNG tank the cost of the flexible connections has been estimated as 0.3 M€.

Unit costs for different types of concrete structures are needed. Concrete placed on the ground has been assumed to cost 300 €/m^3, a figure that increases to 450 €/m^3 for concrete placed at an elevation that requires formwork and structural supports.

If the local geotechnical conditions are such that if the tank requires a pile foundation, the placement of seismic isolators does not entail the need for any additional concrete, one device would be placed in each pile, more or less directly under the base slab of the tank. However, if a surface slab suffices, the placement of isolation devices requires constructing a double mat and concrete pedestals between the two slabs, with the devices placed in the upper part of the pedestals. It has been assumed that, except for its periphery, a shallow slab is only 0.7 m thick, while in the case of a double slab a thickness of 1 m

is required for both slabs; pedestals are constructed every $12\,m^2$ of slab and they are assumed to be 2 m high and 1 m in diameter.

As the seismic demand increases, the walls of the steel tank may need to be thicker and there is also the possibility that steel anchors are needed. The required steel thickness is a function of the expected pressures in the liquid, which are of course affected by the earthquake. The steel needed for both, container and anchors, is cryogenic, adequate for withstanding the low operating temperatures. A unit cost of 5 €/kg has been used here.

Anchorage is not required with the usual aspect ratios of tanks until the PGA reaches about 0.3 g. When required, the minimum cost of anchorage has been taken as 0.35 M€, increasing with the amount of steel required by the anchor system.

When the base slab is placed directly on the ground, the slab must be heated to keep the ground from freezing underneath. If the base slab is elevated and air circulates freely below, then heating is no longer necessary. This arrangement, however, is only possible when there is a double slab or, in the case of pile foundations, if the piles are extended some 2 m above the ground surface before building the slab. The total cost of the installed heating system may be on the region of 1 M€. The energy costs are harder to include because, over the life of the tank, their effect may be strongly affected by variables like inflation rates, interest rates and electricity costs. Here the energy savings have been taken as equivalent to the upfront saving of 10 years of energy consumption, with a unit cost of 0.1 €/kWh. The energy savings for a $160{,}000\,m^3$ tank can then be estimated at 1 M€.

5. Calculation of seismic response

As mentioned earlier, some of the calculations were initiated within the framework of the EC-funded IN-DEPTH project and useful information has also been incorporated based on the publications of [Bergamo et al. 2006a; Bergamo et al. 2006b; Castellano et al. 2006] and [Gregoriou et al. 2006].

The specific dimensions used for the tank are as follows:

Inner tank:	diameter	78.00 m	Spherical roof:	internal radius	80.00 m
Outer tank wall:	internal diameter	80.00 m		thickness	0.40 m
	height	40.15 m	Slab:	diameter	81.60 m
	thickness	0.80 m		thickness	1.0 m

The height and the thicknesses of the inner tank depend on the level of acceleration, so no specific values are indicated above.

The calculations performed involve the response of an isolated tank and that of a nonisolated tank for progressively increasing levels of the response spectra presented earlier. As already mentioned, the isolated tank is assumed to be supported on devices that are vertically rigid and take the first horizontal period of the tank to 2.5 s with 15% damping. For both tanks, the following tasks are carried out:

– Determination of the liquid masses (impulsive and convective), mobilized in relation with the horizontal response of the tank, on the assumption of a full inner tank.

– Determination of the liquid masses (responding rigidly and in the first breathing mode), mobilized in relation with the vertical response of the tank, on the assumption of a full inner tank.
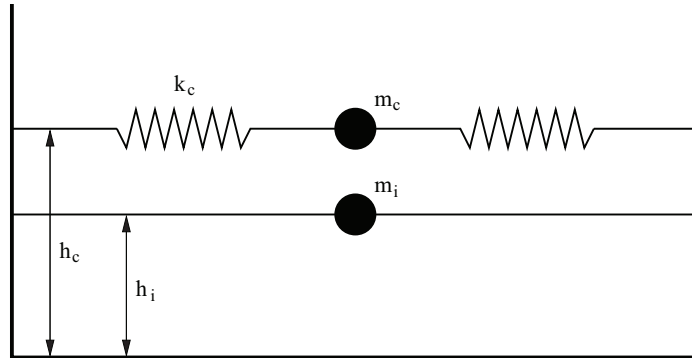
Figure 3. Effective liquid masses in horizontal oscillations.

– Determination of the lower natural frequencies of the inner tank, for both horizontal and vertical excitation.

– Use of the response spectrum method, with suitable combinations of the horizontal and vertical components, in order to determine the need for increasing material quantities, as well as the points beyond which the design is no longer possible.

The calculations follow the methodology proposed by the ASCE Standard 4-98 [ASCE 2000] and the Guidelines for the Seismic Design of Oil and Gas Pipeline Systems [ASCE 1984]. For the vertical excitation this methodology is supplemented with that proposed by [Veletsos and Tang 1986]. Under horizontal excitation the impulsive mass, which moves rigidly attached to the inner tank and hence oscillates at 2.08 Hz, turns out to be 48% of the total; the remaining 52% is the convective mass, with a first sloshing frequency of 0.104 Hz. The situation can be visualized in Figure 3. For vertical oscillations, the rigid mass, which follows the motion of the tank's base, represents 42% of the total mass; the remaining 58% of the liquid mass vibrates in the first breathing mode at 2.08 Hz (its precise similarity with the horizontal frequency is a mere coincidence). As an example, Figure 4 shows a finite element
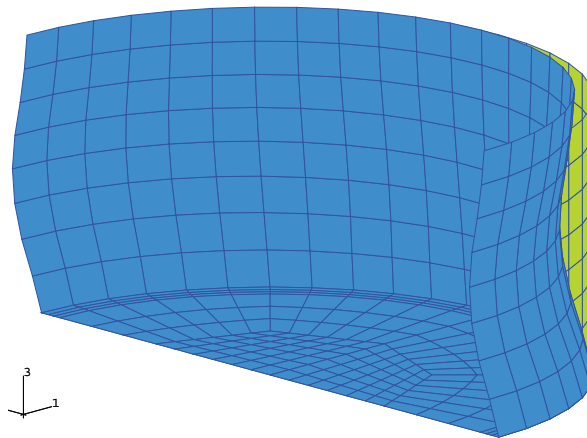

Figure 4. First horizontal mode of the full inner tank.

model of an LNG tank; the deformed shape corresponds to the first horizontal mode of the full inner tank on the assumption of a rigid foundation.

It is important to note that the effects arising from the various liquid masses have to be combined by direct addition. By contrast the effects of the different components of the earthquake have been combined assuming 100% of the horizontal component with 30% of the vertical one, and vice versa. Finally, the structural effects associated with different modes of the tank have been combined with the SRSS rule.

An important contribution to the cost may arise from the need of additional cryogenic steel for the inner tank. The thickness at the various elevations must suffice for dealing with three demands: *hydrostatic conditions*, *OBE conditions*, and *SSE conditions*.

It is seldom obvious which of the latter two cases is more limiting, even though the SSE is clearly greater than the OBE, because standards use different evaluation rules and different values of the allowable steel stresses for OBE and SSE conditions. In the calculation of the inner tank, both the horizontal and vertical excitations have to be considered and combined as described above.

Finally, the calculations of corner uplift have been conducted following the methodology described in API 620 [API 2004].

The following milestones are determined by the calculations for the spectrum corresponding to soil type C. The ranges describe the effect of the different foundations used in the analyses (piles and surface slab):

(a) For nonisolated tanks, when the peak ground acceleration (PGA) reaches

> $0.25\,g$–$0.30\,g$: there is corner uplift unless anchorage is provided.
> $0.50\,g$–$0.65\,g$: the inner tank starts to slide during the earthquake.
> $\sim 1.00\,g$: there is global uplift of the inner tank.

(b) For isolated tanks, when the peak ground acceleration (PGA) reaches

> $0.80\,g$–$0.90\,g$: the inner tank starts to slide during the earthquake.
> $\sim 1.00\,g$: there is global uplift of the inner tank.

Although the isolation does not affect the response of the tank to vertical excitations, the accelerations that produce global uplift actually turn out to be slightly higher for the nonisolated case, but this is a consequence of the thinner shell thickness required in the isolated case.

Equivalent results have also been obtained for the other two spectra (soil types B and D). For nonisolated tanks, corner uplift appears for the same range of accelerations for soil types C and D; however, for soil type B, this effect appears at an acceleration about 30% higher. Global sliding is more sensitive to the type of spectrum: the triggering acceleration for soil type C is about 20% higher than for soil type D, and is also 20% higher for soil type B than for soil type C. Finally, the accelerations at which global uplift appears have a smaller range of variation, between 5 and 10%.

For isolated tanks, the sensitivity to the type of spectrum is generally lower: the accelerations triggering global sliding vary between 5 and 10% with the type of spectrum; the accelerations that cause global uplift have a very small range of variation, below 5%.

As a function of the peak ground acceleration, based on the previous results for soil type C, the following statements can be made regarding the feasibility of the design:

– Up to $0.25\,g$–$0.30\,g$: both isolated and nonisolated tanks are possible without anchorage

    – From 0.25 g–0.30 g to 0.50 g–0.65 g: an isolated tank is still possible without anchorage, but a nonisolated tank requires anchorage.

    – From 0.50 g–0.65 g to 0.80 g–0.90 g: only an isolated tank is possible, which can still be unanchored.

    – From about 0.8 g–0.90 g onwards: no tanks can be built using current standards and methodology, since even an isolated tank will undergo gross sliding during the earthquake.

The comments made earlier in relation with the influence of the soil type and its associated spectral shape are also applicable in relation with the figures given above.

6. Differential costs

By combining the structural and cost information, it becomes possible to compare the different situations and design strategies. Three cases will be shown:

    – a conventional design, without seismic isolation, whether supported on a surface slab or on piles;

    – a seismically isolated tank, which already required a pile foundation in any case and has an isolating device per pile;

    – a seismically isolated tank, which did not require a pile foundation for other reasons and therefore had to be provided with a double slab and pedestals for placing the devices.

The only costs considered are those incurred as a consequence of the seismic demands and only if they vary between the three cases. For example, a larger earthquake implies greater sloshing waves and hence an increased height of the inner and outer tanks, but this cost will not be taken into account because it is identical in all cases. The curves presented are therefore useful only for establishing cost differences between the various strategies, since the absolute values do not reflect the common costs. More specifically, the following costs are included:

For the nonisolated tank:
    – increased thickness of inner tank
    – anchorage of inner tank

For the isolated tank on piles:
    – isolation system
    – flexible pipe connections
    – increased thickness of inner tank
    – anchorage of inner tank

For the isolated tank on a surface slab:
    – dual slab and pedestals
    – savings in heating system and energy
    – isolation system
    – flexible pipe connections
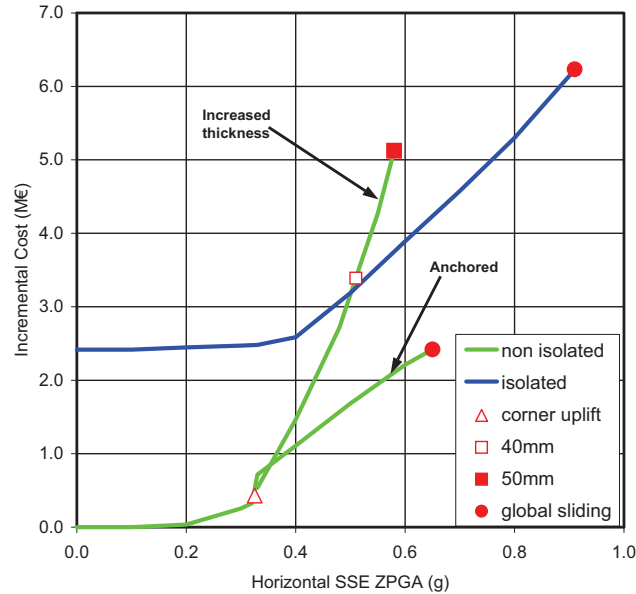   – increased thickness of inner tank
    – anchorage of inner tank

Figure 5. Cost evolution with seismic demand: slab foundation.
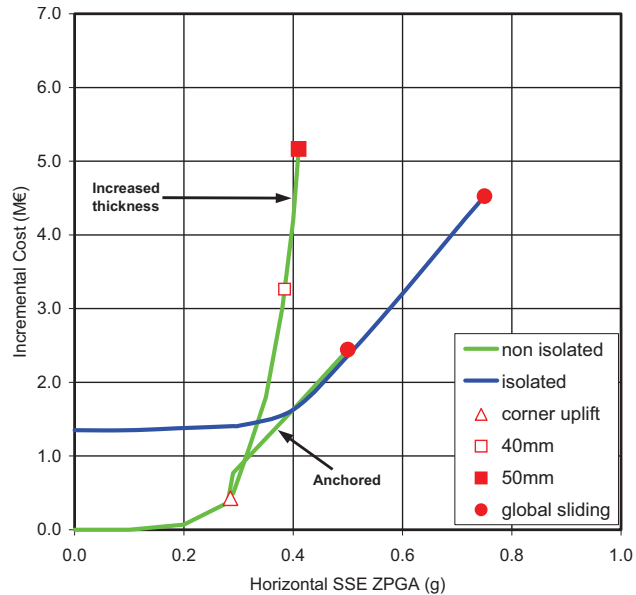

Figure 6. Cost evolution with seismic demand: pile foundation.

The results are combined and compared in Figure 5 for the tank resting on a slab and in Figure 6 for that on a pile foundation. The curves reflect the progressive increases in material quantities imposed by larger seismic demands. Both figures correspond to the case in which an SC spectrum is used for the motions, though the differences with the results obtained with the other spectra are relatively small.

For nonisolated tanks there is a point (identified by a triangle in the figures) beyond which something must be done to avoid damage by corner uplift. A possible solution is to anchor the tank: the discrete jump in one of the "nonisolated" curves is associated with the introduction of this anchorage; in the other "nonisolated" curve the problem is tackled by increasing the thickness of the inner tank. The cost of increasing the thickness quickly becomes higher than that of providing anchorage.

For the specific case of a tank supported on a pile foundation, seismic isolation is not absolutely required until the PGA reaches about 0.50 g, but anchorage must be provided beyond 0.25 g. When considering anchorage, the following should be taken into account:

– Anchorage introduces other "costs" of difficult quantification, beyond the cost of the steel. Technically, it creates undesirable stress concentrations at points of the inner tank, as well as thermal bridges across the thermal insulation under the bottom. Practically, it implies considerable complications and delays in the construction schedule because the anchor straps must be left embedded and protruding when pouring the slab concrete, on which the perimetral beam, thermal insulation and eventually the inner tank will be placed.

– Even though anchorage is a relatively frequent practice, there are some questions as to its reliability during an earthquake. Anchor straps need to be flexible in bending when radial displacements of the inner tank take place; but they are therefore considerably stiffer for movements in the circumferential direction. For straps being deformed in this direction, it is difficult to ensure that they respond in an adequate fashion (for example, without risk of brittle fracture at weld locations).

As a consequence of these considerations, although it is difficult to offer a precise quantification, an isolated tank may be preferable to a nonisolated tank at least in the upper part of the 0.25 g–0.50 g range of peak ground accelerations.

For a tank on a pile foundation the cost of the anchored tank equals that of the isolated tank for accelerations beyond about 0.4 g. However, for tanks on a slab foundation, the incremental cost of the isolated tank always exceeds that of the anchored one for the same range of accelerations. The primary reason is that the isolation of a tank on a slab foundation requires building an additional slab and pedestals, but these extra costs are only partially compensated by the energy savings. On the other hand, the greater stiffness used here for the pile foundation leads to a slightly more expensive inner tank.

For a tank on piles, the solution of increasing the inner tank thickness is practically always more expensive than that of isolating the tank. For a tank founded on a slab, this occurs only beyond 0.5 g, an acceleration level at which the thickness required at the base of the inner tank is about 40 mm.

7. Conclusions

The problems caused by earthquakes on LNG tanks have been reviewed and analyses have been carried out to determine the potential contributions of seismic isolation towards solving those problems or delaying their appearance. The study was centered on a typical modern LNG tank, capable for 160,000 m^3. From the work conducted, the following conclusions can be offered:

a) Seismic isolation may be used to decrease the effects of the horizontal but not the vertical excitations. As a consequence the latter tend to become comparatively much more important in isolated tanks.

b) It then becomes important to take into account that for vertical motions the liquid mass is distributed as a rigid mass and another mass that oscillates with the first breathing mode of the tank, just as for horizontal motions it is distributed into impulsive and convective masses.

c) When the design peak ground accelerations are below about 0.25 g–0.30 g, a nonisolated tank is perfectly adequate and some 2 M€ cheaper than an isolated tank. Seismic isolation therefore cannot be justified on technical grounds for sites with such moderate hazard levels.

d) When the design peak ground accelerations are in the range of 0.25 g–0.30 g to about 0.50 g–0.65 g, a nonisolated tank is still possible but it needs to be anchored, which introduces some uncertainties and involves additional costs of difficult quantification. Even neglecting the latter, the cost difference between the nonisolated and the isolated tank decreases with increasing seismic demands and it even disappears beyond 0.4 g for the isolated 160,000 m^3 tank on piles.

e) If the design peak ground acceleration exceeds about 0.50 g, nonisolated designs are no longer feasible since it becomes impossible to ensure that the inner tank does not undergo gross sliding during the earthquake. Thus, in the range of 0.50 g–0.65 g to 0.90 g, only seismically isolated tanks can be proposed.

f) When the design peak ground acceleration exceeds 0.90 g even an isolated tank is not feasible due to the inevitability of sliding.

g) Irrespective of other circumstances, global uplift of the inner tank (the tank loses any contact with the base) is predicted when the design peak ground acceleration attains about 1.0 g for both isolated and nonisolated tanks.

As a final comment, all calculations were based on the response spectrum method. This is a rather conservative procedure, but well established in the industry and which poses few uncertainties. The calculations could have been carried out using direct integration of synthetic accelerograms and generally the results would have been less demanding. The response spectrum method was adopted because of its wider industrial acceptance and the possible sensitivity of the results to the specific accelerograms.

References

[AASHTO 2000] *Guide specifications for seismic isolation design*, 2nd edition, American Association of State Highway and Transportation Officials, Washington, DC, 2000. 3rd edition published in 2010.

[API 2004] *Design and construction of large, welded, low-pressure storage tanks*, 10th edition, American Petroleum Institute, Washington, DC, 2004. API STD 620. Addendum 1. 11th edition published in 2010 with addenda 1 & 2.

[ASCE 1984] *Guidelines for the seismic design of oil and gas pipeline systems*, Committee on Gas and Liquid Fuel Lifelines of the ASCE Technical Council on Lifeline Earthquake Engineering, New York, 1984.

[ASCE 2000] *Seismic analysis of safety-related nuclear structures and commentary* (*ASCE 4-98*), Standard No. 004-98, American Society of Civil Engineers, Reston, VA, 2000.

[Bergamo et al. 2006a] G. Bergamo, M. G. Castellano, F. Gatti, A. Poggianti, and P. Summers, "Seismic isolation of spheres at petrochemical facilities", in *First European Conference on Earthquake Engineering and Seismology* (Geneva, 2006), Swiss Society for Earthquake Engineering and Structural Dynamics, Zürich, 2006. Paper # 1009.

[Bergamo et al. 2006b] G. Bergamo, M. G. Castellano, F. Gatti, and V. Rebecchi, "Parametric analyses for the seismic isolation of LNG tanks", in *First European Conference on Earthquake Engineering and Seismology* (Geneva, 2006), Swiss Society for Earthquake Engineering and Structural Dynamics, Zürich, 2006. Poster Presentation ID 1046.

[Bergamo et al. 2007] G. Bergamo, M. G. Castellano, F. Gatti, J. Marti, A. Poggianti, and P. Summers, "Seismic protection at petrochemical facilities: main results from INDEPTH project", in *Proceedings of the ASSISi 10th World Conference on Seismic Isolation, Energy Dissipation and Active Vibrations Control of Structures* (Istanbul, 2007), 2007.

[Böhler and Baumann 1999] J. Böhler and T. Baumann, "Different numerical models for the hysteretic behaviour of HDRB's on the dynamic response of base-isolated structures with lumped-mass models under seismic loading", pp. 267–273 in *Constitutive models for rubber* (Vienna, 1999), edited by A. Dorfmann and A. Muhr, Balkema, Rotterdam, 1999.

[BSI 1993] *Flat-bottomed, vertical, cylindrical storage tanks for low temperature service*, BS 7777, British Standards Institution, London, 1993, Available at http://tinyurl.com/bsi7777.

[Castellano et al. 2006] M. G. Castellano, A. Poggianti, and P. Summers, "Seismic retrofit of spheres using energy-dissipating braces", in *First European Conference on Earthquake Engineering and Seismology* (Geneva, 2006), Swiss Society for Earthquake Engineering and Structural Dynamics, Zürich, 2006. Paper # 1001.

[CEN 2004] *Eurocode 8: Design of structures for earthquake resistance - Part 1: General rules, seismic actions and rules for buildings*, EN 1998-1:2004, European Committee for Standardization, Brussels, 2004, Available at http://tinyurl.com/bs-en-1998-1-2004.

[CEN 2006] *Design and manufacture of site built, vertical, cylindrical, flat-bottomed steel tanks for the storage of refrigerated, liquefied gases with operating temperatures between $0°C$ and $-165°C$*, EN 14620, European Committee for Standardization, Brussels, 2006, Available at http://tinyurl.com/bs-en-14620.

[CEN 2007] *Installation and equipment for liquefied natural gas. Design of onshore installations*, EN 1473, European Committee for Standardization, Brussels, 2007, Available at http://tinyurl.com/bs-en-1473-2007.

[Cho et al. 2004] K. H. Cho, M. K. Kim, Y. M. Lim, and S. Y. Cho, "Seismic response of base-isolated liquid storage tanks considering fluid-structure-soil interaction in time domain", *Soil Dyn. Earthq. Eng.* **24**:11 (2004), 839–852.

[Christovasilis and Whittaker 2008] I. P. Christovasilis and A. S. Whittaker, "Seismic analysis of conventional and isolated LNG tanks using mechanical analogs", *Earthq. Spectra* **24**:3 (2008), 599–616.

[Crespo et al. 2006] M. Crespo, S. Omnes, and J. Marti, "Benefits of seismic isolation for LNG tanks", in *First European Conference on Earthquake Engineering and Seismology* (Geneva, 2006), Swiss Society for Earthquake Engineering and Structural Dynamics, Zürich, 2006. Paper # 1083.

[Gregoriou et al. 2006] V. P. Gregoriou, S. V. Tsinopoulos, and D. L. Karabalis, "Base isolated LNG tanks: seismic analyses and comparison studies", in *First European Conference on Earthquake Engineering and Seismology* (Geneva, 2006), Swiss Society for Earthquake Engineering and Structural Dynamics, Zürich, 2006. Paper # 1128.

[Kim et al. 2002] M. K. Kim, Y. M. Lim, S. Y. Cho, K. H. Cho, and K. W. Lee, "Seismic analysis of base-isolated liquid storage tanks using the BE-FE-BE coupling technique", *Soil Dyn. Earthq. Eng.* **22**:9–12 (2002), 1151–1158.

[Malhotra 1997] P. K. Malhotra, "Method for seismic base isolation of liquid-storage tanks", *J. Struct. Eng.* (*ASCE*) **123**:1 (1997), 113–116.

[Malhotra 1998] P. K. Malhotra, "New method for seismic isolation of liquid-storage tanks", *Earthq. Eng. Struct. Dyn.* **26**:8 (1998), 839–847.

[Manabe and Sakurai 2007] H. Manabe and T. Sakurai, "Seismic analysis of an SPB tank installed in the offshore GBS LNG terminal", *IHI Eng. Rev.* **40**:2 (2007), 69–73.

[Naeim and Kelly 1999] F. Naeim and J. M. Kelly, *Design of seismically isolated structures: from theory to practice*, Wiley, New York, 1999.

[NFPA 2006] *NFPA 59A: Standard for the production, storage, and handling of liquefied natural gas (LNG)*, National Fire Protection Association, Quincy, MA, 2006, Available at http://tinyurl.com/NFPA-59A-2006. Revised in 2009.

[Rötzer et al. 2005] J. Rötzer, H. Douglas, and H. Maurer, "Hazard and safety investigations for LNG tanks, 1: Earthquakes", *LNG J.* (July/August 2005), 23–24.

[Shrimali and Jangid 2002] M. K. Shrimali and R. S. Jangid, "Earthquake response of liquid storage tanks with sliding systems", *J. Seismol. Earthq. Eng.* **4**:2 & 3 (2002), 51–61.

[Shrimali and Jangid 2004] M. K. Shrimali and R. S. Jangid, "Seismic analysis of base-isolated liquid storage tanks", *J. Sound Vib.* **275**:1–2 (2004), 59–75.

[Skinner et al. 1993] R. I. Skinner, W. H. Robinson, and G. H. McVerry, *An introduction to seismic isolation*, Wiley, New York, 1993.

[Tajirian 1998] F. F. Tajirian, "Base isolation design for civil components and civil structures", in *Structural engineering world wide 1998: proceedings of the Structural Engineers World Congress* (San Francisco, 1998), edited by N. K. Srivastava, Elsevier, Amsterdam, 1998.

[Veletsos and Tang 1986] A. S. Veletsos and Y. Tang, "Dynamics of vertically excited liquid storage tanks", *J. Struct. Eng. (ASCE)* **112**:6 (1986), 1228–1246.

[Veletsos and Tang 1990] A. S. Veletsos and Y. Tang, "Soil-structure interaction effects for laterally excited liquid storage tanks", *Earthq. Eng. Struct. Dyn.* **19**:4 (1990), 473–496.

[Wang et al. 2001] Y.-P. Wang, M.-C. Teng, and K.-W. Chung, "Seismic isolation of rigid cylindrical tanks using friction pendulum bearings", *Earthq. Eng. Struct. Dyn.* **30**:7 (2001), 1083–1099.

JOAQUÍN MARTÍ: joaquin.marti@principia.es
PRINCIPIA Ingenieros Consultores, Velázquez, 94, 28006 Madrid, Spain

MARÍA CRESPO: maria.crespo@principia.es
PRINCIPIA Ingenieros Consultores, Velázquez, 94, 28006 Madrid, Spain

FRANCISCO MARTÍNEZ: francisco.martinez@principia.es
PRINCIPIA Ingenieros Consultores, Velázquez, 94, 28006 Madrid, Spain

SUBMISSION GUIDELINES

ORIGINALITY

Authors may submit manuscripts in PDF format online at the Submissions page. Submission of a manuscript acknowledges that the manuscript is original and has neither previously, nor simultaneously, in whole or in part, been submitted elsewhere. Information regarding the preparation of manuscripts is provided below. Correspondence by email is requested for convenience and speed.

LANGUAGE

Manuscripts must be in English. A brief abstract of about 150 words or less must be included. The abstract should be self-contained and not make any reference to the bibliography. Also required are keywords and subject classification for the article, and, for each author, postal address, affiliation (if appropriate), and email address if available. A home-page URL is optional.

FORMAT

Authors can use their preferred manuscript-preparation software, including for example Microsoft Word or any variant of TeX. The journal itself is produced in LaTeX, so accepted articles prepared using other software will be converted to LaTeX at production time. Authors wishing to prepare their document in LaTeX can follow the example file at www.jomms.org (but the use of other class files is acceptable). At submission time only a PDF file is required. After acceptance, authors must submit all source material (see especially Figures below).

REFERENCES

Bibliographical references should be complete, including article titles and page ranges. All references in the bibliography should be cited in the text. The use of BibTeX is preferred but not required. Tags will be converted to the house format (see a current issue for examples); however, for submission you may use the format of your choice. Links will be provided to all literature with known web locations; authors can supply their own links in addition to those provided by the editorial process.

FIGURES

Figures must be of publication quality. After acceptance, you will need to submit the original source files in vector format for all diagrams and graphs in your manuscript: vector EPS or vector PDF files are the most useful. (EPS stands for Encapsulated PostScript.)

Most drawing and graphing packages—Mathematica, Adobe Illustrator, Corel Draw, MATLAB, etc.—allow the user to save files in one of these formats. Make sure that what you're saving is vector graphics and not a bitmap. If you need help, please write to graphics@mathscipub.org with as many details as you can about how your graphics were generated.

Please also include the original data for any plots. This is particularly important if you are unable to save Excel-generated plots in vector format. Saving them as bitmaps is not useful; please send the Excel (.xls) spreadsheets instead. Bundle your figure files into a single archive (using zip, tar, rar or other format of your choice) and upload on the link you been given at acceptance time.

Each figure should be captioned and numbered so that it can float. Small figures occupying no more than three lines of vertical space can be kept in the text ("the curve looks like this:"). It is acceptable to submit a manuscript with all figures at the end, if their placement is specified in the text by means of comments such as "Place Figure 1 here". The same considerations apply to tables.

WHITE SPACE

Forced line breaks or page breaks should not be inserted in the document. There is no point in your trying to optimize line and page breaks in the original manuscript. The manuscript will be reformatted to use the journal's preferred fonts and layout.

PROOFS

Page proofs will be made available to authors (or to the designated corresponding author) at a Web site in PDF format. Failure to acknowledge the receipt of proofs or to return corrections within the requested deadline may cause publication to be postponed.

Seismic Isolation and Protection Systems vol 1, no 1, 2010